



## Results analysis and validation – D5.3

Project Number:	ICT-2009-257385
Project Title:	Opportunistic networks and Cognitive Management Systems for Efficient Application Provision in the Future Internet - OneFIT
Document Type:	Deliverable

Contractual Date of Delivery:	31.12.2012
Actual Date of Delivery:	14.01.2013
Editors:	Ó. Moreno, J.L. González
Participants:	See contributor's list
Workpackage:	WP5
Estimated Person Months:	47 PMs
Nature:	PU <sup>1</sup>
Version:	1.0
Total Number of Pages:	125
File:	OneFIT_D5.3_20121231.docx

### Abstract

This deliverable describes the validation processes followed to assess the performance of the algorithms and protocols for the operator governed opportunistic networking as defined in the OneFIT Project.

Therefore, this document includes the description of the set-up of the different validation platforms, the design of the test plans for each one of them, and the analysis of the results obtained from the tests.

A per-scenario approach rather than a per-platform approach has been followed, so an additional analysis has been performed, gathering the results related to each scenario, in order to validate the premises stated to each one of them. The OneFIT concept has been therefore validated for all foreseen business scenarios.

### Keywords List

Validation platform, implementation, Opportunistic Networks, scenarios, test-bed

<sup>1</sup> Dissemination level codes: **PU** = Public  
**PP** = Restricted to other programme participants (including the Commission Services)  
**RE** = Restricted to a group specified by the consortium (including the Commission Services)  
**CO** = Confidential, only for members of the consortium (including the Commission Services)

## Executive Summary

This document addresses the validation tests and the corresponding obtained results from the OneFIT [1] validation platforms. Comprehensive descriptions of the specification and the implementation of these platforms can be found in deliverables D5.1 [2] and D5.2 [3] respectively.

In first place, a description of the process followed to validate the OneFIT concept is shown. The validation process is based on five different business scenarios on which the performance of the OneFIT mechanisms will be assessed separately. To achieve this, nine validation platforms have been developed, each of them addressing different aspects of the OneFIT architecture, protocols and life cycle. The nine platforms complement each other, so that global conclusions on the validity of the OneFIT concept can be extracted.

Individual validation for each of the business scenarios is performed. On a per-scenario basis, it is showcased how each one of the related platforms is configured in order to be adapted to the peculiarities of the scenario. Moreover, plans to test every platform, obtaining the most relevant set of KPIs for the given scenario, and to interpret the results are presented. Subsequently, the results obtained from each platform are shown and interpreted in the context of the current scenario. Finally, in order to properly validate every scenario, a synergetic analysis of the results of all the platforms involved in the scenario validation is performed. These analyses focus on the OneFIT solution as a whole, rather than in the particular results of the individual aspects addressed in the platforms, thus providing a holistic approach on how the OneFIT concept is able to deal with the challenges posed by the scenario. More specifically:

- The results of implementing the first scenario prove that an Opportunistic Network approach efficiently copes with the problems of an infrastructure network that needs to temporary extend its coverage in order to provide service to a number of users that are out of reach. This is achieved by creating an ad-hoc network among the target nodes and infrastructure-reachable nodes that uses the radio resources allocated by the operator after analysing the context information. Indicatively, as more nodes are accepted in the ON, the ON's duration is increased as well.
- The results from the experiments of the second scenario prove that the OneFIT approach efficiently tackles situations, where a specific area of the infrastructure network needs to temporary serve more users than it is designed to, or to solve a congestion situation. The solution to this problem is to create an ON among neighbouring non-congested nodes or to reroute traffic to deployed femtocells that absorb the excess of traffic from the infrastructure, under the requirements and policies stated by the operator after analysing the context and the availability of resources. Validation proved a significant reduction of the average energy consumption in the congested BS, since users have switched to alternative BSs through ONs and a slight increase in the average energy consumption of the non-congested BSs, since they have acquired traffic from the congested one. In addition, a reduction in the energy consumption of a terminal after its attachment to a nearby femtocell is observed due to the fact that less energy is needed in order to communicate with the new serving AP.
- The results from the tests of the third scenario prove that creating Opportunistic Networks in the context of a situation where the operator needs to establish an ad-hoc network for a specific purpose (e.g. provide a proximity service, offload traffic, etc.) using the minimum amount of infrastructure resources is an efficient solution to address such situations. Results also show good QoS values for the D2D links, the efficiency of the spectrum selection algorithms and the feasibility of developing end services specifically designed to run on top of ONs.

- The fourth scenario proposes a situation where a number of closely located users request a set of applications to establish a communication with some entities beyond the service area region. The creation of an ON among these users allow a series of benefits, such as the aggregation of traffic, a reduction on the resource demand or cooperative caching of data. Due to the similarities of these use cases and those of Scenarios 3 and 5, no specific validation of Scenario 4 has been carried out, and most of the conclusions from those scenarios can be extrapolated for the fourth one.
- The results from the validation experiments related to the fifth scenario prove that the OneFIT approach can provide opportunistic resource management in the backhaul side of the infrastructure. Implementation of the OneFIT scenario 5 focuses on wireless mesh networks (802.11 based) since specifics of this networking technology (mesh topology, self-reconfiguration and healing, multi-hop wireless communication among wireless routers, backhaul communication over shared spectrum etc.) provide the most possibilities for cognitive backhaul resource management. Also, these networks can benefit the most (performance gains are most noticeable) from opportunistic backhaul resource management. Performed validation experiments show that the OneFIT system can provide opportunistic backhaul bandwidth aggregation and sharing in wireless mesh networks. Also, the OneFIT system provides context aware selection of infrastructure nodes (wireless mesh network APs, BSs, femtocells etc.) with the goal of providing opportunistic aggregation/virtualization and sharing of backhaul resources (bandwidth and storage).

Finally, this document presents all the insight obtained in the previous synergetic analyses, and states the ultimate conclusions regarding the suitability of the OneFIT concept to address and fulfil the necessities of the Future Mobile Internet, according to the premises of the foreseen business scenarios. These conclusions are the closure of the technical work in the OneFIT project, and a measure of the validity of the concept developed during the life of the project.

## Contributors

First Name	Last Name	Affiliation	Email
Óscar	Moreno	TID	omj@tid.es
José Luis	González	TID	jluis@tid.es
Jordi	Pérez-Romero	UPC	jorperez@tsc.upc.edu
Oriol	Sallent	UPC	sallent@tsc.upc.edu
Alessandro	Raschellà	UPC	alessandr@tsc.upc.edu
Anna	Umbert	UPC	annau@tsc.upc.edu
Jens	Gebert	ALUD	Jens.Gebert@alcatel-lucent.com
Rolf	Fuchs	ALUD	Rolf.Fuchs@alcatel-lucent.com
Panagiotis	Demestichas	UPRC	pdemest@unipi.gr
Andreas	Georgakopoulos	UPRC	andgeorg@unipi.gr
Vera	Stavroulaki	UPRC	veras@unipi.gr
Kostas	Tsagkaris	UPRC	ktsagk@unipi.gr
Yiouli	Kritikou	UPRC	kritikou@unipi.gr
Lia	Tzifa	UPRC	etzifa@unipi.gr
Nikos	Koutsouris	UPRC	nkouts@unipi.gr
Dimitris	Karvounas	UPRC	dkarvoyn@unipi.gr
Marios	Logothetis	UPRC	mlogothe@unipi.gr
Asimina	Sarli	UPRC	Mina.sarli@gmail.com
Aimilia	Bantouna	UPRC	abantoun@unipi.gr
Louisa-Magdalene	Papadopoulou	UPRC	lpapadop@unipi.gr
Aristi	Galani	UPRC	agalani@unipi.gr
Panagiotis	Vlacheas	UPRC	panvlah@unipi.gr
Petros	Morakos	UPRC	pmorakos@unipi.gr
Alexandros	Antzoulatos	UPRC	alexant@unipi.gr
Markus	Mueck	IMC	Markus.Dominik.Mueck@intel.com
Christian	Drewes	IMC	Christian.Drewes@intel.com
Florian	Nehring	IMC	Florian.Nehring@intel.com
Guenter	Moser	IMC	Guenter.Moser@intel.com
Milenko	Tosic	LCI	milenko.tosic@lacidelleing.com
Dragan	Boskovic	LCI	dragan.boskovic@lacidelleing.com
Ognjen	Ikovic	LCI	ognjen.ikovic@lacidelleing.com
Mirko	Cirilovic	LCI	mirko.cirilovic@lacidelleing.com
Seiamak	Vahid	UNIS	s.vahid@surrey.ac.uk
Mir	Ghoraishi	UNIS	m.ghoraishi@surrey.ac.uk
Pega	Stéphane	TCS	stephane.pegas@thalesgroup.com
Bourdellès	Michel	TCS	Michel.bourdelles@thalesgroup.com
Abdoulaye	Bagayoko	NTUK	abdoulaye.bagayoko@necotech.fr
Christian	Mouton	NTUK	christian.mouton@necotech.fr

Dorin	Panaitopol	NTUK	dorin.panaitopol@nectech.fr
Thomas	Delsol	NTUK	thomas.delsol@nectech.fr

## Table of Acronyms

Acronym	Meaning
3G	3 <sup>rd</sup> Generation
3GPP	3 <sup>rd</sup> Generation Partnership Project
ACL	Agent Communication Language
ADC	Analog to Digital Converter
AP	Access Point
BPSK	Binary Phase Shift Keying
BS	Base Station
BT	Bluetooth
BW	Bandwidth
C4MS	Control Channels for the Cooperation of the Cognitive Management Systems
CCK	Complementary Code Keying
CDF	Cumulative Distribution function
CDN	Content Delivery Network
CMON	Cognitive Management system for the Opportunistic Network
CPU	Central Processing Unit
CSCI	Cognitive management System for the Coordination of the Infrastructure
D2D	Device-to-Device
DAC	Digital to Analog Converter
DHCP	Dynamic Host Configuration Protocol
DSM	Dynamic Spectrum Management
E2E	End to End
ED	Energy Detection
eNB	Enhanced Node-B
FIPA	Foundation for Intelligent Physical Agents
FPGA	Field Programmable Gate Array
FTP	File Transfer Protocol
GMSK	Gaussian Minimum Shift Keying
GPRS	General Packet Radio Service
GW	Gateway
HD	High Definition
HDTV	High Definition Television
ISM	Industrial, Scientific and Medical

IP	Internet Protocol
JADE	Java Agent Development
LAN	Local Area Network
MAC	Media Access Control
MF	Matched Filter
MIH	Media-Independent Handover
MILP	Mixed Integral Linear Program
MIMO	Multiple Input Multiple Output
MME	Minimum-Maximum Eigenvalue
MPR	Multipoint Relay
OFDM	Orthogonal Frequency Division Multiplex
OLSR	Optimized Link State Routing
ON	Opportunistic Network
ONE	Opportunistic Network Environment
OneFIT	Opportunistic Networks and Cognitive Management Systems for Efficient Application Provision in the Future Internet
PC	Personal Computer
PD	Probability of Detection
PER	Packet Error Rate
PFA	Probability of False Alarm
QAM	Quadrature Amplitude Modulation
QCI	QoS Class Identifier
QoE	Quality of Experience
QoS	Quality of Service
QPSK	Quadrature Phase Shift Keying
RAN	Radio Access Network
RAT	Radio Access Technology
RF	Radio Frequency
ROC	Receiver Operating Characteristic
RX	Receiver
SISO	Single Input Single Output
SNMP	Simple Network Management Protocol
SNR	Signal to Noise Ratio
SOI	Spectrum Opportunity Index
SoTA	State of the art
SpHO	Spectrum Handover

---

TCP	Transmission Control Protocol
TX	Transmitter
UDP	User Datagram Protocol
UE	User Equipment
USB	Universal Serial Bus
USRP	Universal Software Radio Peripheral
WARP	Wireless Open-Access Research Platform
wCDN	Wireless Content Delivery Network
WLAN	Wireless Local Area Network
WMN	Wireless Mesh Network
WP	Work Package



## Table of Contents

<b>1. Introduction</b> .....	<b>15</b>
<b>2. Description of the validation process</b> .....	<b>16</b>
2.1 Validation scenarios.....	17
2.1.1 Scenario 1 “Opportunistic coverage extension” .....	17
2.1.2 Scenario 2 “Opportunistic capacity extension” .....	17
2.1.3 Scenario 3 “Infrastructure supported ad-hoc networking” .....	17
2.1.4 Scenario 4 “Opportunistic traffic aggregation in the RAN” .....	18
2.1.5 Scenario 5 “Opportunistic resource aggregation in the backhaul” .....	18
2.2 Validation platforms .....	19
2.2.1 Platform 1 “Prototyping platform for the management of opportunistic networks” .....	19
2.2.2 Platform 2 “Opportunistic networking demonstrator” .....	20
2.2.3 Platform 3 “Opportunistic service provision demonstrator” .....	20
2.2.4 Platform 4 “Opportunistic ad-hoc network demonstrator” .....	21
2.2.5 Platform 5 “Prototyping platform for opportunistic coverage extension and related support functions” .....	22
2.2.6 Platform 6 “Direct D2D communication test-bed” .....	24
2.2.7 Platform 7 “Cognitive Radio testbed” .....	25
2.2.8 Platform 8 “Spectrum opportunity identification and spectrum selection test-bed” .....	25
2.2.9 Platform 9 “Open platform wireless mesh network test-bed” .....	28
<b>3. Validation of Scenario 1 “Opp. coverage extension”</b> .....	<b>30</b>
3.1 Set-up of test platforms .....	30
3.1.1 Platform 1 “Prototyping platform for the management of opportunistic networks” .....	30
3.1.2 Platform 2 “Opportunistic networking demonstrator” .....	30
3.1.3 Platform 4 “Opportunistic ad-hoc network demonstrator” .....	31
3.1.4 Platform 5 “Indoor/Office opportunistic coverage extension and related support functions” .....	32
3.1.5 Platform 7 “Cognitive Radio testbed” .....	34
3.2 Obtained results .....	38
3.2.1 Results from platform 1 “Prototyping platform for the management of opportunistic networks” ...	38
3.2.2 Results from platform 2 “Opportunistic networking demonstrator” .....	39
3.2.3 Results from platform 4 “Opportunistic ad-hoc network demonstrator” .....	41
3.2.4 Results from platform 5 “Indoor/Office opportunistic coverage extension and related support functions” .....	43
3.2.5 Results from platform 7 “Cognitive Radio testbed” .....	50
3.3 Results analysis and conclusions .....	67
<b>4. Validation of Scenario 2 “Opp. capacity extension”</b> .....	<b>68</b>
4.1 Set-up of test platforms .....	68
4.1.1 Platform 1 “Prototyping platform for the management of opportunistic networks” .....	68
4.1.2 Platform 2 “Opportunistic networking demonstrator” .....	69
4.1.3 Platform 4 “Opportunistic ad-hoc network demonstrator” .....	69
4.2 Obtained results .....	70
4.2.1 Results from platform 1 “Prototyping platform for the management of opportunistic networks” ...	70
4.2.2 Results from platform 2 “Opportunistic networking demonstrator” .....	72
4.2.3 Results from platform 4 “Opportunistic ad-hoc network demonstrator” .....	73
4.3 Results analysis and conclusions .....	73
<b>5. Validation of Scenario 3 “Infrastructure supported D2D networking”</b> .....	<b>75</b>
5.1 Set-up of test platforms .....	75
5.1.1 Platform 2 “Opportunistic networking demonstrator” .....	75
5.1.2 Platform 3 “Opportunistic service provision demonstrator” .....	75
5.1.3 Platform 4 “Opportunistic ad-hoc network demonstrator” .....	79
5.1.4 Platform 6 “Direct D2D communication test-bed” .....	79
5.1.5 Platform 8 “Spectrum opportunity identification and spectrum selection test-bed” .....	82
5.2 Obtained results .....	85
5.2.1 Results from platform 2 “Opportunistic networking demonstrator” .....	85
5.2.2 Results from platform 3 “Opportunistic service provision demonstrator” .....	88
5.2.3 Results from platform 4 “Opportunistic ad-hoc network demonstrator” .....	95

---

5.2.4 Results from platform 6 “Direct D2D communication test-bed” .....	95
5.2.5 Results from platform 8 “Spectrum opportunity identification and spectrum selection test-bed” .	101
5.3 Results analysis and conclusions .....	107
<b>6. Validation of Scenario 5 “Opp. resource aggregation in the backhaul” .....</b>	<b>109</b>
6.1 Set-up of test platforms .....	109
6.1.1 Platform 9 “Open platform wireless mesh network test-bed” .....	109
6.2 Obtained results .....	115
6.2.1 Results from platform 9 “Open platform WMN test-bed” .....	115
6.3 Results analysis and conclusions .....	120
<b>7. Global conclusions.....</b>	<b>122</b>
<b>8. References.....</b>	<b>124</b>

## List of Figures

Figure 1: Platforms-to-scenarios mapping.....	16
Figure 2: OneFIT scenario 1: Opportunistic coverage extension .....	17
Figure 3: OneFIT scenario 2: Opportunistic capacity extension .....	17
Figure 4: OneFIT scenario 3: Infrastructure supported ad-hoc networking .....	18
Figure 5: OneFIT scenario 4: Opportunistic traffic aggregation in the RAN .....	18
Figure 6: OneFIT scenario 5: Opportunistic resource aggregation in the backhaul .....	19
Figure 7: Opportunistic Networking Demonstrator Overview .....	20
Figure 8: Elements of the demonstration platform.....	21
Figure 9: Protocol stack adaptation .....	22
Figure 10: cognitive radio demonstrator Overview.....	23
Figure 11: WLAN Configuration (Joint channel and access point selection) test-bed Overview.....	24
Figure 12: cognitive radio demonstrator Overview.....	25
Figure 13: Scenario considered in the demonstration .....	26
Figure 14: Implementation of the demonstration scenario by means of USRPs .....	27
Figure 15: Open platform WMN test-bed.....	29
Figure 16: Implementation of scenario 1.....	30
Figure 17: Configuration for the “opportunistic ad-hoc network demonstrator” .....	31
Figure 18: Configuration for “Opportunistic Network Support” .....	32
Figure 19: Configuration for “Multi Homing Support” .....	33
Figure 20: Configuration for “Best Available Connection” .....	33
Figure 21: Spectrum Sensing Setup .....	34
Figure 22: Center Frequencies of Channel 1:14.....	35
Figure 23: Scenario used in testing for spectrum opportunity identification .....	37
Figure 24: Set-up of an external interference source .....	37
Figure 25: Indicative duration of connections .....	39
Figure 26: Percentage of aborted messages.....	39
Figure 27: Throughput and Coverage extension gains .....	41
Figure 28: Sequence diagram of the message exchanges .....	42
Figure 29: Number of exchanged packets .....	43
Figure 30: The three key platform features in the novel SW environment.....	44
Figure 31: The operator policies selected for the operation of the key platform features.....	44
Figure 32: Power consumption on LENOVO X61s without connectivity .....	45
Figure 33: Power consumption on LENOVO X61s with LAN connectivity .....	45
Figure 34: Power consumption on LENOVO X61s with WLAN connectivity .....	46
Figure 35: Power consumption on LENOVO X61s with WLAN shared for 2 TV streams .....	46
Figure 36: Power consumption on LENOVO X61s with 3G Macro BS connectivity .....	47
Figure 37: Power consumption on LENOVO X61s with 3G Femto connectivity .....	47
Figure 38: Variation of power consumption on LENOVO X61s.....	48
Figure 39: Average power consumption on LENOVO X61s .....	49
Figure 40 ROC Curve for Energy Detection.....	51
Figure 41 Energy Detection PD vs. PFA.....	51
Figure 42 Energy Detection PD vs. SNR .....	52
Figure 43 Energy Detection Performance - Varying Lengths (SNR = -10dB).....	52
Figure 44 Energy Detection - Change PFA .....	53
Figure 45 Cyclostationarity based detection - PD vs. SNR .....	53
Figure 46 Cyclostationarity Detection Performance - Varying Lengths.....	54
Figure 47 Matched Filter - PD vs. PFA.....	54
Figure 48 Matched Filter - PD vs. SNR .....	55
Figure 49 Covariance based Detection .....	55

Figure 50 MME based Detection .....	56
Figure 51 Detection Delay vs. Number of Samples.....	57
Figure 52 Blind Technique - PD vs. SNR .....	58
Figure 53 Blind Technique PFA vs. SNR.....	58
Figure 54 Comparison, PD vs. SNR .....	60
Figure 55 Comparison, PD vs. SNR .....	60
Figure 56 Comparison - 2400 Samples.....	61
Figure 57 Performance Comparison ED vs. Blind Technique – 2 Frames .....	62
Figure 58 Comparison ED vs. Blind Technique - For 10 Frames.....	63
Figure 59 ED vs. Blind Technique - PD vs. SNR.....	64
Figure 60 Blind Technique - Probability of False Alarm .....	64
Figure 61 Probability of Missed Detection.....	65
Figure 62 Decision Time .....	66
Figure 63: Implementation of capacity extension through neighbouring terminals.....	68
Figure 64: Implementation of capacity extension through femtocells .....	69
Figure 65: Indicative results from capacity extension through neighboring terminals (no mobility) ..	70
Figure 66: Indicative results from capacity extension through neighboring terminals (mobility level of 2m/s).....	71
Figure 67: Indicative results from capacity extension through femtocells.....	71
Figure 68: Indicative results from capacity extension through femtocells.....	72
Figure 69: Throughput in the capacity extension scenario.....	73
Figure 70: Sensor reporting when the ON is off (above) and when it is established (below) .....	76
Figure 71: Target simulation area .....	77
Figure 72: Demographic configuration .....	77
Figure 73: Screenshot of <b>Chanalyzer Pro</b> .....	80
Figure 74: Screenshot of <b>Ping Test Easy</b> .....	81
Figure 75: Screenshot of <b>CommView</b> for nodes transmit power measurements.....	81
Figure 76: Example of configuration with UE/STA2=AP assumption operating in channel 3.....	82
Figure 77: Considered scenario for testing the spectrum opportunity identification functionality ....	83
Figure 78: Set-up of an external interference source .....	83
Figure 79: Different cases for transferring data between two devices .....	86
Figure 80: Throughput Measurements .....	87
Figure 81: Number of connected nodes .....	88
Figure 82: CO <sub>2</sub> emission measurement.....	89
Figure 83: NO <sub>x</sub> emission measurement .....	89
Figure 84: Fuel consumption measurement .....	90
Figure 85: Generated noise measurement .....	91
Figure 86: Number of connected nodes .....	92
Figure 87: CO <sub>2</sub> emission measurement.....	93
Figure 88: NO <sub>x</sub> emission measurement .....	93
Figure 89: Fuel consumption measurement.....	94
Figure 90: Generated noise measurement .....	95
Figure 91: Initial Topology for WLAN establishment .....	96
Figure 92: Configuration for UE/STA#1=AP assumption.....	97
Figure 93: Configuration for UE/STA#2=AP assumption.....	97
Figure 94: Configuration for UE/STA#3=AP assumption.....	98
Figure 95: Per-link PER for the various configurations .....	100
Figure 96: Measured Spectrum Opportunity Index.....	101
Figure 97: Spectrum Selection under changes in the interference conditions .....	103
Figure 98: Screenshot of Terminal 1 at the start of the ON creation .....	103
Figure 99: Screenshot of the Infrastructure Node at the start of the ON creation .....	103

Figure 100: Screenshot of Terminal 1 after the ON link has been established .....	104
Figure 101: Screenshot of Terminal 1 after switching on the external interferer .....	104
Figure 102: Screenshot of the Infrastructure Node at ON reconfiguration.....	104
Figure 103: Screenshot of Terminal 1 after the ON reconfiguration.....	105
Figure 104: Screenshot of Terminal 2 after the ON reconfiguration.....	105
Figure 105: Results of experiment 1: (a) Random selection, (b) Fittingness factor-based selection .	106
Figure 106: Results of experiment 2: (a) Random selection, (b) Fittingness factor-based selection .	106
Figure 107: Results of experiment 3: (a) Random selection, (b) Fittingness factor-based selection .	107
Figure 108: Results of experiment 4: (a) Random selection, (b) Fittingness factor-based selection .	107
Figure 109: The test-bed used for realization of the scenario 5 use case .....	110
Figure 110 – Set up of the open platform WMN test-bed for validation of the GW selection algorithm .....	111
Figure 111: Test-bed setup for estimation of impact of multipath routing on QoS provided to end users.....	113
Figure 112 – User mobility results in change in request distribution and GW selection .....	115
Figure 113: Average throughput achieved by U1 and U2.....	117
Figure 114: Packet loss percentage suffered by U1 and U2 .....	117
Figure 115: Average jitter on a path for U1 and U2.....	117
Figure 116: Average throughput achieved by U1 and U2.....	118
Figure 117: Packet loss percentage suffered by U1 and U2 .....	118
Figure 118: Average jitter on a path for U1 and U2.....	118
Figure 119 – Jitter levels measured at U4 side .....	119
Figure 120 – Packet loss percentage measured at U4 side .....	120

## List of Tables

Table 1: Average power consumption on LENOVO X61s.....	49
Table 2 Decision Time .....	56
Table 3 Sample and SNR of Sensing Techniques.....	61
Table 4: Test case 1 node distribution .....	78
Table 5: Test case 2 node distribution .....	78
Table 6: Example of Channel Table from Chanalyzer Pro .....	80
Table 7: Experiment assumptions.....	84
Table 8: Activity patterns of the external interference and the ON link .....	85
Table 9: Statistics on connected nodes.....	88
Table 10: Statistics on pollution measurements.....	90
Table 11: Statistics on fuel consumption measurements.....	90
Table 12: Statistics on generated noise measurements .....	91
Table 13: Statistics on connected nodes.....	92
Table 14: Statistics on pollution measurements.....	94
Table 15: Statistics on fuel consumption measurements.....	94
Table 16: Statistics on generated noise measurements .....	95
Table 17: Inputs for proposed AP and Channel selection algorithms.....	99
Table 18: Per-link PER estimation for the various configurations .....	100
Table 19: Spectrum blocks obtained as a result of the spectrum opportunity identification algorithm .....	101
Table 20: Spectrum HO rate for the random selection .....	107
Table 21: Setup and results of the proof of concept experiments for backhaul bandwidth aggregation validation .....	112
Table 22: Experimental setup .....	116

## 1. Introduction

The OneFIT project has developed a complete solution to cope with the challenges of the Future Internet, based on opportunistic and cognitive mechanisms to trigger the creation of ad-hoc, heterogeneous, decentralised, temporal, geographically located and infrastructure-managed networks among user terminals, access points and infrastructure nodes.

To assess the validity of the OneFIT concept, a full Workpackage of the project has been devoted to the development, implementation and testing of a number of platforms and prototypes designed to test the performance of the solution under certain assumptions. This document summarizes the results from all the experiments performed on the platforms and the conclusions that can be extracted about the validation process are presented.

The validation process relies on the business scenarios described in D2.1 [4]. Hence, independent validation tests have been performed and conclusions extracted, for each one of them. These tests have been in turn completed using several different validation platforms, so the results from each one complement each other and a more general view of the performance of the system for every particular scenario has been obtained.

This document is devoted to present the way the validation process has been undertaken, the results that have been achieved and the conclusions that can be extracted from them to assess the validity of the OneFIT project.

## 2. Description of the validation process

This chapter is intended to describe how the validation activities inside the OneFIT project have been carried out, although a thorough description of each platform's implementation details and results can be found in subsequent chapters.

As can be found in deliverable D2.1 [4], five different business scenarios to be validated have been described. Short descriptions of these scenarios are shown below. To carry out these validations, a total of nine testbeds have been developed by different partners, focusing on different aspects of the OneFIT solution (see D5.2 [3] for comprehensive descriptions). Each platform addresses part of the use cases (or all of them) of one or more scenarios. The mapping of validation platforms to scenarios is shown in the following figure:

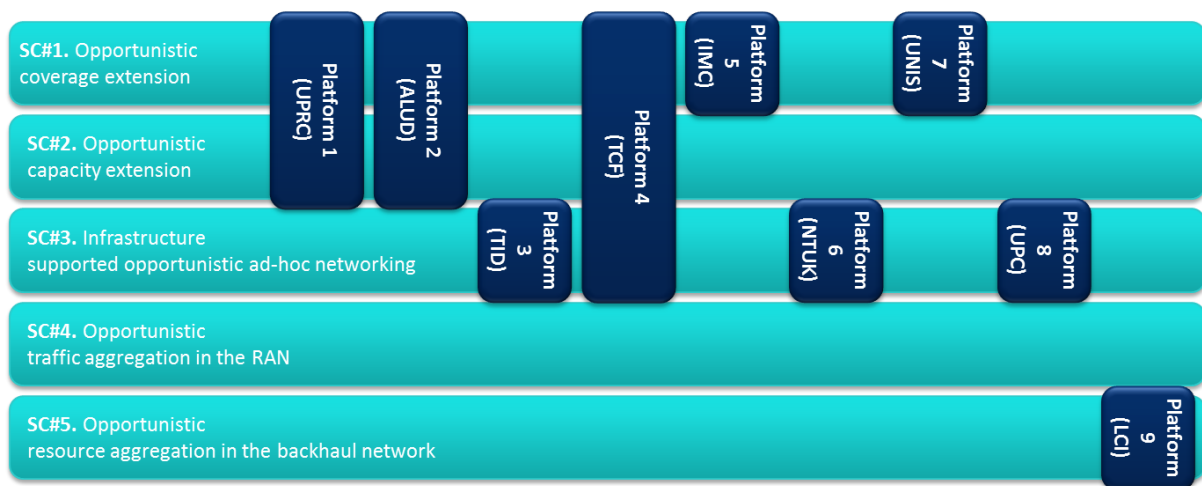


Figure 1: Platforms-to-scenarios mapping

For Scenario 4, there is no platform covering its validation, due mainly to the similarities that can be found among its use cases and those of Scenarios 3 and 5. Therefore, to avoid the duplication of resources devoted to validation, the assessment of Scenario 4 will be performed indirectly via the appropriate results of similar tests.



## 2.1 Validation scenarios

### 2.1.1 Scenario 1 “Opportunistic coverage extension”

In this scenario, one or more devices are outside of the coverage area of the infrastructure, and, subsequently, an opportunistic network is created in order to let them get access to their serving applications. The opportunism of the solution lies in the selection of the participating nodes and UEs (based on geographical, context, profile and policy information) and in the use of the available and most appropriate chunks of spectrum.

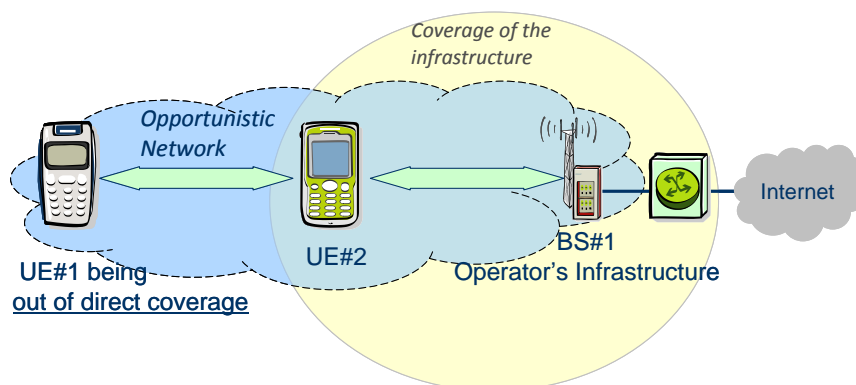


Figure 2: OneFIT scenario 1: Opportunistic coverage extension

### 2.1.2 Scenario 2 “Opportunistic capacity extension”

This scenario depicts a localized area where a traffic hot-spot in some infrastructure nodes is detected and an opportunistic network is created in order to re-route the traffic to non-congested access points (that may or may not be part of the operator’s infrastructure). As in the previous case, the use of context information is key to select the most appropriate set of participating nodes and to opportunistically select the proper spectrum band.

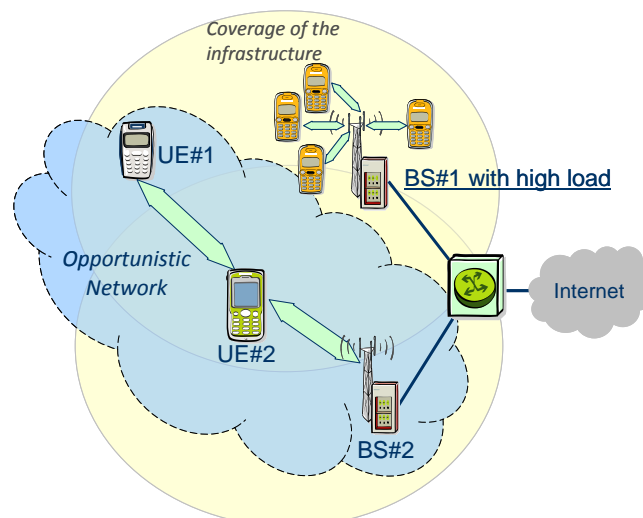


Figure 3: OneFIT scenario 2: Opportunistic capacity extension

### 2.1.3 Scenario 3 “Infrastructure supported ad-hoc networking”

In this scenario, the opportunistic network may be completely infrastructure-less, but still operator-governed. Operator governance is materialized through the provision of resources and policies, and the exchange of information and knowledge on context and profiles. The rationale for creating an

ON in this scenario is to exploit the geographical vicinity of the terminals to provide them a set of services that take advantage of the proximity, the D2D links and the opportunistic context.

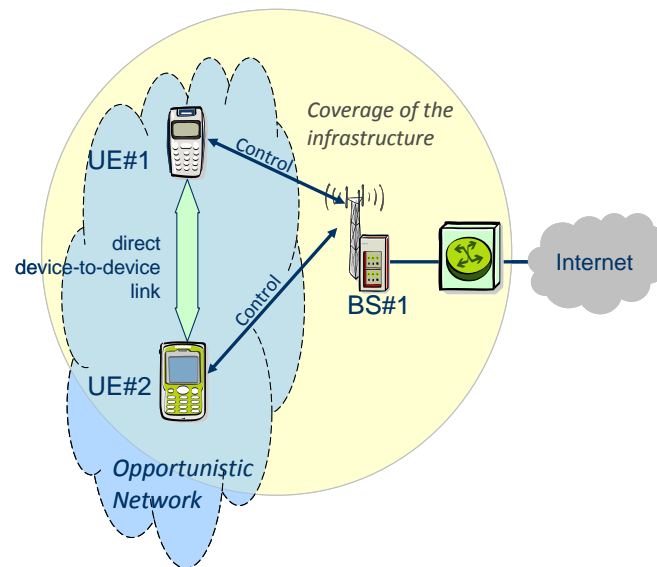


Figure 4: OneFIT scenario 3: Infrastructure supported ad-hoc networking

#### 2.1.4 Scenario 4 “Opportunistic traffic aggregation in the RAN”

In this scenario, there are a number of users in a certain service area region. These users request a set of applications that communicate with entities beyond the service area and that cause a significant demand for resources. Therefore, the operator drives the users region into forming an ON with, at least, one node of the infrastructure that bridges the communications with the remote entities. The ON thus enables the aggregation of traffic to/from multiple terminals, the cooperative caching of data and an improvement on the utilization of networks resources.

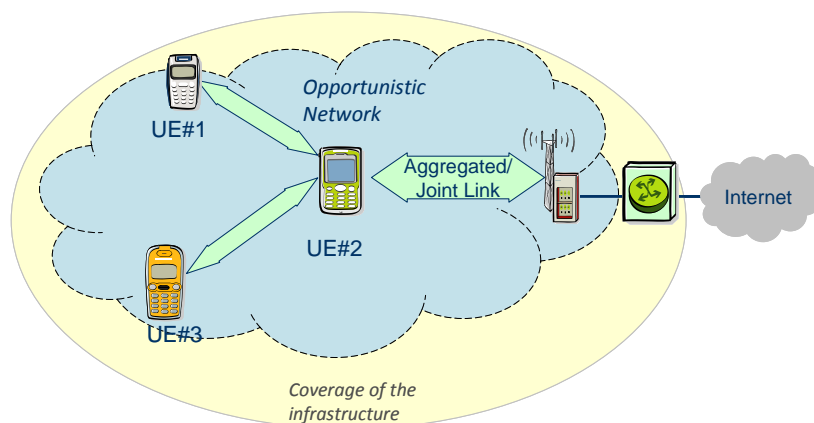


Figure 5: OneFIT scenario 4: Opportunistic traffic aggregation in the RAN

#### 2.1.5 Scenario 5 “Opportunistic resource aggregation in the backhaul”

In this scenario, an ON is created across multiple infrastructure nodes in order to aggregate backhaul traffic and match the bandwidth of wireless access technologies with the adequate bandwidth on the backhaul/core network side. The ON can also be used to gather processing and storage resources across multiple nodes in order to pre-process the traffic data and limit the bandwidth resources needed for its transmission or its storage.

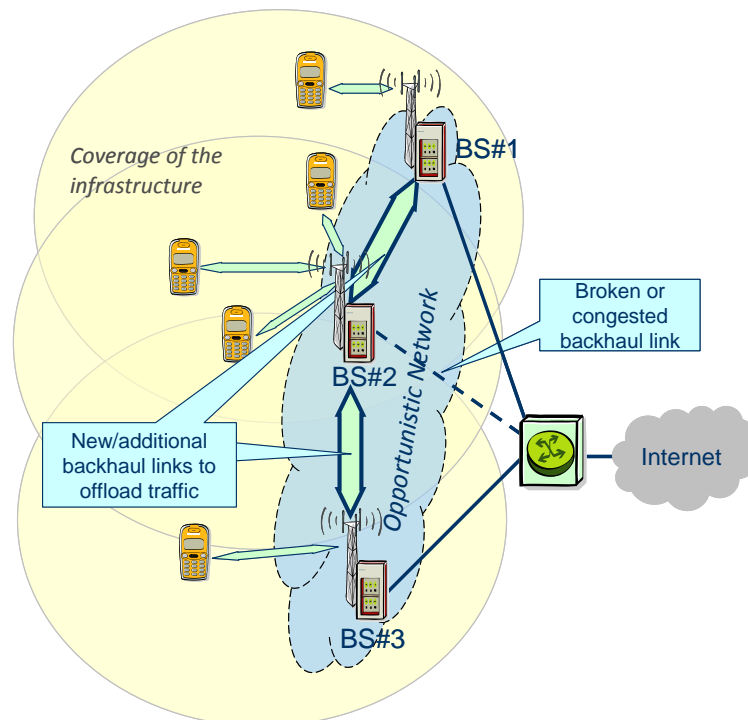


Figure 6: OneFIT scenario 5: Opportunistic resource aggregation in the backhaul

## 2.2 Validation platforms

### 2.2.1 Platform 1 “Prototyping platform for the management of opportunistic networks”

The prototyping platform for the management of ONs is used in order to validate various OneFIT scenarios (by focusing on coverage extension and capacity extension through neighbouring terminals and through femtocells scenarios). Proposed algorithms from WP4 have been implemented in the platform and have been tested in order to provide a proof-of-concept. Also, as part of the platform a modified version of the Opportunistic Network Environment (ONE) simulator [16] is utilized. It has been modified accordingly, in order to include also communication with infrastructure and to integrate our developed JADE [17] prototype so as to enable the exchange of actual FIPA ACL messages [18] among agents. The ONE simulator has been chosen for the experiments due to its inherent capabilities in measuring performance of traditional ONs. It is customizable in terms of traffic generation, mobility of terminals, number of nodes and number of interfaces per node. It is also possible to simulate BS or femtocell entities. The implementation comprises the suitability determination phase, the ON creation phase and the termination phase.

Main implemented functionalities are mapped to the CSCI and CMON as follows:

- The context awareness functional block of the CSCI is responsible for acquiring the status of infrastructure elements and the status of terminals;
- The decision making mechanism of the CSCI is responsible for the identification of terminals that are located in a problematic area (congested or out of coverage) and need access to alternate infrastructure elements through neighbouring terminals;
- The decision making mechanism of the CMON is responsible for the formation of ON paths for each terminal in the congested area that needs to be redirected to alternate BSs and allocates the terminals to alternate BSs;
- The control functional entity of the CMON is responsible for the solution enforcement.

The aforementioned functionalities and the direct mapping to the functional entities of the OneFIT architecture is described also in detail in [3].

### 2.2.2 Platform 2 “Opportunistic networking demonstrator”

The opportunistic networking demonstrator is used to verify the OneFIT scenarios on coverage extension and capacity extension, to verify the architecture [5], to verify the algorithms for the suitability determination, creation, maintenance and release of opportunistic networks [9] as well as to verify the C4MS protocol [6][7].

This prototype consists of several devices, one or more access points and at least one PC hosting the cognitive radio system management functionality on infrastructure side as shown in Figure 7.

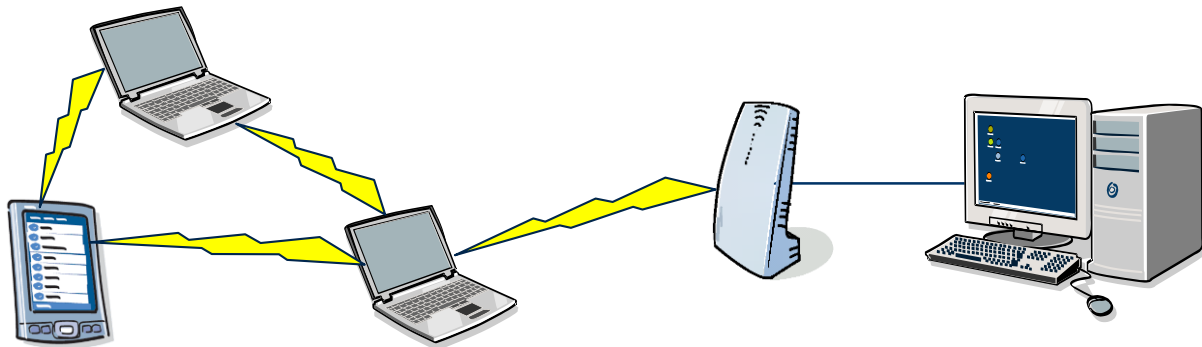


Figure 7: Opportunistic Networking Demonstrator Overview

The most relevant features of this prototype are:

- Use of real terminals supporting different radio access technologies;
- Decisions based on real signal measurements.
- Need for ON occurs due to mobility of users (e.g. moving out of coverage in the coverage extension scenario) or service requirements (e.g. service request for direct device-to-device communication).
- Spectrum Selection: DSM decides on which spectrum to use for the relay (as well as for the access points)
- Reconfiguration: CSCI/CMON triggered switching on and off of the second radio interface of the relaying device, activation/de-activation of the relaying function;
- Mobility procedures: Handover to relay;
- Routing: Update of routing tables after handover;
- IEEE 802.21 MIH based C4MS implementation.

A more detailed implementation description of this demonstrator can be found in D5.2 [3].

### 2.2.3 Platform 3 “Opportunistic service provision demonstrator”

This demonstrator evaluates the feasibility of building novel end-user services that take advantage of the underlying Opportunistic Network capabilities of both infrastructure and user terminals. Therefore, this demonstration does not aim to evaluate the performance of ON procedures and algorithms. Instead, it is assumed that OneFIT mechanisms work, so that an end-user application can be built upon them; after that, service-oriented aspects such as the reliability, the resilience or the scalability of the available tools will be assessed. To that end, an example service has been designed to capitalize on the opportunistic features of the network: a pollution-monitoring service intended for a City Council that needs to control the pollution levels at certain intense traffic areas of the city.

The service relies on the vehicles on-board sensors to send data to a remote server, by means of opportunistic networks created among vehicles in the same area.

A specific test-bed that emulates the behaviour of a high-mobility wireless scenario, where a significant number of nodes enter and exit the ON while it is alive, and the OneFIT mechanisms has been developed. This test-bed is based on a vehicle traffic simulator that uses real cartography with an OneFIT abstraction layer deployed over it. The simulation is therefore split into two different layers: the traffic simulation layer that obtains the position of vehicles and their behaviour over the time and the network simulation layer that evaluates the performance of the ON established over them.

In the test-bed's ONs, mobile nodes are assumed to be the simulated vehicles, which move throughout city streets following certain traffic rules. Fixed infrastructure nodes are located in defined positions and they mimic the features of real 3G base stations. According to the OneFIT architecture and procedures, an ON is created among one or more mobile nodes and one or more infrastructure nodes. In each ON, those vehicles with 3G capabilities act as gateways between non-3G mobile nodes in the ON and the infrastructure nodes. Thus, gateway vehicles will collect all the logs from the surrounding vehicles and send them to the monitoring server.

The network emulation block is the part of the test-bed that mimics the behaviour of the wireless network and the OneFIT mechanisms. In particular, an abstraction layer that simulates the behaviour of the OneFIT-based vehicle-to-vehicle communications has been developed. It consists of a simplified model of the OneFIT procedures that hides the underlying complexity (C4MS protocol stack and specific algorithms). This abstraction layer thus implements the ON management phases in a simplified way: candidate nodes are selected during Suitability Phase; connections will be established during the Creation Phase using a very basic routing scheme; during the Maintenance Phase, nodes entering and exiting the ON will be controlled; and Termination Phase will consist of dissolving the connections.

#### 2.2.4 Platform 4 "Opportunistic ad-hoc network demonstrator"

Demonstration will address the use case of OneFIT's scenarios 1, 2 and 3.

The demonstration platform includes (see Figure 8):

- Network of ad-hoc radio nodes, with Wi-Fi connections, two of them with 2 Wi-Fi/3GPP accesses.
- 3GPP Base stations

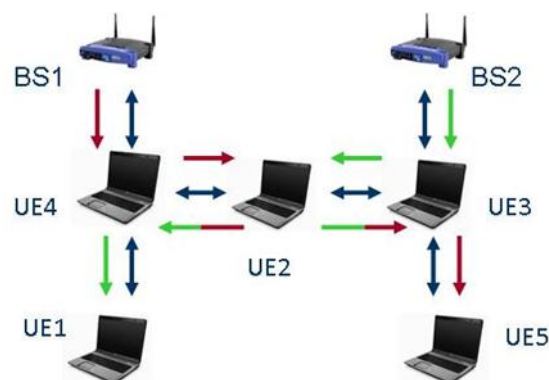


Figure 8: Elements of the demonstration platform

#### Prerequisites

The network (operator governed) has completed the network discovery phase from each other. The proposed algorithms are related to the maintenance phase. In the suitability determination phase, current routing protocols (as DYMO) are used with distance as metric.

The Software/hardware used is:

- Operating system: Linux kernel 3.0.0-12 (Ubuntu 11.10)
- Wi-Fi Cards: Centrino Wireless – N 1000 (Intel)
- Link with BS: 3GPP sticks or Ethernet link or Wi-Fi stick.

#### Implementation of a Virtual Network Interface on the radio nodes

The integration of the new algorithm at network layer has been applied with a modification of the Wifi linux protocol stack, with the definition of adaptors with the application layer, and with the Wifi driver, in order to smoothly integrate new protocols to be tested easily with any kind of applications (as VLC etc...).

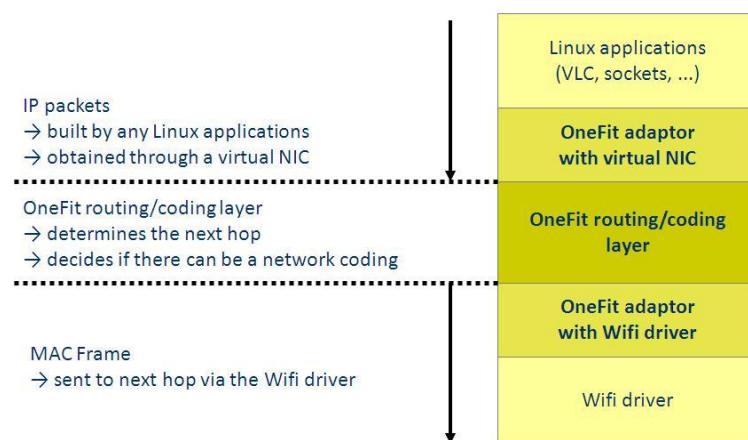


Figure 9: Protocol stack adaptation

#### Thales & NTUK platforms integration

Thales and NTUK integrated their platform with, on one hand the MANET part of the network corresponding to the TCs platform, and on the other hand the femto access part corresponding to the NTUK platform, described in section 2.2.6. In scenario one is described more in detail this platform with the results given in the MANET part of the network.

### **2.2.5 Platform 5 “Prototyping platform for opportunistic coverage extension and related support functions”**

The Prototyping platform for opportunistic coverage extension and related support functions is briefly summarized in the illustration below.

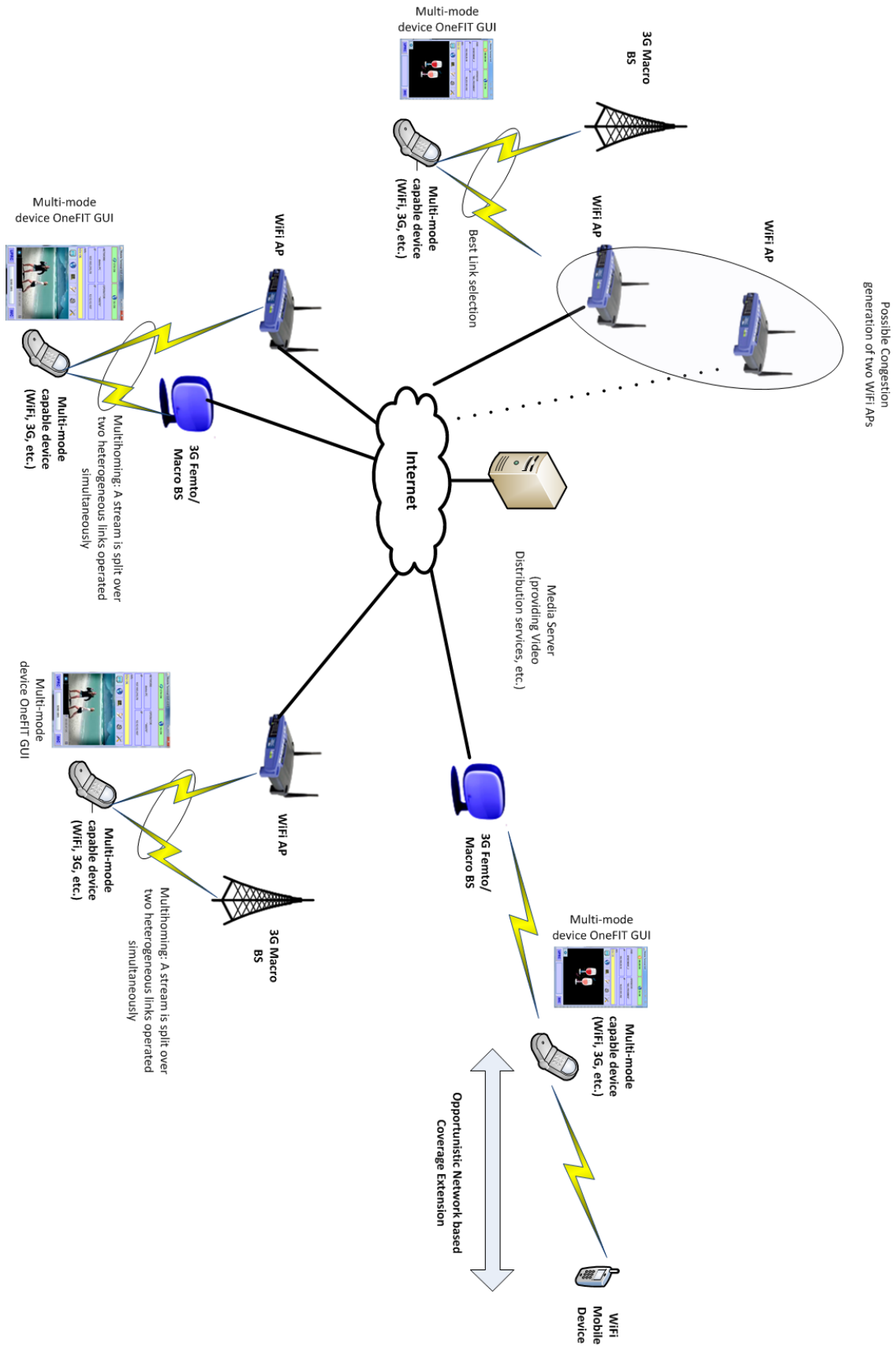


Figure 10: cognitive radio demonstrator Overview

In particular, the various components of the above illustrated platform allow for the following validation steps:

- Opportunistic Coverage Extension via Mobile Device Multi-Hop Communication;
- Congestion creation and detection caused by WiFi Access Points. A congestion detection feature within the Mobile Devices identifies the congestion and redirects the traffic to the most suitable Access Technology.
- Multi-Homing Communication: A data-stream is split over a multitude of Radio Access Technologies, for example over 3G and WiFi. The loss of one single link thus guarantees that the QoS is not entirely lost on the User side. Full QoS can be re-established as soon as the connections to the required links are set-up again.

### 2.2.6 Platform 6 “Direct D2D communication test-bed”

For the demonstration scenario, we considered two Wi-Fi channels and three PCs having both Wi-Fi capability and Access Point (AP) functionality. The PCs were located in different places within an office (Figure 11). Three devices with Wi-Fi capability try to establish a WLAN in order to communicate. An external WLAN manager finds a compliant AP and channel configuration that meets given per-link PER requirements. We consider that there are only two available Wi-Fi channels, so the WLAN Manager should choose between channels #3 and #11. Each device can be used as the AP.

We use “Chanalyzer Pro” of Metageek to visualize the 2.4 GHz band and to make measurements in the different Wi-Fi channels. In order to estimate the transmit power of the devices we use “CommView for Wi-Fi” of TamoSoft. A free software “Ping Test Easy” is used to estimate per-link PER. the evaluation consisted in estimating the PER for each link for each configuration (channel, AP assumption), then to compare the different configurations in order to find the best ones.

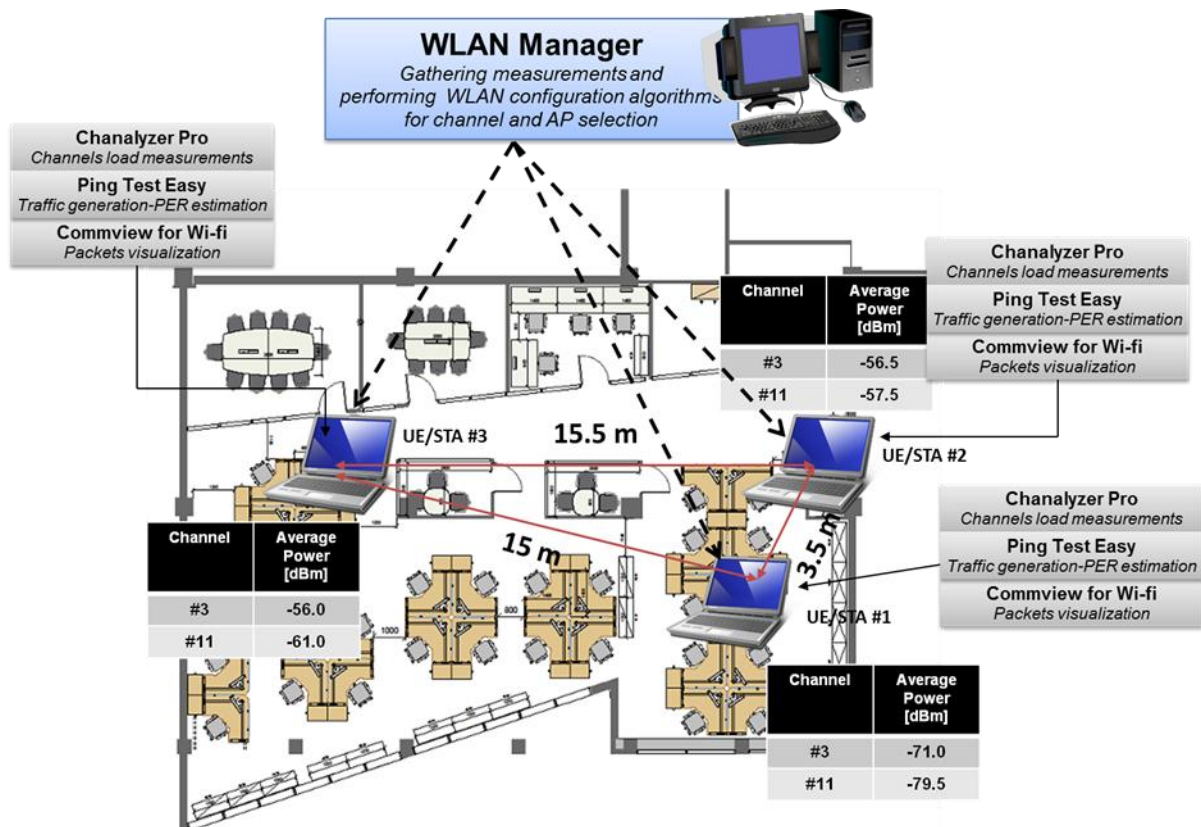


Figure 11: WLAN Configuration (Joint channel and access point selection) test-bed Overview.



### 2.2.7 Platform 7 “Cognitive Radio testbed”

The cognitive radio testbed demonstrator is used to demonstrate sensing and routing in multi-hop extensions of OneFIT scenarios 1 & 2 (coverage and capacity extension). This prototype consists of several devices (WARP boards acting as user devices and AP/infrastructure nodes), one or more access points, two PCs acting as application (i.e. video traffic) source/sink and one PC as controller connected via switch, as shown in Figure 12.

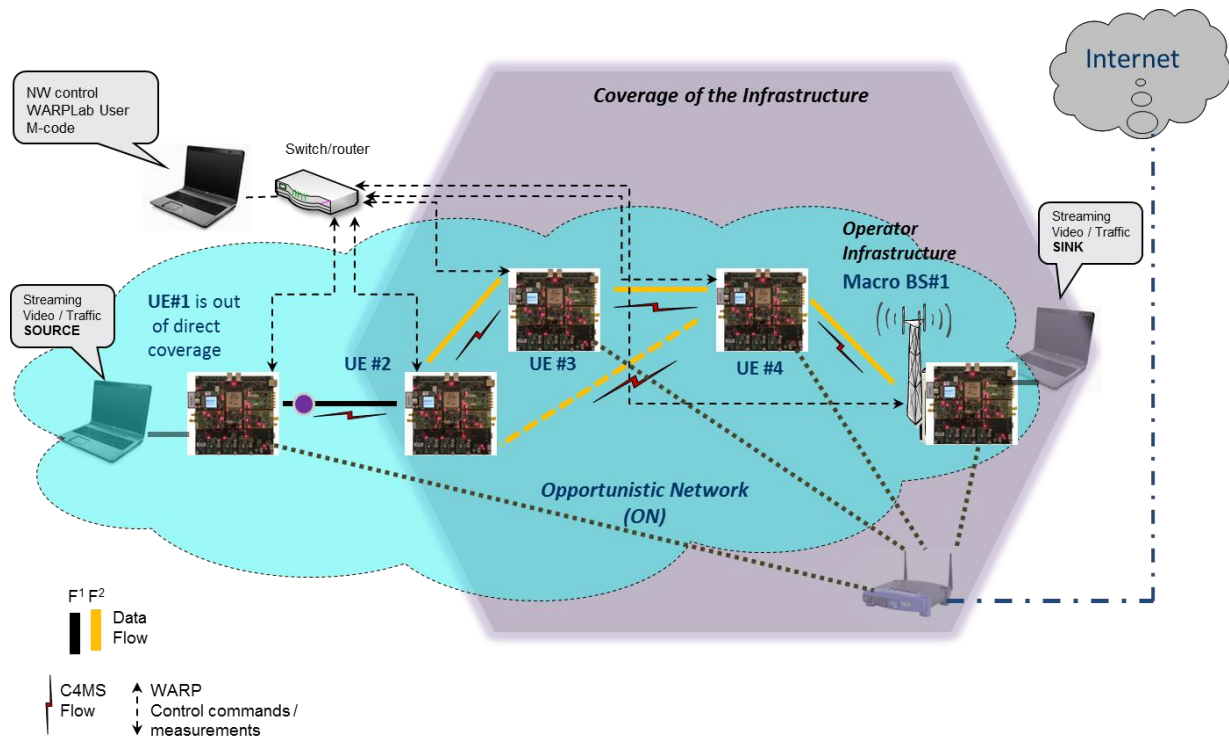


Figure 12: cognitive radio demonstrator Overview

The main features of this prototype are:

- Use of software-radio based nodes;
- Decisions based on real signal measurements.
- Need for ON occurs due to mobility of users (e.g. moving out of coverage in the coverage extension scenario) or service requirements
- Spectrum identification/selection: spectrum sensing techniques identify available opportunities and decides on which spectrum to use
- Reconfiguration: CSCI/CMON triggered switching of the second radio interface of the relaying device, activation/de-activation of the relaying function;
- Routing: setup & update of routing tables

A more detailed description of this demonstrator can be found in D5.2 [3].

### 2.2.8 Platform 8 “Spectrum opportunity identification and spectrum selection test-bed”

The objective of this test-bed is to show the behaviour of the spectrum opportunity identification and spectrum selection procedures in an ON. For that purpose, the “Scenario 3: Infrastructure supported opportunistic ad-hoc networking” [1] is considered where two devices need to communicate through an ON controlled by the infrastructure, as graphically illustrated in the upper

part of Figure 13. Both spectrum opportunity identification and spectrum selection functionalities reside in the infrastructure node, namely in the DSM and the CSCI/CMON entities. The result of executing these functions, with the specific frequency band assigned for the ON link between the two terminals is notified using the C4MS protocol.

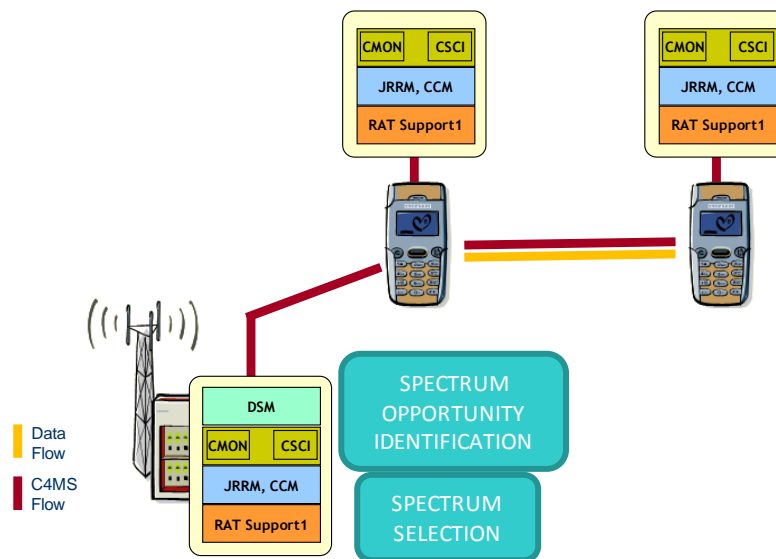


Figure 13: Scenario considered in the demonstration

The hardware and software components of the demonstrator are presented in the following.

### 2.2.8.1 Hardware components of the testbed

The testbed demonstrator is built on the basis of Universal Software Radio Peripheral (USRP) boards [4], which are used to implement the infrastructure node and the terminals, as illustrated in Figure 14 that corresponds to the specific implementation of the scenario in Figure 13. USRP#1 will implement the infrastructure and the associated spectrum identification and selection functionalities, while USRP#2 and USRP#3 are the terminals exchanging data.

Each USRP integrated board incorporates AD/DA Converters (ADCs/DACs), a Radio Frequency (RF) front end, and a Field Programmable Gate Array (FPGA) which does some pre-processing of the input signal. A typical setup of the USRP board consists of one mother board and up to four daughter boards. On the mother board, there are four slots, where up to 2 RX and 2 TX daughter boards can be plugged in. The daughter boards are used to hold the radio frequency receiver and the radio frequency transmitter. There are 4 high-speed 12-bit ADCs and 4 high-speed 14-bit DACs. All the ADCs and DACs are connected to the FPGA that performs high bandwidth math, such as interpolation and decimation. The DACs clock frequency is 128 Ms/s, while ADCs work at 64 Ms/s to digitize the received signal. A USB controller sends the digital signal samples to a PC in I/Q complex data format (4 bytes per complex sample), resulting in a maximum rate of 8 Ms/s. Consequently, the FPGA has to perform filtering and digital down-conversion (decimation) to adapt the incoming data rate to the USB 2.0 and PC computing capabilities. The maximum RF bandwidth that can be handled is thus 8 MHz.

There exist different kinds of daughter boards that allow a very high USRP reconfigurability and working at several frequency bands. The daughter boards integrated in the USRP motherboard of this testbed are *XCVR2450 Transceivers*. They work in the frequency ranges 2.4 - 2.5 GHz and 4.9 - 5.9 GHz.

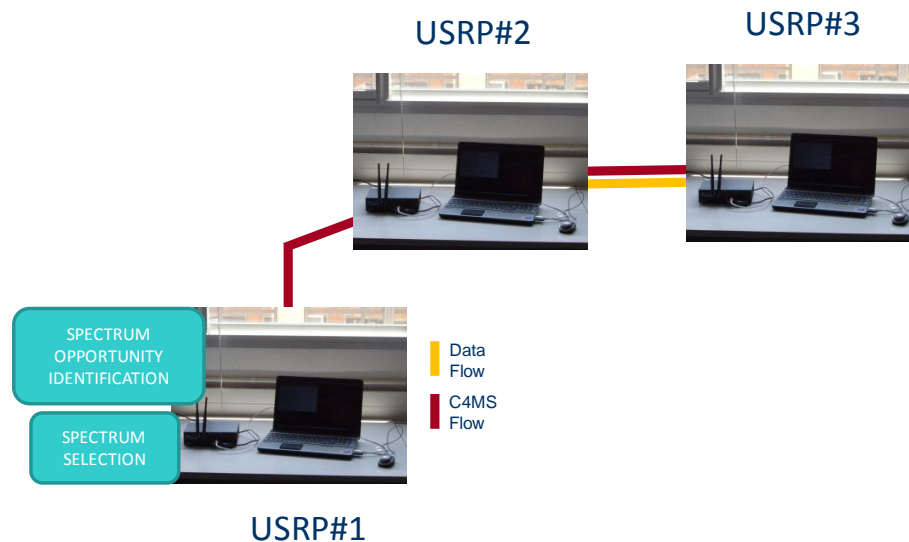


Figure 14: Implementation of the demonstration scenario by means of USRPs

### 2.2.8.2 Software components of the testbed

Identification of spectrum opportunities is performed by both a hardware platform (i.e., USRP) and a software component implemented with GNU Radio toolkit. It is a software for learning about, building and deploying software radios [13]. GNU Radio is free and open source. It provides a library of signal processing blocks and the glue to tie it all together. In GNU Radio, the programmer builds a radio by creating a graph (as in graph theory) where the vertices are signal processing blocks and the edges represent the data flow between them. All the signal processing blocks are written in C++ and Python is used to create a network or graphs and glue these blocks together. GNU Radio has been used to develop the modules that implement the spectrum opportunity and spectrum selection algorithms and to enable the data and control communication between USRP transceivers.

#### Spectrum Opportunity Identification algorithm

The spectrum opportunity identification algorithm executes two different procedures: the measurement procedure and the spectrum block formation.

In the measurement procedure, the total analysed band is subdivided into  $N$  smaller portions of equal band  $\Delta f$ . The measurement algorithm performs an energy detection sensing (during a period of time  $\Delta t$ ) for each  $\Delta f$  portion until measuring the total band, starting from frequency  $F_{min\_band}$ . This measurement is repeated  $Num\_Meas$  times. Then, based on the multiple measurements carried out, the Spectrum Opportunity Index (SOI) is obtained for each portion, defined as the fraction of measurements in which this portion has been detected as available. The power threshold to decide if a portion is free is set based on [14].

In the spectrum block formation procedure, the consecutive spectrum blocks with SOI above a certain threshold are grouped in blocks. Each block is constituted by a maximum of  $P_{max}$  portions. For each block, the algorithm returns the 2-tuple  $SB_k = \{f_k, BW_k\}$  where  $f_k$  is the central frequency of the block and  $BW_k$  the bandwidth.

### Spectrum Selection algorithm

The spectrum selection algorithm uses as input the set of available spectrum pools resulting from the spectrum opportunity identification, together with the characteristics of each pool in terms of available bit rate based on radio considerations. The algorithm output is the list of spectrum assignments to each of the existing links. The algorithm presented in [15] is considered for the implementation in the testbed. It makes use of the fittingness factor concept as a metric to capture how suitable a specific spectrum pool is for a specific radio link. The algorithm is based on estimating the fittingness factor for each link and available spectrum block based on a knowledge database that is maintained with different fittingness factor statistics.

#### **2.2.8.3 Signalling procedures**

Since the target of the demonstration is the spectrum opportunity identification and spectrum selection, the demonstration implements only the ON creation and ON maintenance stages of the ON life cycle. It is assumed that the decision to create an ON among the two devices has been previously made in the ON suitability phase.

The cognitive control channel signalling is implemented with the C4MS protocol using the implementation option based on IEEE 802.21 “Media-Independent Handover (MIH) Services” [8].

The detailed message sequence charts corresponding to the implemented ON creation and ON maintenance procedures were presented in deliverable D5.2 (in particular, see section 3.3.2.1 for the ON creation and 3.3.3.1 for the ON maintenance).

#### **2.2.9 Platform 9 “Open platform wireless mesh network test-bed”**

The open platform wireless mesh network (WMN) test-bed is developed in order to test and evaluate scenario 5 specific use cases from WMN point of view (in unlicensed spectrum). This network technology is identified as one which can benefit the most from opportunistic resource management in the wireless backhaul side of the network. Mesh topology provides many possibilities for resource management through sharing and aggregation.

The OneFIT algorithms [10] “Application cognitive multipath routing in wireless mesh networks”, “Content conditioning and distributed storage virtualization/aggregation for context driven media delivery” and their variants are validated on this platform. Validation experiments for these algorithms are organized in a way which allows validation of the Scenario 5 from WMN perspective.

The OneFIT building blocks (CMON and CSCI logic) are implemented in the centralized network management server. The SNMP protocol is used as a variant of the C4MS (see section 5 of D5.1 [3]) protocol for contextual data gathering and exchange of control messages. The OLSR protocol is used for route discovery and establishment tasks related to the C4MS protocol (see [3]).

The test-bed is shown in Figure 15. It is configured and controlled via a web based dashboard. This dashboard application is used for experiment setup, and presentation of the monitored parameters and experimental results. A more detailed description of the test-bed (and control dashboard) and its role in the OneFIT validation platform can be found in D5.2 [3]. Description of MikroTik router boards, which are used as open platform WMN nodes, can be found in D5.2 [2].

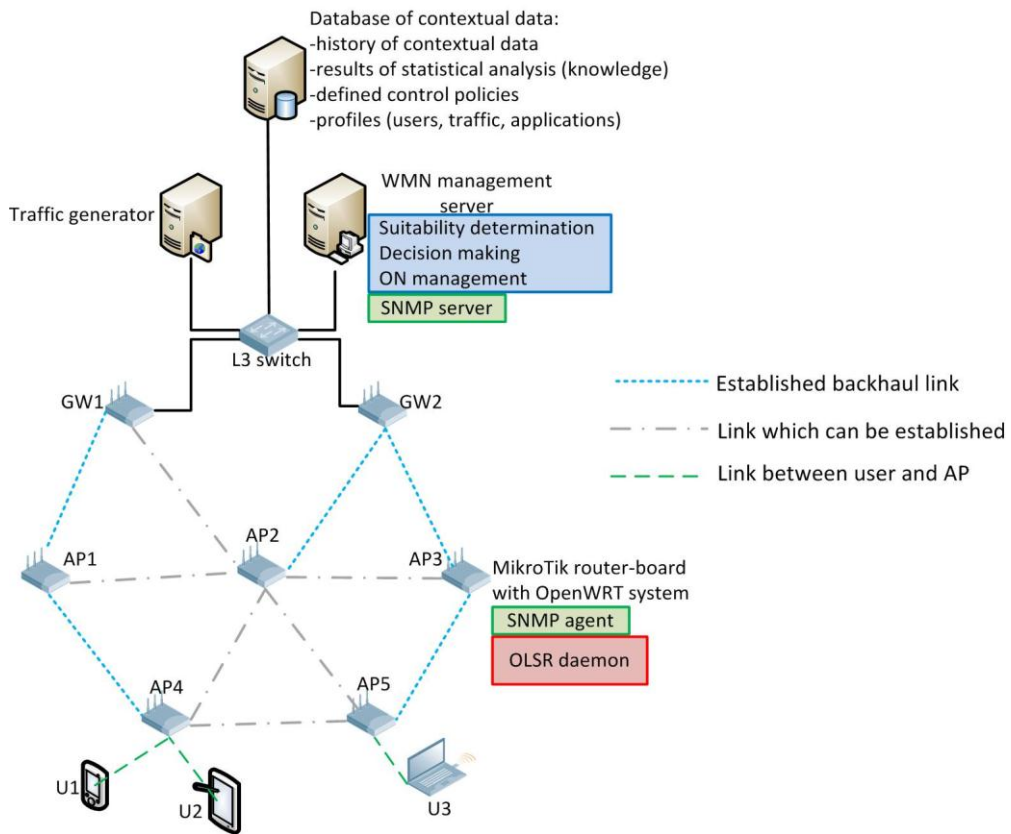


Figure 15: Open platform WMN test-bed

## 3. Validation of Scenario 1 “Opp. coverage extension”

### 3.1 Set-up of test platforms

#### 3.1.1 Platform 1 “Prototyping platform for the management of opportunistic networks”

##### 3.1.1.1 Configuration

According to the provided implementation, a configurable number of infrastructure elements (e.g. base stations) and terminals are available in the environment. Terminals have two available interfaces (namely a 3GPP-based interface to connect to the infrastructure elements of the cellular network and a short-range interface in order to be able to connect between each other). Moreover, the mobility level of each terminal and the traffic/message generation from each terminal are configurable.

##### 3.1.1.2 Test plan

Regarding the scenario 1, initially all simulated base stations are online and ONs are not needed yet, since terminals are connected directly to the infrastructure. As soon as a base station goes offline (e.g. due to a failure), terminals which have the ability to connect to neighbouring terminals will connect to each other in order to gain to a nearby base station. The aforementioned approach is visually represented in the figure that follows. In Figure 16a infrastructure elements are online and ONs are not needed yet. In Figure 16b, a base station goes offline (e.g. the centre one, as presented in the figure) and terminals which are near to other terminals with connection to an alternative base station will form an ON, in order to gain access to the neighbouring base station. As soon as the base station goes online, the ON is not needed anymore and it is terminated.

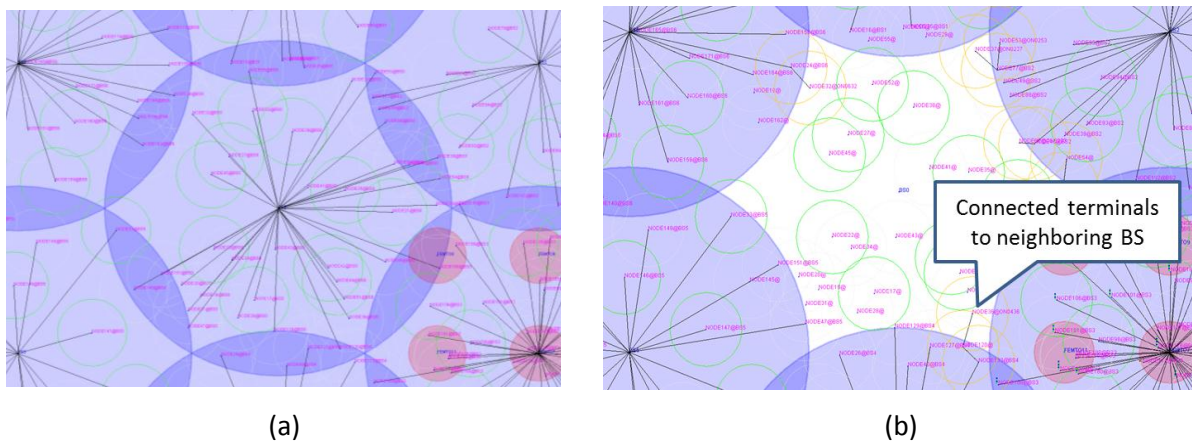


Figure 16: Implementation of scenario 1

#### 3.1.2 Platform 2 “Opportunistic networking demonstrator”

##### 3.1.2.1 Configuration

At the beginning of this scenario, all devices are directly connected to one of the infrastructures access points or base stations. All relaying functions are inactive.

The devices send their capabilities via C4MS to the infrastructure. Further on, all devices are sending periodic and/or event based measurements (e.g. received signal strength) to the infrastructure.

##### 3.1.2.2 Test plan

One of the terminals is now moving out of coverage of the infrastructure.

First, the test is made with the opportunistic networking feature being disabled. By moving through the environment, the area is determined where coverage is available and where coverage is lost. A map is created manually showing coverage, and, when being in coverage, showing average signal strength and throughput at a given place.

Then the test is made with the opportunistic networking feature being enabled. By moving again through the environment, the same signal strength and coverage can be observed. However, when moving out of coverage, a trigger (measurement report) is sent from the device to the infrastructure that coverage may be lost soon.

This event triggers the suitability determination in the infrastructure to find at least one terminal being able to act as relay to support the device moving out of coverage. A detailed description of this algorithm can be found in D4.2 [10]. When an ON was created with a suitable device, the coverage is extended. The map described above is now updated to show coverage, average signal strength and throughput at a given place with opportunistic networking being enabled.

The map shows then coverage and throughput for both cases, ON disabled and ON enabled and the area in which the coverage is extended can be visualised as well as throughput gains at the cell edge.

### 3.1.3 Platform 4 “Opportunistic ad-hoc network demonstrator”

#### 3.1.3.1 Configuration

The configuration targeted is the following:

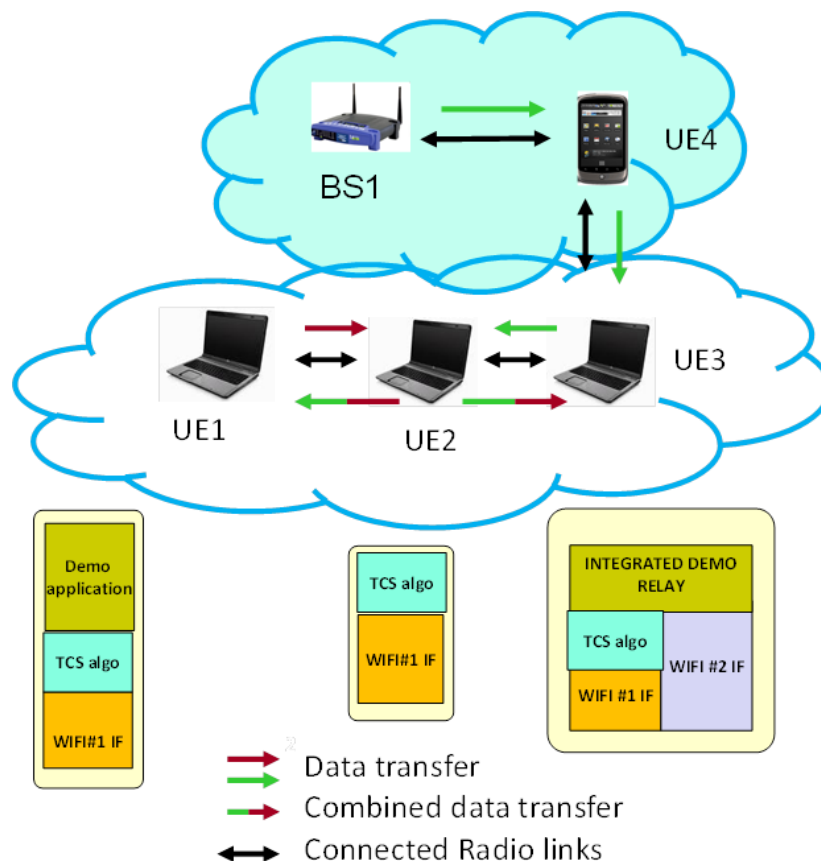


Figure 17: Configuration for the “opportunistic ad-hoc network demonstrator”

The configuration is based on user equipment in ad-hoc mode (part of the TCS platform) and one of these user equipment connected with a specific wifi connection to a mobile, itself able to connect to a base station. The scenario offers the execution of different traffic flows, implying data transfer

from/to the UE in the ad-hoc part of the opportunistic network to the infrastructure part. These flows offer topological situation the multi-flow algorithm co-determination may be applied.

### 3.1.3.2 Test plan

The proposed optimization algorithms will be validated:

- By the measurements of the throughputs circulating within the radio nodes, using supervision tools as Wireshark [25].
- By the evaluation of the traffic overhead in terms of new control messages sent and information included on the IP packets.

## 3.1.4 Platform 5 “Indoor/Office opportunistic coverage extension and related support functions”

### 3.1.4.1 Configuration

In order to validate and exploit this platform component, the three implemented key features are tested, validated and exploited for further (power based) measurements:

- Opportunistic Network Support;
- Multi Homing Support;
- Best Available Connection.

#### Configuration for “Opportunistic Network Support”:

In this configuration, a multi-hop communication is set-up – it illustrates future operators’ features which enable a multi-hop based extension of the available network coverage.

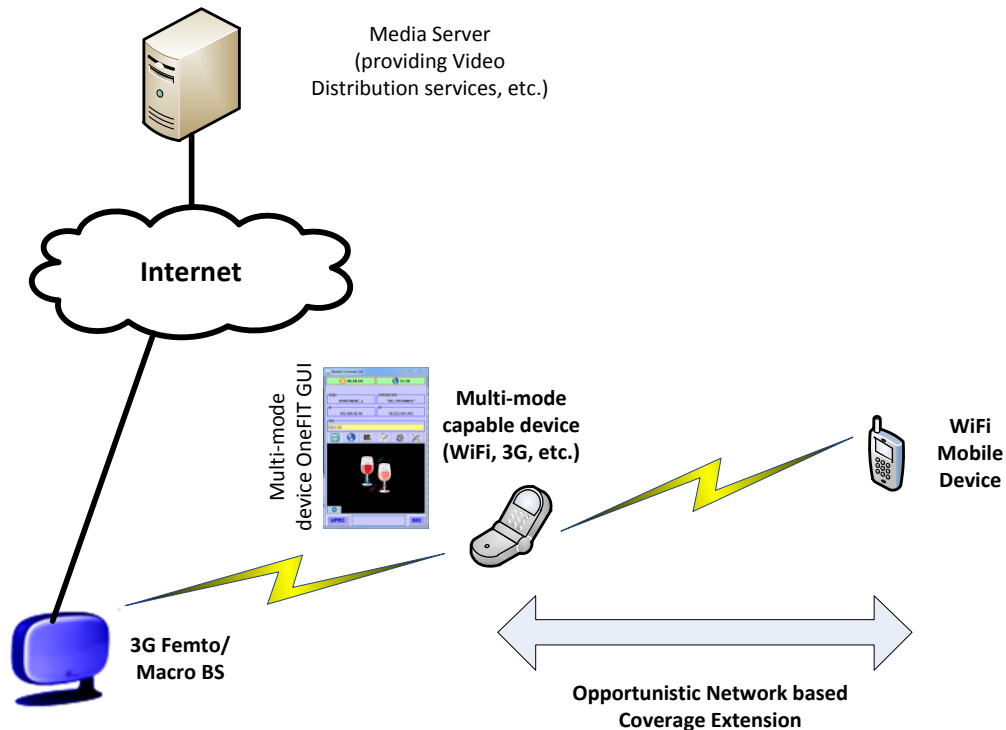


Figure 18: Configuration for “Opportunistic Network Support”.



Configuration for “Multi Homing Support”:

In this configuration, a multi-RAT communication is set-up – it illustrates future features which enable the user to fully exploit the entire heterogeneous radio context. In particular, the split of a Video stream is illustrated over simultaneously operated RATs.

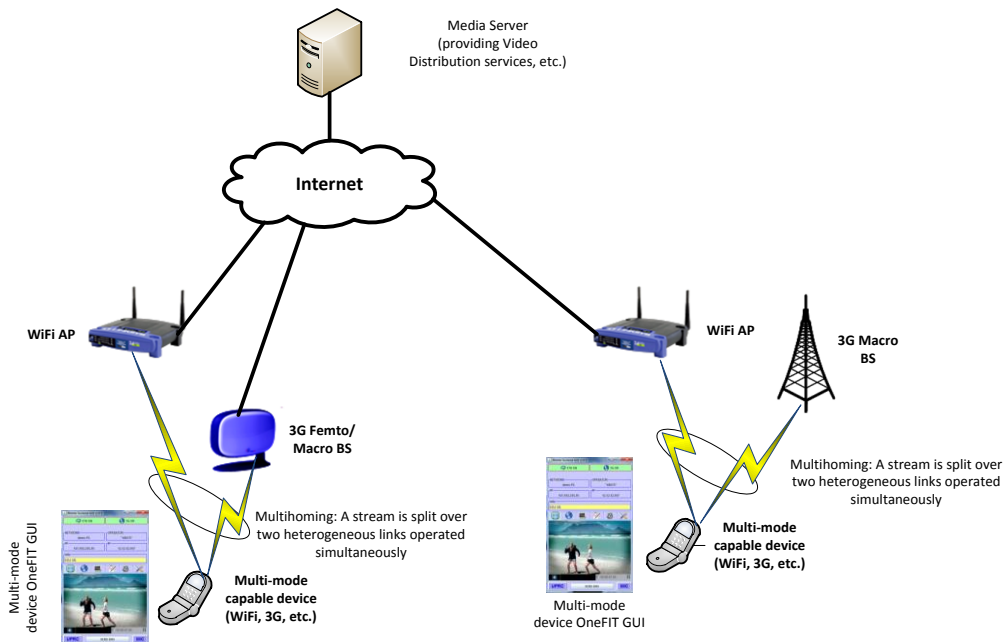


Figure 19: Configuration for “Multi Homing Support”.

Configuration for “Best Available Connection”:

In this configuration, the best available connection is used, exploiting in particular an automatized congestion detection mechanism.

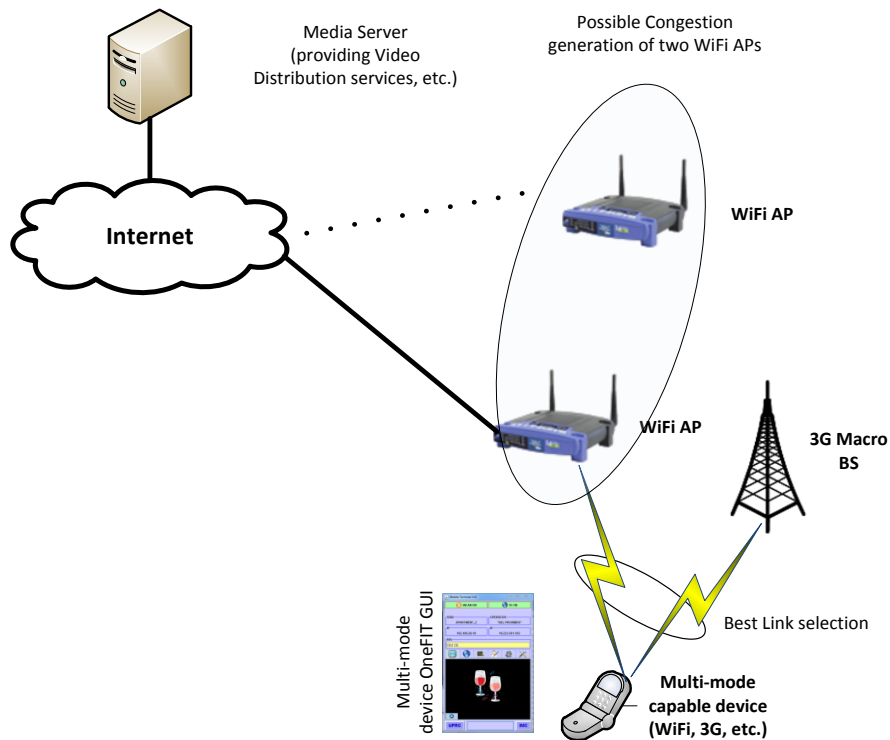


Figure 20: Configuration for “Best Available Connection”.

### 3.1.4.2 Test plan

The test plan mainly foresees two parts:

- Functional verification of the upper configurations;
- Power Measurements in order to acquire Power Consumption indicators for various configurations.

### 3.1.5 Platform 7 “Cognitive Radio testbed”

Validation of platform followed two phases: In the initial phase, task of performance evaluation of spectrum sensing techniques is considered where stand-alone SoTA sensing techniques are developed, deployed and tested on WARP nodes. In the second phase, network-layer functionality (LINUX + drivers) is introduced/added to WARP platforms and a demonstration of scenario #1 + routing in multihop is considered.

#### 3.1.5.1 PHASE i Platform

Accurate spectrum sensing is a prime requirement for opportunistic spectrum use for cognitive radio technology. Cognitive radios are required to monitor the spectrum for any vacant band to operate and Spectrum Sensing is considered a key enabling technology for cognitive radios. In this part, we provide a comparison of six state-of-the-art spectrum sensing techniques using WARP-based cognitive radio test-bed. These techniques are

- Energy based detection
- Matched Filter based detection
- Cyclostationary feature based detection
- Minimum/Maximum Eigen value based detection
- Covariance based detection
- Blind detection

The following sections discuss in the detail the setup/configuration and methodology used to conduct the comparison of spectrum sensing techniques.

#### 3.1.5.2 Configuration

The setup used is depicted in Figure 21 below. The required bit streams can be downloaded to the WARP board using the Xilinx tools. Most of the WARPLab functions work with 1x1 SISO as well as 2x2 and 4x4 MIMO setup. For this phase, only one transmitter and one receiver are required so the SISO model and functions are used. This configuration can be easily extended to use more than one receiver.

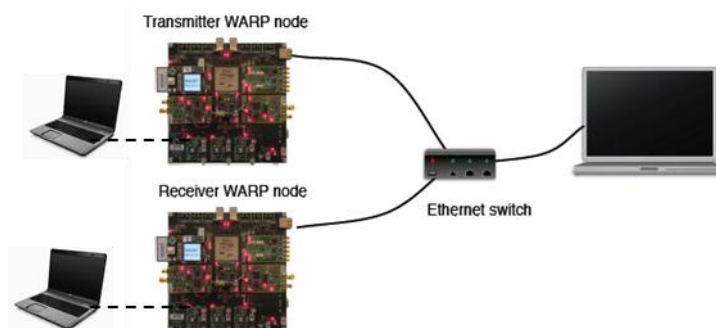


Figure 21: Spectrum Sensing Setup

For a spectrum sensing setup, the objective was to communicate with the boards and perform spectrum sensing on WARP boards. A few key parameters for the spectrum sensing experiments are briefly described below.

### Carrier Channel

The first parameter is the carrier channel. WARP board can be tuned to one of the 14 available carrier channels. The antenna that comes with the WARP kit is matched to 2.4GHz. Each band is 22MHz wide. The figure below shows the center frequencies of each band.

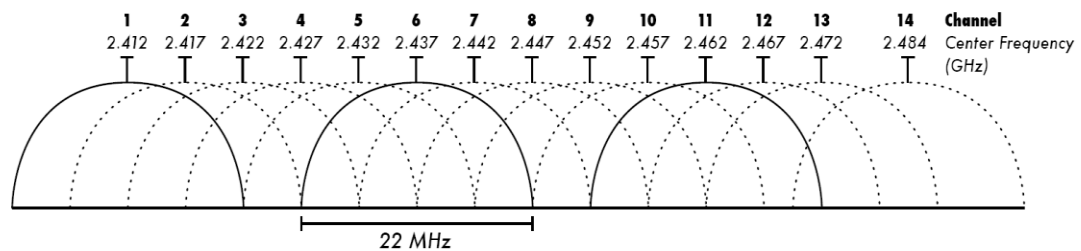


Figure 22: Center Frequencies of Channel 1:14

### IQ/Rate

The default WARP hardware clocks the ADCs and DACs at 40MHz. The WARPLab reference design generates and captures raw I/Q samples at 40MHz; it applies no digital filtering or rate change. The transmitter and receiver buffers for each radio hold  $2^{14}$  samples, so each over-the-air cycle lasts  $\sim 400\mu\text{s}$  which is  $(2^{14} \text{ samples}) / (40\text{e}6 \text{ samples/sec})$  [21]. For the experiments random data was generated which was then mapped to BPSK, QPSK, QAM symbols. The signal occupied 20MHz bandwidth.

### Transmitter Gain

Transmitter gain is applied at two stages, at the baseband level and the RF level. The baseband gain can be set by choosing a value from [ 0 : 3 ], which is 1.5dB/step. The RF gain can be set by choosing a value from [ 0 : 63 ], which is 1dB/step. The dB per step value is a rough estimate provided in the WARP documentations. For the experiments transmitter gain was setup at low-moderate values, as both the transmitter and receiver were in door. When set at the maximum gain, transmitted power is roughly about 20dB.

### Receiver Gain

Receiver gain can also be applied at two stages, at the baseband level and the RF level. The baseband gain can be set by choosing a value from [ 0 : 31 ], which is 2dB/step. The RF gain can be set by choosing a value from [ 1 : 3 ], which is 15dB/step. For the experiments RF receiver gain was always set to 1, which is the lowest setting. The baseband gain was varied as per requirement. Gains were adjusted to have the desired signal to noise ratio.

### Auto Gain Control

WARP boards can work on Automatic Gain Control or Manual Gain Control. For the experiments, manual gain control was selected.

### Buffer Size

Each daughter card has a buffer which can store up to  $2^{14}$  samples. For each instance the required number of samples required were written to the transmitter and transmitted. At the receiver side the transmission was captured and samples were stored in the buffer for reading later. The testing

for standalone techniques were done by choosing various sample sizes. Firstly the minimum sample size on which a technique will give probability of detection = 90% for a given SNR. The results will be discussed in the later chapters. It was however observed that for some of the techniques sample size is important for good performance, whereas for others it didn't make much of a difference.

#### SNR Setting

The signal to noise ratio was maintained in two ways:

- The receiver gain was adjusted manually so that the signal strength is equal to the transmitted power. Noise was added at the receiver before the decision block. For comparison with the simulation results, this method was used.
- No noise was added in the receiver block. The SNR settings were controlled by adjusting the transmitter gain. For ROC curves this method was used.

#### **3.1.5.3 Spectrum Sensing on WARP**

After testing for correct setup for transmission, reception and signal strength measurement, next step is to integrate the standalone sensing techniques in the communication system framework. A total of six techniques are evaluated. Once the WARP nodes are configured, random data sequence is generated, modulated and sent over the carrier channel. The raw receiver data is read from the WARP board and sensing technique is applied to make the decision of presence or absence of the signal.

#### **3.1.5.4 Test plan**

The test plan for this phase consists of one test:

##### Test 1: Evaluations of the sensing techniques

The purpose of this test is to evaluate each of the six sensing techniques based on the following criterion:

- Probability of Detection
- Probability of False Alarm
- Probability of Missed Detection
- Decision Time
- Complexity/Robustness

#### **3.1.5.5 PHASE ii Platform**

In the second phase, network-layer functionality (LINUX + drivers) is introduced/added to WARP platforms and a demonstration of ON-formation in scenario #1+ routing in multihop is considered.

#### **3.1.5.6 Configuration**

##### Configuration for test #2 - Spectrum opportunity identification/selection

The indoor office scenario illustrated in Figure 23 is considered. The location where the testbed is situated has coverage via 3 WiFi access points (AP2, AP3 and AP4) that occupy channels at 2.412, 2.437 and 2.462 GHz. The testbed with the ON is located in room marked "tesbed".

To test the spectrum sensing/opportunity identification algorithm, the measurement procedure considered the total band from 2.4 GHz to 2.5 GHz divided in 1000 portions of 100 kHz. Different sensing techniques are used for sensing each portion during 100 ms. The detection threshold is set for a PFA (false alarm probability) of 1%.

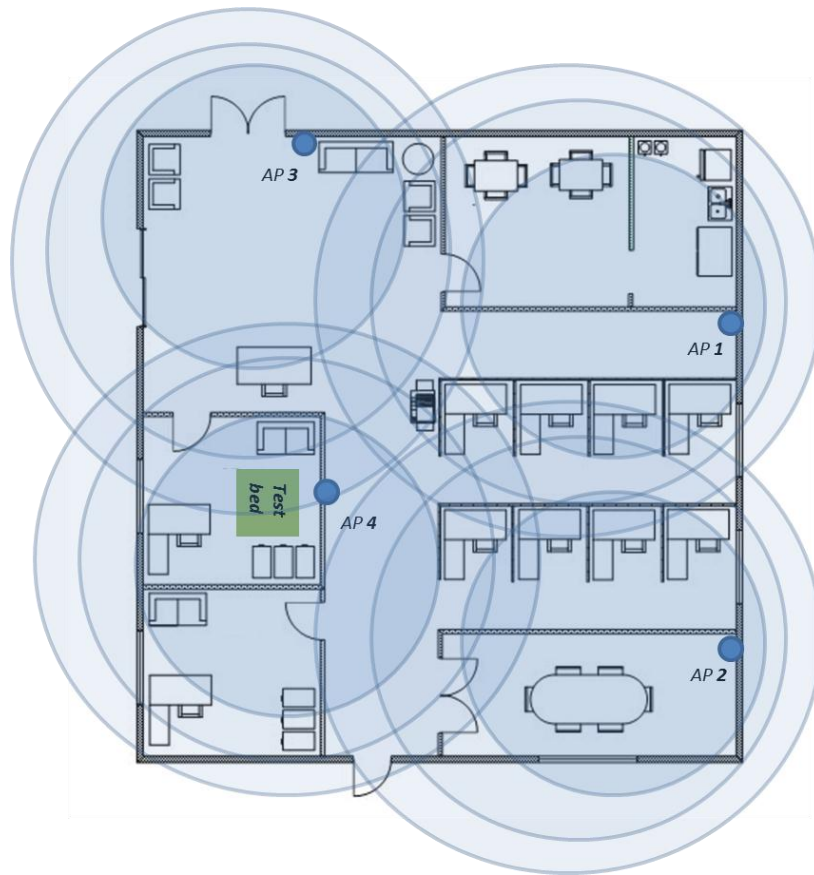


Figure 23: Scenario used in testing for spectrum opportunity identification

Configuration for Test 3 - Demonstration of ON formation [ONEFIT scenario #1, use-case 1 - ON phases 1, 2].

The configuration for this test is shown in Figure 24. Once the spectrum is assigned, OLSRd on UE#1 starts route setup procedure towards destination i.e. BS#1 via UEs 2, 3 and 4 acting as relays. Once a route is established, data transmission begins. In this test, an additional AP is introduced as an interference source that can be manually configured in the spectrum block allocated to any of the links, as shown in Figure 24.

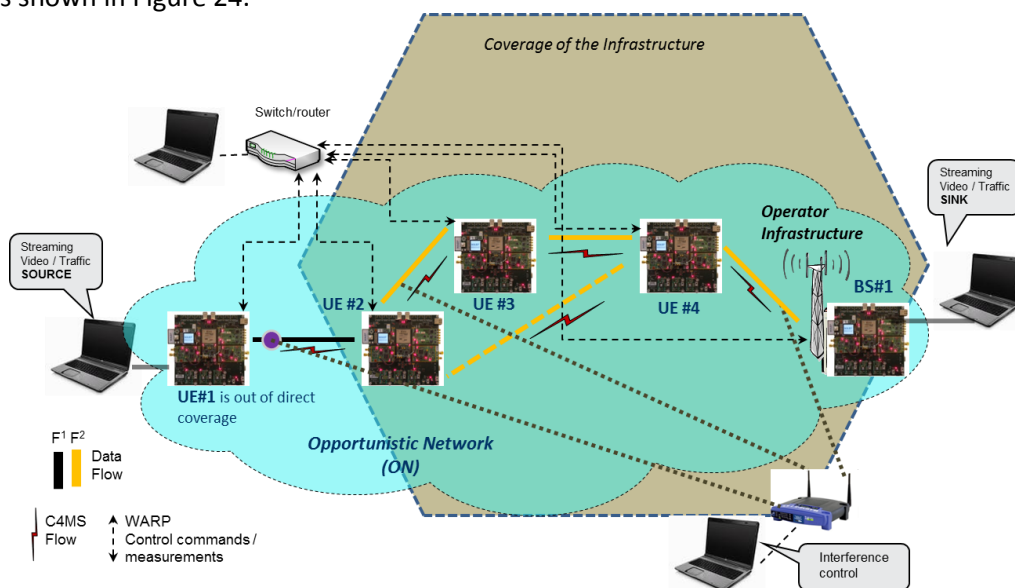


Figure 24: Set-up of an external interference source

Setup Scenario 1, UC 1:-

- All UEs are operating in 2.4 GHz ISM band.
- “out-of-coverage” UE#1 is operating @ F1;
- All “in-coverage” UEs (2, 3, 4, & BS#1) operating @ F2.
- With suitability-determination & creation phases conducted successfully, UE#2 (edge relay node) second radio interface (towards UE#1) is required to switch/operate on F1, so E2E path can be established and video session (UE#1 > BS#1) can be started.

#### Configuration for test #4 - Reactivity/adaptation of routing algorithm to interference

The configuration for this test is shown in Figure 24 (similar to test 3).

### **3.1.5.7 Test plan**

The test plan for this phase consists of:

#### Test 2: Spectrum opportunity identification/selection

This test aims to evaluate the behaviour of the spectrum opportunity identification algorithm.

#### Test 3: Demonstration of ON formation [ONEFIT scenario #1, use-case 1].

The purpose of this test is to show ON-formation.

#### Test 4: Reactivity/adaptation of routing algorithm to interference, node/link loss - ON phase 3.

The purpose of this test is to examine the adaptability of standard OLSR (a link-state based proactive protocol) to changes in link-level channel availability (due to interference or mobility or power-down). For this purpose:

- A relay node is powered down. The target of the test is to show re-routing is initiated, new E2E path is established (following some delay) and application/video stream can resume after minor disruption/delay. With UE#3 powered down, the original path (1-2-3-4-BS) is changed to: 1-2-4-BS.
- An external interference source is activated to operate on the same frequency as that of the ON links. The target of the test is to show that operation of standard routing protocols that remain unaware of channel availability at link-level can result in route updates/re-routing and the corresponding control signalling overheads.

In the case of OLSR, changes in the neighbourhood of a node are detectable. For instance, MPR set is re-calculated whenever a neighbour appearance / loss is detected or when changes in the 2-hop neighbourhood are detected. Upon such changes, the routing tables are re-calculated which does not incur additional control overheads by itself however, new TC messages are issued due to changes in topology and topology table is updated.

The main metrics considered are:

- Packet delivery ratio (application throughput), packet loss, jitter
- # of re-routing attempts

## **3.2 Obtained results**

### **3.2.1 Results from platform 1 “Prototyping platform for the management of opportunistic networks”**

For the evaluation of scenario 1 a specific algorithm has been developed (“selection of nodes through a fitness function” as described in the deliverables of WP4). A customized version of the ONE [16] simulator has been utilized in order to obtain results. Figure 25 illustrates the indicative

duration of connections in static nodes (subject to their energy level). As the figure suggests, as more nodes are accepted in the ON, an increase of the ON's duration may be observed.

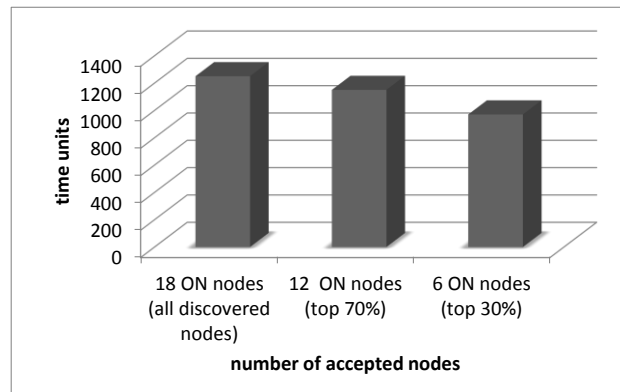


Figure 25: Indicative duration of connections

Moreover, Figure 26 illustrates the percentage of aborted messages with respect to the number of accepted ON nodes. As the figure suggests, as more nodes are accepted in the ON, an increase in the percentage is observed since it is more likely to experience a failure in a link. Also, the number of aborted messages corresponds to the messages which are dropped due to a link drop at the moment of their transmission (so the message is not successfully transmitted to the receiving node).

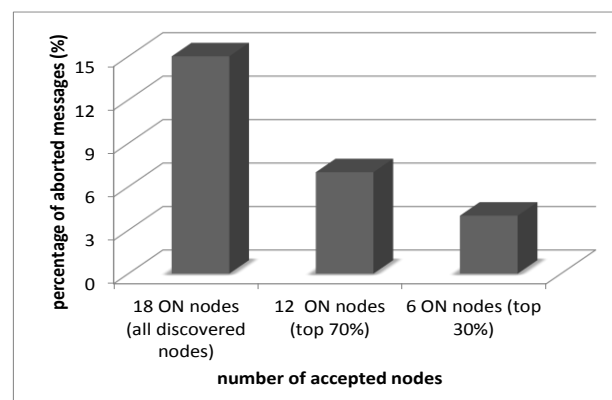


Figure 26: Percentage of aborted messages

## 3.2.2 Results from platform 2 “Opportunistic networking demonstrator”

### 3.2.2.1 Proof of Algorithm for Suitability Determination and ON Creation

D5.2 [3] Section 3.3.1.1 describes an algorithm for the suitability determination for the coverage extension scenario. With the opportunistic networking demonstrator, it was proven that this algorithm detects situations where a device is going out of coverage. The algorithm uses configurable thresholds on signal strength or alternatively on estimated throughput on when to detect a going out of coverage situation. One challenge is to define these thresholds in such a way that an ON is not created too early in order to save resources but also that an ON is not created too late to avoid service interruptions.

Further on, the opportunistic networking demonstrator is used to verify the procedures for ON Creation and Release. These procedures include the reconfiguration of a device to provide a relaying function and a handover procedure for the mobile going out of coverage towards that relay.

If a service will continue seamlessly after ON Creation depends on the relaying and mobility mechanism:

- If the Relay works as L2-Relay and performs a bridging of the messages, the device going out of coverage keeps its IP Address and the service will continue seamlessly.
- If the Relay works as L3-Relay without mobility procedures, the Relay usually includes a DHCP Server and creates an own IP-Subnet. In this case, the device going out of coverage will get a new IP-address after the ON creation and an on-going service is likely to be interrupted.
- If mobility procedures like the GPRS Tunnelling Protocol defined by 3GPP or Mobile IP are used, then seamless service continuity is also possible with a L3-Relay.

### 3.2.2.2 Signalling Evaluation

The Opportunistic Networking Demonstrator is also used to evaluate the C4MS signalling for the different scenarios.

This section gives a short summary on the signalling evaluation while a detailed description is available in D3.3 section 6.1[8].

The signalling can be divided into two parts:

- Signalling for the ON creation and release. At least 6 messages are needed for the ON Creation and 4 messages are needed for the ON release. The messages have a typical C4MS payload size between 20 byte (e.g. ON Creation response) and 120 byte (ON Creation request), the average C4MS message size (C4MS payload without TCP/IP/L2/L1) is 65 byte.
- Measurement reporting: Link reports are regularly exchanged. Please note that these measurements are normally not ON related because link measurements are also exchanged when being normally connected with an infrastructure network. However, in the case of an ON, the measurements of the device being out of direct infrastructure coverage have to be transported over an additional hop via the relaying device, therefore, the signalling load at the relaying device increases. A Measurement report like e.g. a MIH\_Link\_Parameters-Report has typically 90 byte while a Cell Load Report has typically about 50 byte C4MS information. The overall measurement signalling load largely depends on how often such measurements are exchanged, e.g. periodically all 5 seconds or only based on triggers e.g. when a predefined threshold is crossed.

### 3.2.2.3 Throughput and Coverage improvement

The demonstrator is also used for testing on how far the coverage can be extended by using one relaying device.

For this test, several reference locations have been specified in an office environment. Then the provided FTP-throughput has been measured at these device locations with different configurations as shown in Figure 27. These tests have been made using 802.11b due to the capabilities of the relaying device. Locations 1 and 2 are in the same room where the access point is located. Locations 3 to 7 are in the hallway before that room while the other locations are in another hallway around the corner.

As shown in Figure 27, the direct connection (blue curve) provides good coverage (more than 75% of maximum throughput) up to location 8, then it degrades and the coverage is completely lost at point 11.

With a relay at location 5, still 30% of the maximum throughput can be provided at that point where direct coverage is lost (Location 11). Even at the end of the 2<sup>nd</sup> hallway (Location 14), 15% of the maximum throughput is available when using a relay (orange curve).

When using opportunistic networking, the direct connection is used in cases of good direct coverage; else a relaying device is used. Thus, always the better of the two curves is used (green dotted line).



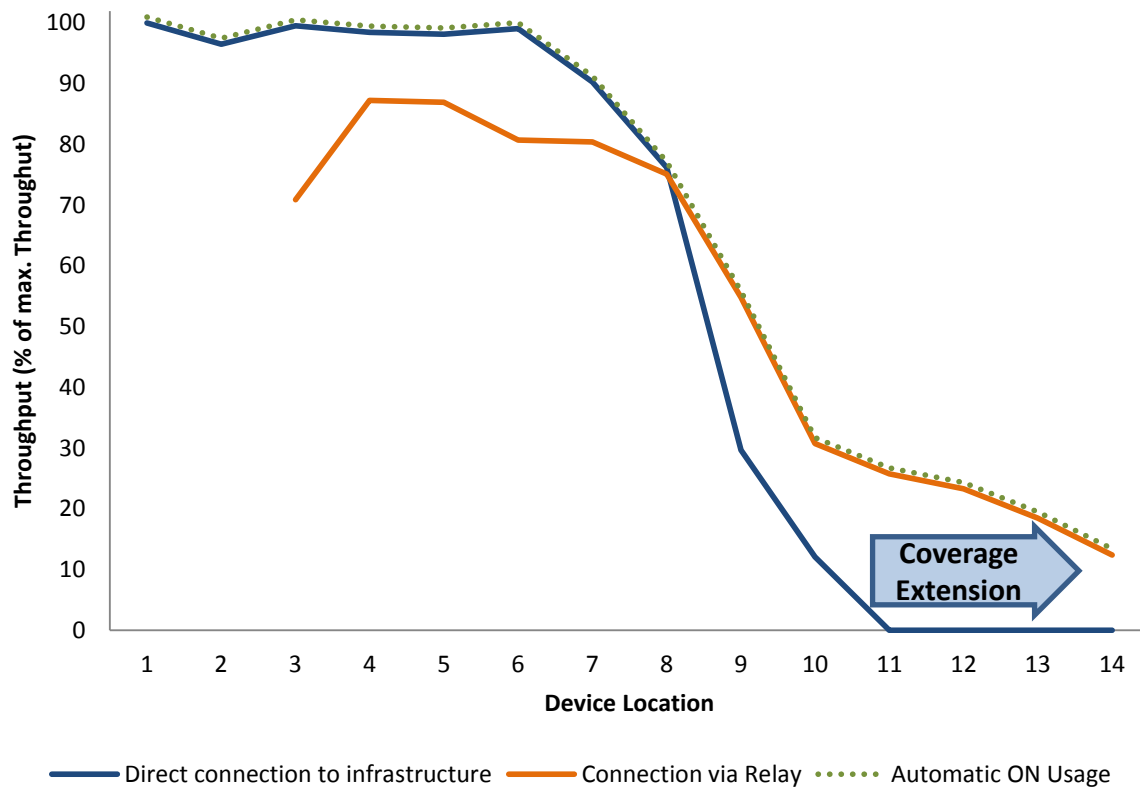


Figure 27: Throughput and Coverage extension gains

### 3.2.3 Results from platform 4 “Opportunistic ad-hoc network demonstrator”

#### Throughput overhead estimate on extra control information exchanges

This section gives implementation details and results on experiments on the protocol on a network of Wifi laptops demonstrator. A video of three laptops demonstration is available from the following link [26], with streaming webcam flows using Real Time Transport Protocol [27].

Figure 28 gives details on the protocol message exchanges between 3 nodes in the case of two flows establishment, from the node 1 to node 3 and from the node 3 to the node 1.

To manage, in a term of synchronisation, the network coding, we use for each node a messages queue of sent and received messages with a determined size as a constant (set to 10 in the experiments). When a relay receives a packet, it stores it into the queue, and waits for a packet from the other flow to code it with. If a packet is going to be stored into a full queue, before storing it, the older packet of the queue is repeated without coding to free a slot of the queue. This choice of implementation can induce a latency in the case of packet losses (mainly in dependent flows like *ping*), but it appeared to be the most efficient way of doing it in a term of throughput gain.

The link stability management is done by polling. Every initial node periodically sends a `Flooding` message to determine if the configuration didn't change. So there is always a mix between control packets and applicative packets.

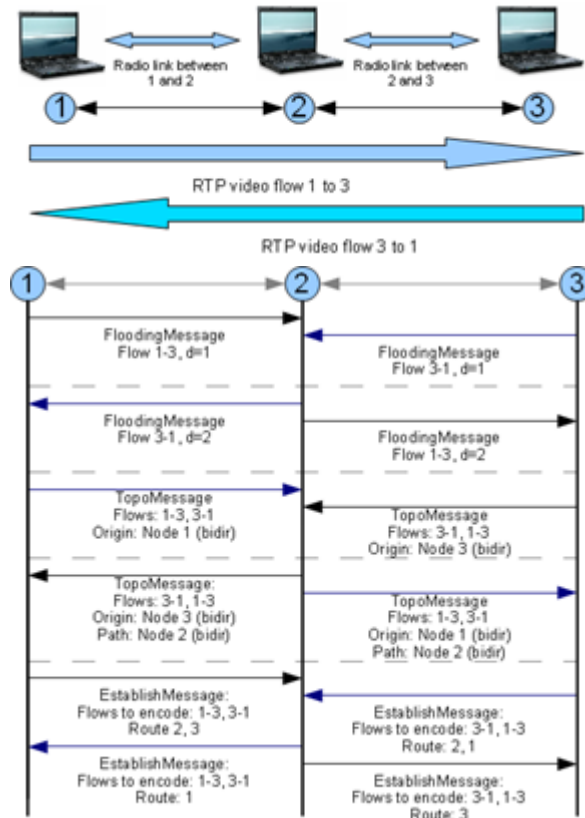


Figure 28: Sequence diagram of the message exchanges

In this example, 20 IP packets of 1324 bytes are transmitted per second, which gives a global traffic of received and sent packets per second for the three nodes of 211840 bytes without optimization, and 185360 bytes with optimization.

The overhead in terms of IP packets header is of 40 bytes per packets (identifier of the 2 packet flows, size of the data, information in the case the packets have different size) which means an overhead of 3%.

Per polling period, set here as 4 seconds, the three nodes send 4 flooding, 4 Topo and 4 Establish messages of respective 54, 116, 64 bytes size, for a global throughput for these messages of 936 bytes every 4 seconds.

The added throughput per second in this example is of  $936 \div 4$  (extra signaling) +  $40 \times 20$  (overhead in packet headers sent by node 2) each second, which equals 1034 bytes, for a gain of 26480 bytes (ratio 3.9%).

The overhead in terms of messages exchanged is of 12 control messages sent any 4 seconds, when 640 data messages (in the case of no network optimization applied in node 2) are exchanged (ratio of 1.88%),.

As the control messages already exist in routing protocol (as RREQ, RREP messages for AODV), and the size of the information added in the IP packet header may be optimized, the overheads are overestimated, and may be optimized in further studies. However, gains obtained from this experimentation justify the use of such protocol optimizations.

### Throughput gain on data transfer from Wireshark views

Here are given snapshots of Wireshark results on the application on one relay node of a bidirectional flow, with the multiflow routes co determination algorithm switched on/off with two video flows of 45 kbits/sec. in the following figure are given in abscissa the time, and in ordinate the nb packets/sec sent and received. As shown we may see confirmation of the gain of the number exchanged of the combined packets with respect to the packets sent on a classical relay.

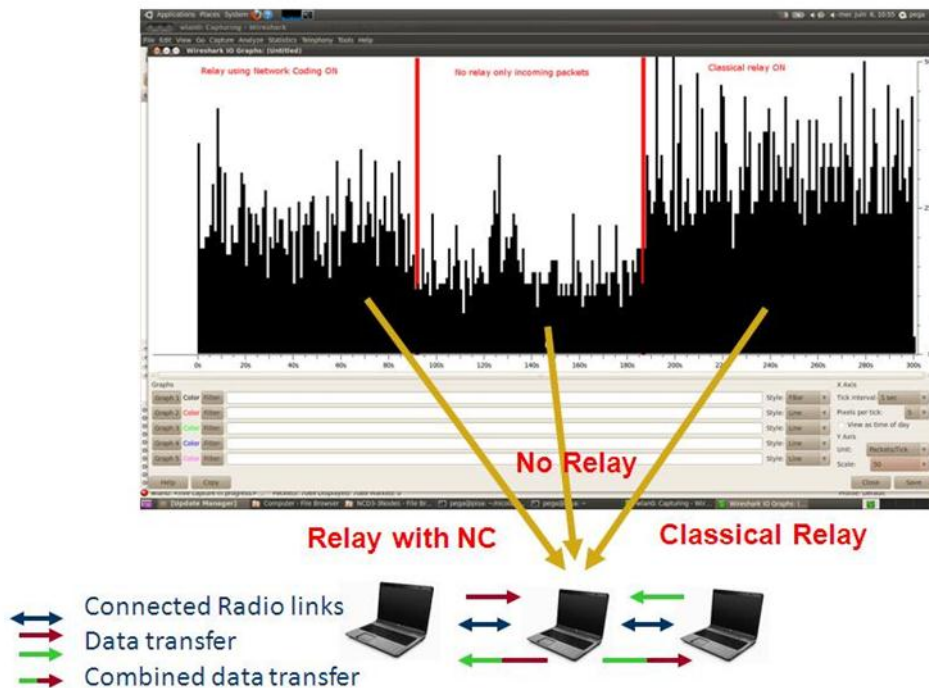


Figure 29: Number of exchanged packets

### Further results

The execution on demonstrator allows to experiment on physical equipment the proof of concept and the capability to assess the optimization gains on integrated platforms. The add-on of the TCS proposed algorithm is its adaptation on multi topologies and flows. Results on these adaptations have been provided in the D4.2 and D4.3 deliverables, and the object of publications.

### **3.2.4 Results from platform 5 “Indoor/Office opportunistic coverage extension and related support functions”**

The results of this platform relate main to two Cases:

- All features of the newly developed SW components in combination with all HW extensions are tested and validated. In particular, support functions are validated related to three main features (“Opportunistic Network Support”, “Multi Homing Support” and “Best Available Connection”) subject to the operator policies which can be selected as shown below.

The validation process is finalized by demonstrating that the implemented features work in alignment to the functional specifications. All corresponding functions have been successfully validated.



Figure 30: The three key platform features in the novel SW environment.

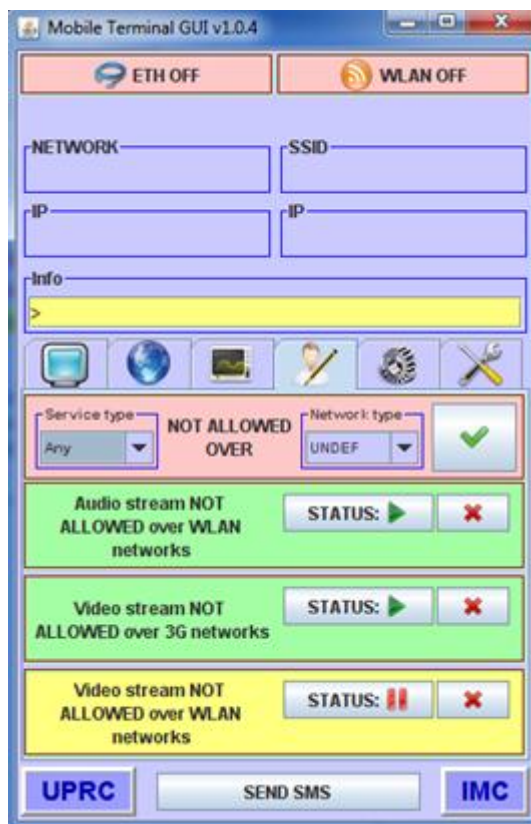


Figure 31: The operator policies selected for the operation of the key platform features.

- Quantitative results are achieved with respect to the overall power consumption of the set-up. Corresponding detailed results are summarized in the sequel. Those allow in particular to identify the optimum target RAT leading to an overall minimum power consumption.

In order to obtain a comparison base-line, the Laptop LENOVO X61s host power consumption was measured without any connectivity being added (the x-axis indicates the time over which the measurements had been taken):

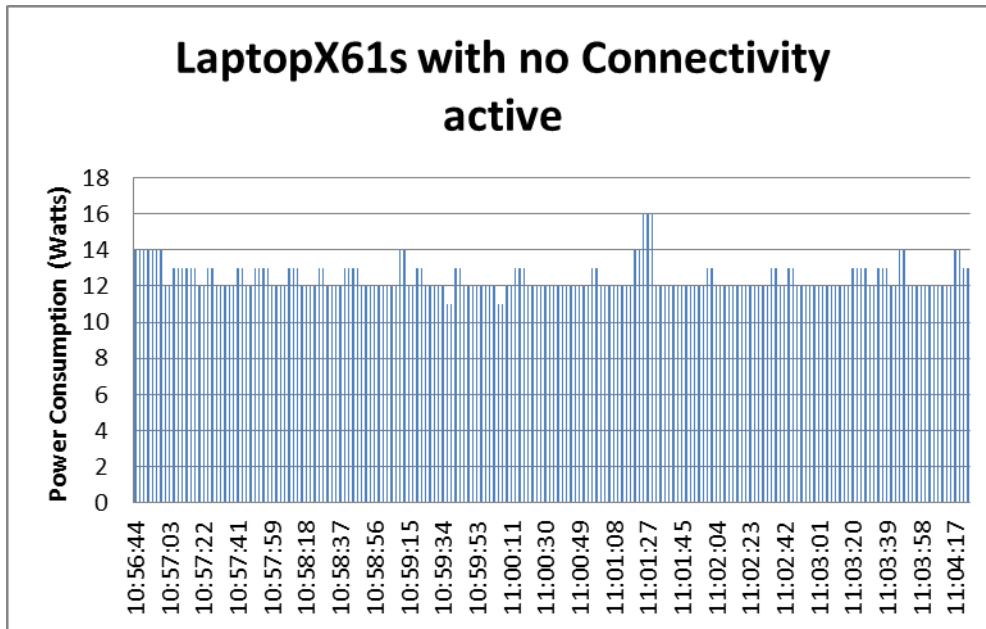


Figure 32: Power consumption on LENOVO X61s without connectivity

Another base-line reference is indicated in the graph below: The LAN connectivity of the reference Laptop X61s is activated and an HDTV video stream is downloaded and shown as provided by <http://www.ustream.tv/nasahdtv>. All wireless connectivity numbers need to be considered with reference to those base-line observations.

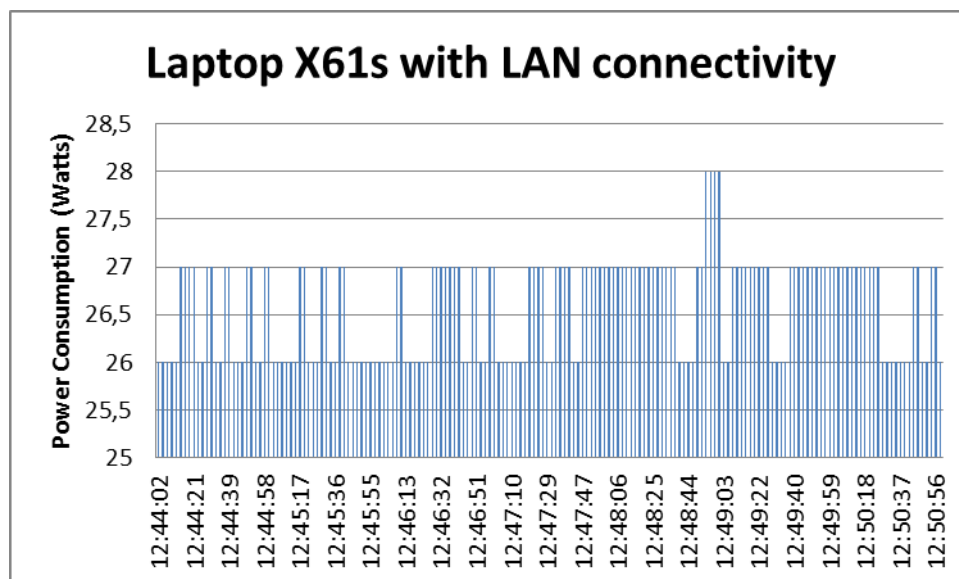


Figure 33: Power consumption on LENOVO X61s with LAN connectivity

As it can be seen below, the WLAN based streaming leads to a considerably higher power consumption compared to LAN based streaming. Again, the HD video stream provided by <http://www.ustream.tv/nasahdtv> was used as an application.

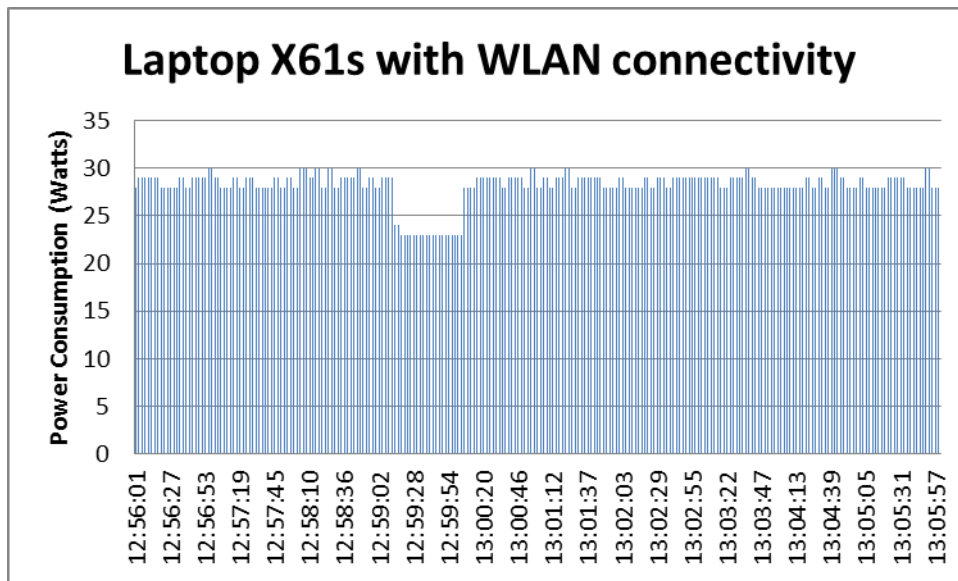


Figure 34: Power consumption on LENOVO X61s with WLAN connectivity

Below, the same WLAN based streaming is used, however two clients use the HD video stream provided by <http://www.ustream.tv/nasahdtv> as an application. For those two clients, two independent WLAN networks are set-up operating at an identical channel, i.e. the resources need to be shared. Notably, the power consumption observed in the clients only varies slightly: 28.168 Watts are used for the WLAN case in which only one client is present for downloading the video stream and 28.227 Watts are used in the case of capacity sharing for two HD TV streams. This difference is in practice negligible.

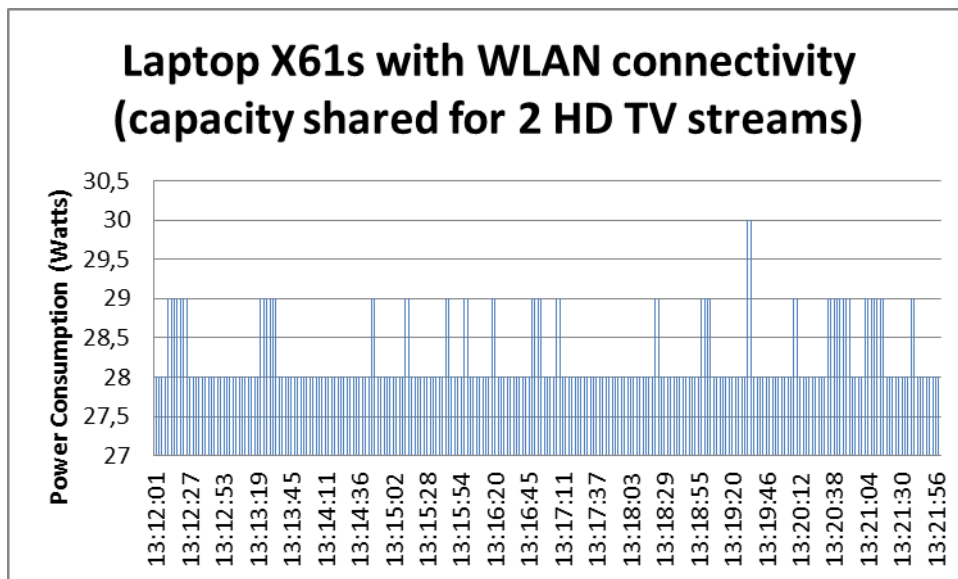


Figure 35: Power consumption on LENOVO X61s with WLAN shared for 2 TV streams

Below, the average power consumption for a 3G connection established based on the XMM6160 modem is shown. The corresponding power consumption is slightly above the one of WLAN (by approx. 3%).

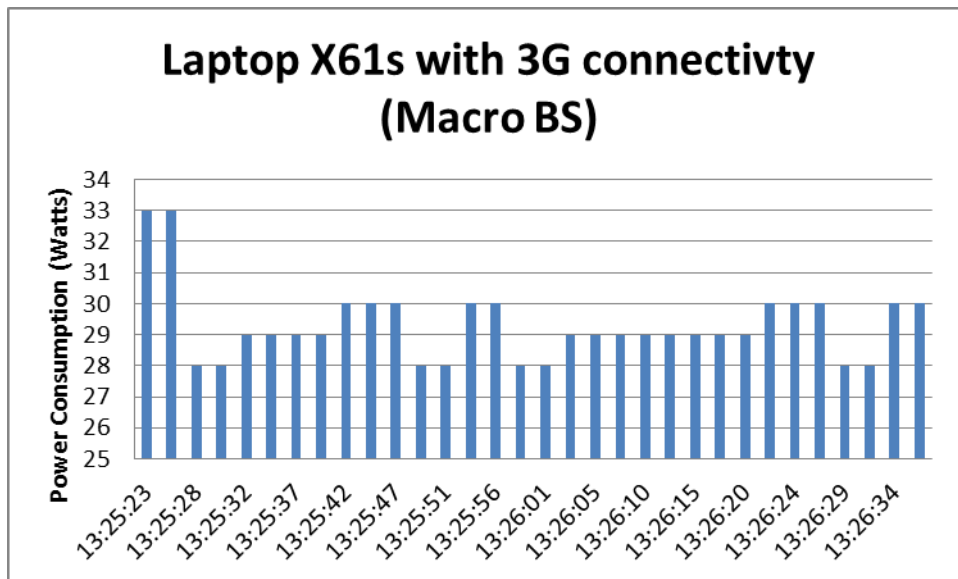


Figure 36: Power consumption on LENOVO X61s with 3G Macro BS connectivity

Using an experimental Femto BS, a Macro BS / Femto BS comparison of the overage power consumption for a 3G connection established based on the XMM6160 modem is shown below. Notably, the corresponding power consumption for Femto BS is dramatically lower compared to the Macro BS connection, by approx. 25% on average. Part of the savings, however, may be due to the slow backbone network connection. Indeed, an experimental network was used since today's commercial solutions do not allow for routing within the IP Sub-nets of 3G operators. Thus, those values may require additional validation by solutions closer to productization.

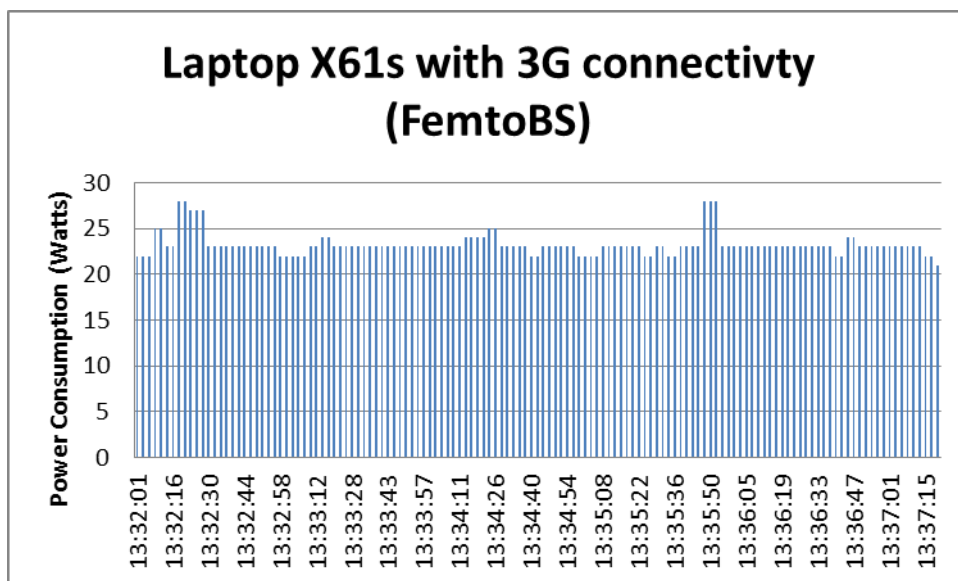


Figure 37: Power consumption on LENOVO X61s with 3G Femto connectivity

An aggregate view on the power consumption measurements is given on the following page.

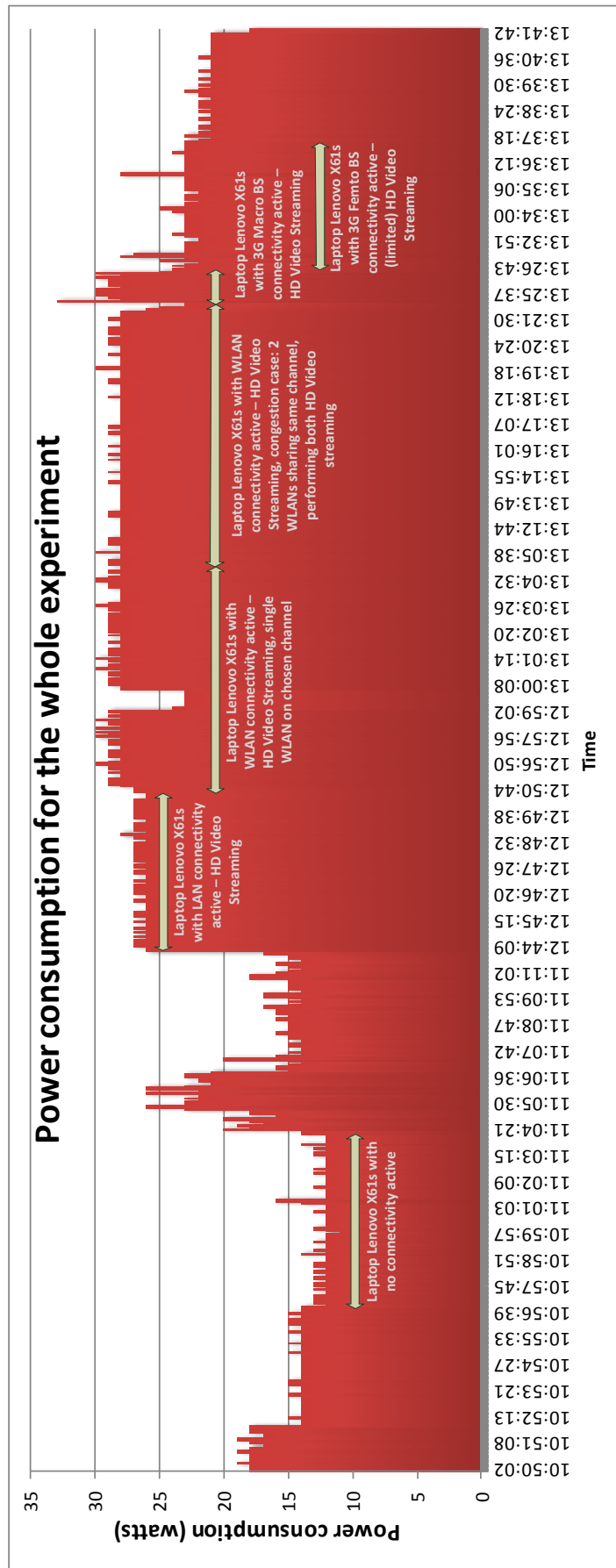


Figure 38: Variation of power consumption on LENOVO X61s



The following table summarize the average power consumption over the measurement intervals indicated above:

Table 1: Average power consumption on LENOVO X61s

Configuration	Average Power Consumption (W)
Laptop X61s without connectivity	12.43
Laptop X61s with LAN connectivity	26.58
Laptop X61s with WLAN connectivity (1 user accessing all resources)	28.17
Laptop X61s with WLAN connectivity (2 user sharing resources over 2 independent WiFi networks)	28.23
Laptop X61s with 3G connectivity (Marco BS)	29.07
Laptop X61s with 3G connectivity (Femto BS)	23.21

Those average numbers are summarized in the graph below:

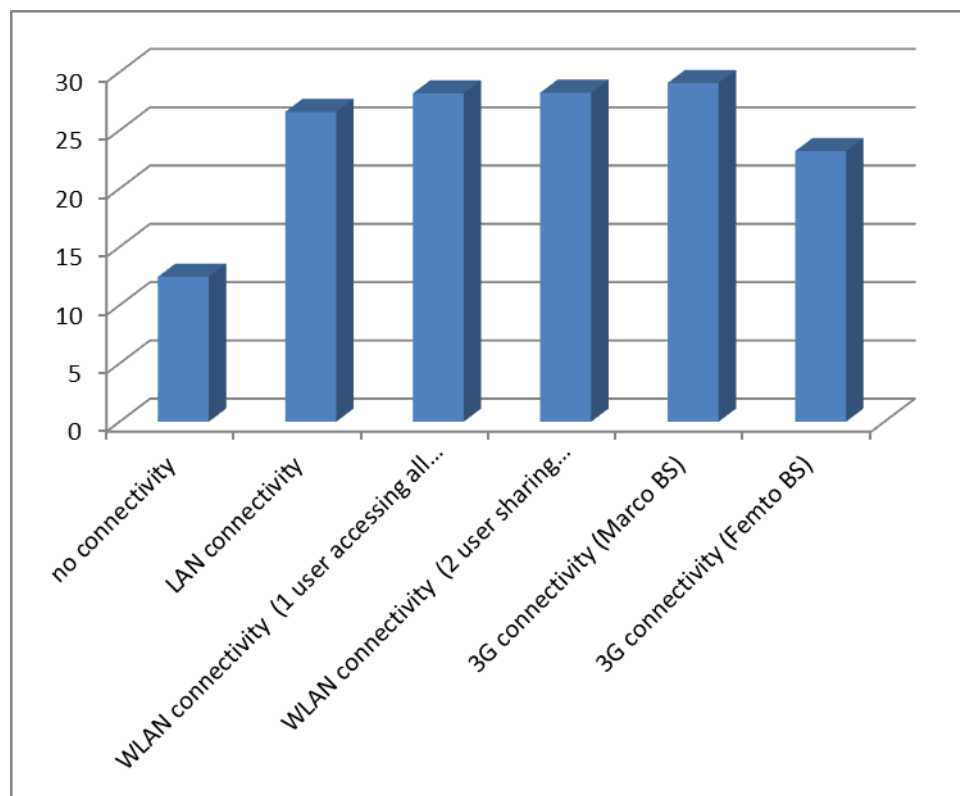


Figure 39: Average power consumption on LENOVO X61s

Based on the upper results, the following conclusions can be drawn for a multi-RAT environment:

Activating any type of connectivity (LAN, WLAN, 3G, etc.) will increase the overall Mobile Device Power Consumption considerably. Whenever possible, the corresponding modems should be switched off.

There is no substantial difference in terms of power consumption between LAN, WLAN (with one user having all resources, two users sharing the available resources, etc.) and 3G (Macro BS based connection). A notable difference is identified for Femto BS. I.e. whenever a highly efficient Femto

BS network is available, it should be preferred over standard WLAN and 3G (Macro BS) connections. However, it should be noted that in our experimental set-up, the backbone connection was operating at a very low data-rate only. Final conclusions to be used in product designs may require further measurements based on a number of commercial Femto BS deployments. For the other wireless connectivity solutions, the selection is expected not to be based on power consumption metrics. Rather, criteria like availability, QoS/QoE, congestion, etc. are expected to be used.

### **3.2.5 Results from platform 7 “Cognitive Radio testbed”**

#### **3.2.5.1 Results – PHASE i**

This phase considered one test:

##### Test 1: Evaluations of the sensing techniques

The purpose of this test is to evaluate each of the six sensing techniques based on common criteria.

#### **3.2.5.2 Statistical Analysis**

To do the statistical analysis of the spectrum sensing techniques, a new framework was designed to repeat the experiment over a range of signal to noise ratios to compute the probability of detection, probability of missed detection and probability of false alarm. This framework initialized both WARP nodes at the start, and then continuous transmission was done from the transmitter node. Capture at the receiver was triggered every time the computer sent a sync packet. The signal was then fed to the decision block where respective sensing technique was applied. The experiments were repeated from 100 to 5000 times at each SNR to get average probabilities. The ROC curves were plotted from the results.

#### **3.2.5.3 Performance Evaluation**

After the individual testing of standalone spectrum sensing techniques, all the six techniques are tested under exactly the same conditions for comparison. The parameters such as number of samples, modulation type, transmitter/receiver parameters and probability of false alarm (where applicable) kept same across all. The techniques were tested and compared under different scenarios. The spectrum sensing techniques were also tested for the computation time. The time was measured in terms of CPU time elapsed in the decision block. The conditions for measurements were same for all techniques.

#### **3.2.5.4 Performance of Spectrum Sensing Techniques**

This section discusses the performance of each spectrum sensing technique using the WARP communication framework, provides comparison with theoretical/simulation results and presents evaluations of various candidate sensing techniques.

##### **3.2.5.4.1 Energy Detection**

Using the WARPLab setup, the receiver operating characteristics (ROC) were measured as shown in Figure 40. The results show that energy detection works well if the measured SNR is above -10dB. Performance begins to fall when the SNR is below -10dB.

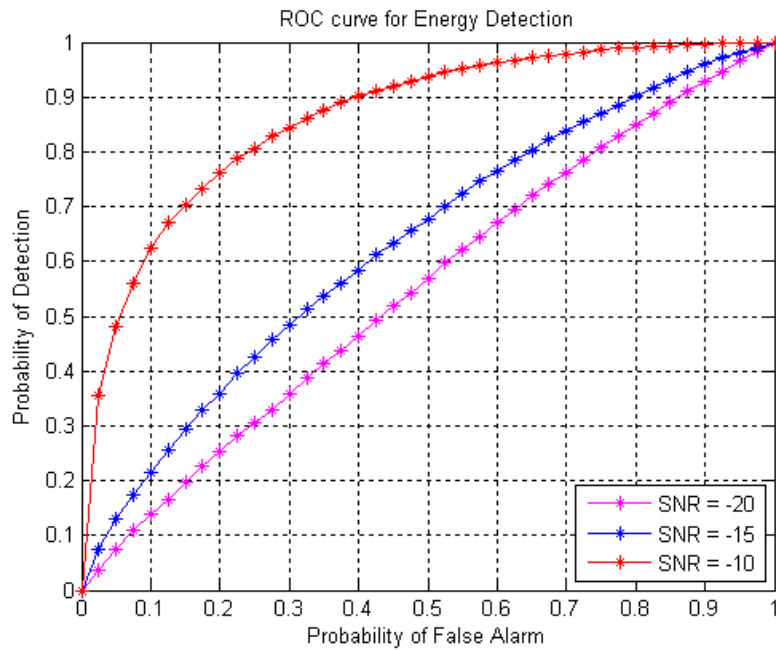


Figure 40 ROC Curve for Energy Detection

For the real-time demonstration, the experiment was conducted to compare the simulation results against the real time.

The first experiment was performed to compare the ROC curve of simulation and the real-time test. The figure below shows the results for probability of false alarm ranging from 0.2 to 0.5 vs. probability of detection. It is observed that simulation and WARP results differ a little. The differences are due to the additional receiver noise and the other environmental factors (RF sources in the lab) that were not considered in the simulation.

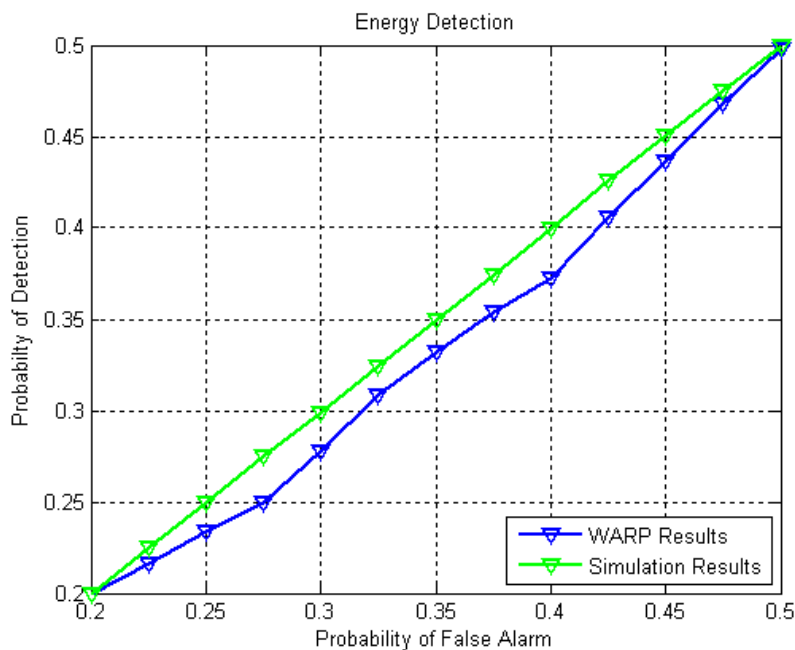


Figure 41 Energy Detection PD vs. PFA

The energy detection technique was then tested for SNR -20dB to 20dB to compute the probability of detection. The following graph shows the results.

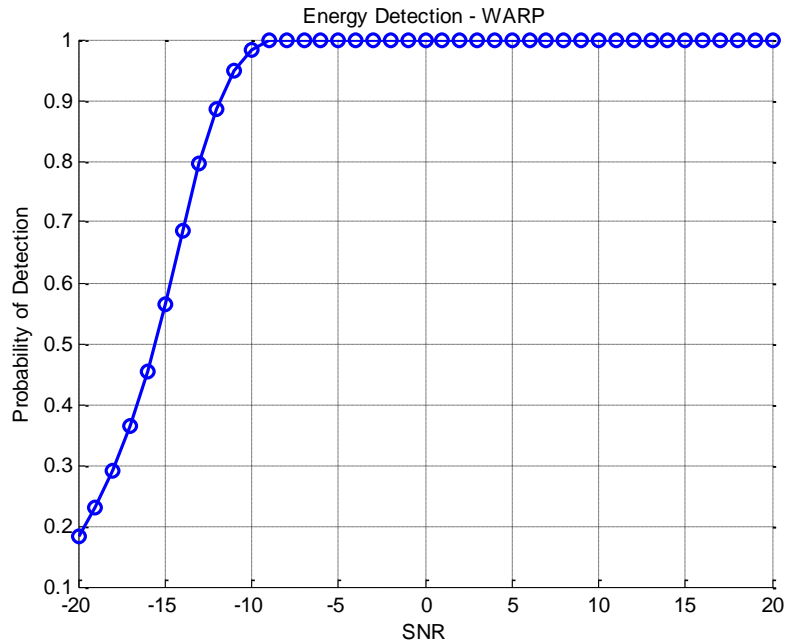


Figure 42 Energy Detection PD vs. SNR

Figure 15 shows results for 8000 samples averaged for 1000 experiments. The probability of detection is 1 for signals above -10dB. However that’s not the complete story, this experiment was performed using the WARP nodes and the length of symbol sequence fed to the decision block was 8000. This motivated further testing with different number of samples. The results for symbol length 800, 2000, 4000 and 8000 are shown below.

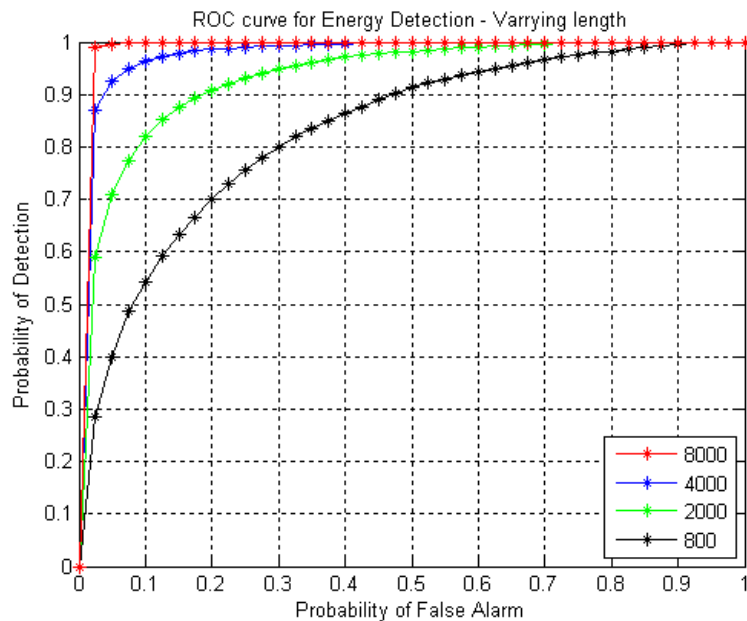


Figure 43 Energy Detection Performance - Varying Lengths (SNR = -10dB)

The threshold is dependent on probability of false alarm, but changing that from 5% to 20% didn’t make much of a difference as depicted in Figure 44. Probability of detection slightly increased in the region below -10dB but it’s of no use having that improvement at the cost of higher false alarm.

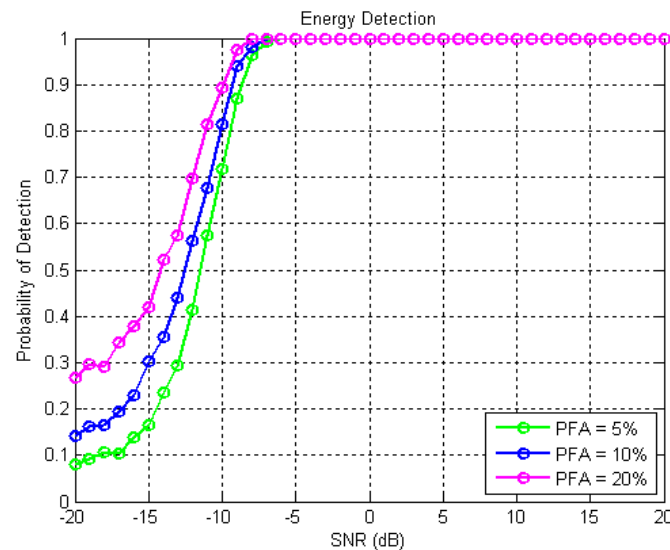


Figure 44 Energy Detection - Change PFA

### 3.2.5.4.2 Observations

The following observations were made:

- Energy detection works better for signals with more than -10dB SNR
- If decision block is fed more samples, the results improve
- The threshold is dependent on probability of false alarm, having a higher value will not be much of use. Probability of false alarm should be kept low to avoid the chance of collision with the primary user.

### 3.2.5.5 Cyclostationary Feature based Detection

Cyclostationarity based detectors are naturally insensitive to uncertainty in the noise variance, as the decision statistic is based on the noise rejection property of the cyclostationary spectrum. Hence the experimental results are not much different from the simulation results.

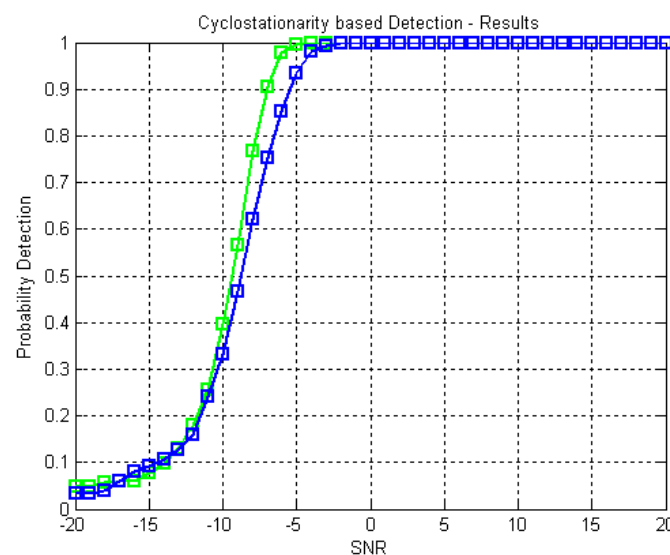


Figure 45 Cyclostationary based detection - PD vs. SNR

The results show that the cyclostationary feature based detection can 99% probability of detection at around -5dB. The graph shows results for 1000 samples averaged for 1000 experiments. For lesser

number of samples, probability of detection is plotted against SNR for 1000, 2000 and 4000 samples. Figure 46 shows that if the sensing block is given more samples the performance improves.

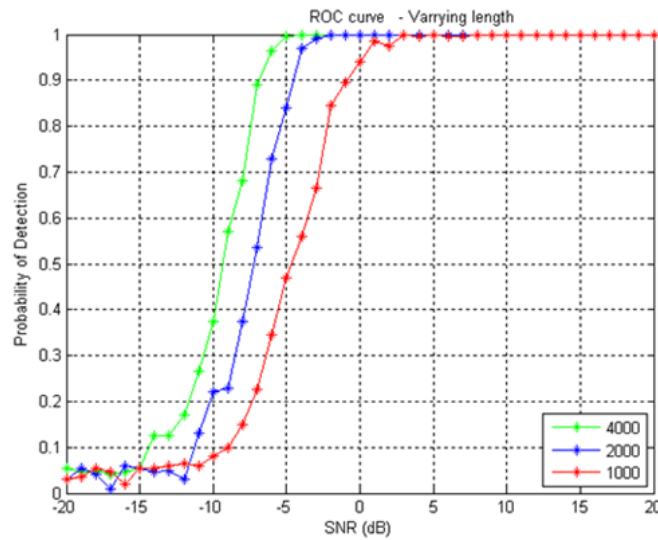


Figure 46 Cyclostationarity Detection Performance - Varying Lengths

**3.2.5.5.1 Observations**

The following observations were made:

- If the sensing block is given more samples the performance improves.

**3.2.5.6 Matched Filter based Detection**

The matched filter technique as mentioned earlier requires the knowledge of the primary user’s signal. As soon as the noisy signal is received, the block convolves the signal with its conjugate time-reversed version to maximize the signal to noise ratio. Test statistic is then compared with the threshold to determine presence or absence of the signal.

The figure below shows the ROC curve obtained from simulations and using WARP node. Experiment was done using 800 symbols at -18dB. Average of 1000 experiments was taken.

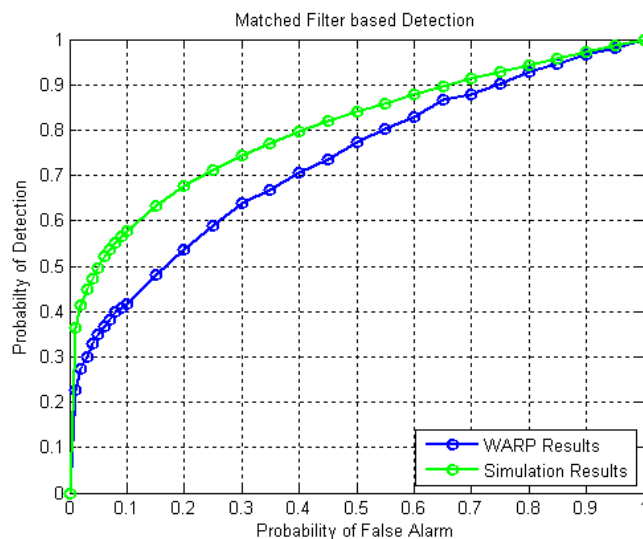


Figure 47 Matched Filter - PD vs. PFA

As shown in Figure 48 for the SNR wall, the probability of false alarm was set to 10% and the tests were conducted for probability of detection for the range -20dB to 20dB. It was observed that probability of detection turned out to be more than 90% for SNR greater than -15dB.

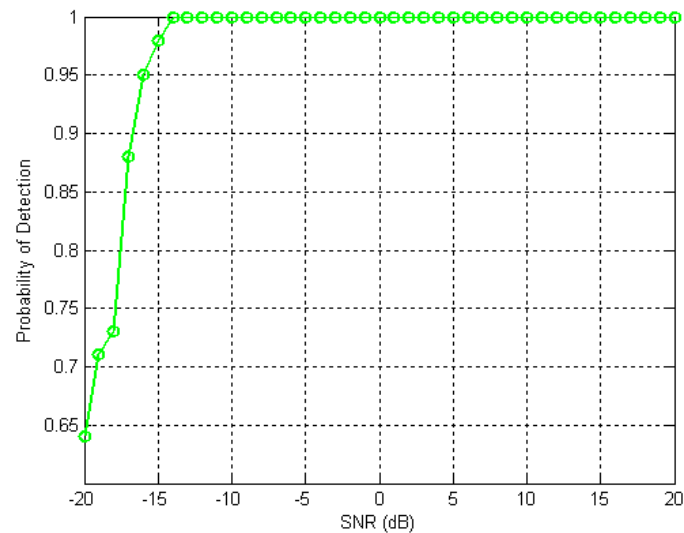


Figure 48 Matched Filter - PD vs. SNR

This might look like an ideal scheme, as it is performing better even at low SNRs but the fact that it needs information about the primary user signal makes it less practical.

Another factor that affects the matched filter performance is the synchronization error. In the experiment transmitter node was triggered to start transmitting particular number of samples at a specified frequency. If the receiver is not synced there's a delay off 100 samples, the performance of the matched filter detector is observed to degrade significantly.

### 3.2.5.6.1 Observations

The following observations were made:

- Performance degrades if mismatch in sync
- Needs perfect knowledge of signal

### 3.2.5.7 Covariance based Detection

The covariance based detection as discussed earlier depends on the correlation of signal samples. Covariance is calculated and compared with the threshold mentioned in earlier chapter. The threshold is defined according to the probability of false alarm.

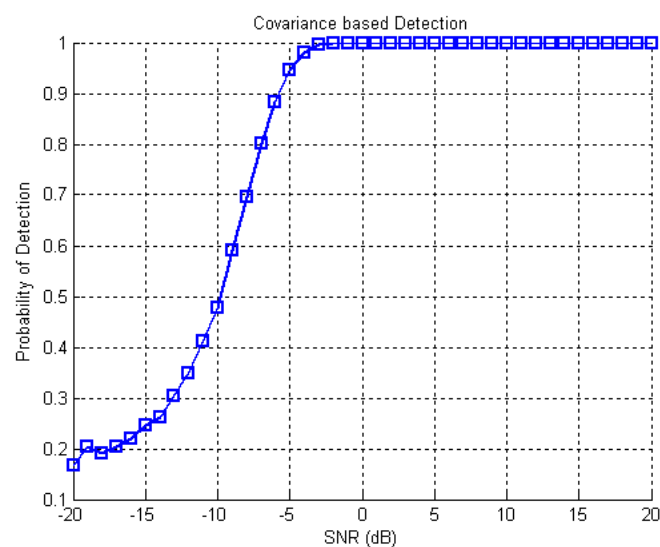


Figure 49 Covariance based Detection

There are many parameters that can be adjusted for the algorithm such as number of samples and smoothing factor to get the ideal threshold for given conditions.

### 3.2.5.7.1 Observations

The following observations were made:

- If the sensing block is given more samples the performance improves.
- Changing smoothing factor improves performance but takes longer time

### 3.2.5.8 Minimum-Maximum Eigen Value based Detection

The minimum-maximum Eigen value based detector computes the covariance of the received data and calculated the maximum and minimum Eigen value. The decision block is fed both maximum and minimum value, over-sampling factor and the smoothing factor to make a decision for a specified probability of false alarm. This method needs no information about signal or channel.

The graph below shows the roc curve for SNR range -20dB to 20dB and probability of false alarm = 10%. The covariance calculation is a computationally intensive task.

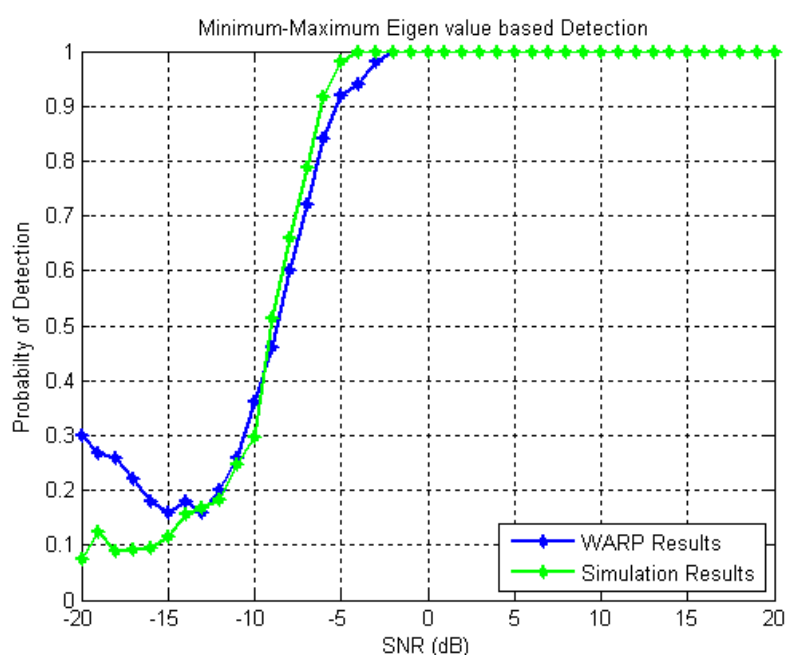


Figure 50 MME based Detection

The graph shows results for 500 samples averaged for 1000 experiments. The comparison of all techniques in the Chapter 5 shows the performance of MME technique for higher with higher number of samples. It was observed that the performance gets better as we increase the samples, but sensing time also increases. A small experiment was conducted to observe the trend of increase in time with the increase in number of samples.

Table 2 Decision Time

Samples	Time for single run of decision block (sec)
500	0.7075
1000	1.4703
2000	2.9000
4000	5.7687
8000	11.4812



It should be noted that these numbers (in Table 2 Decision Time) are only the representative of time taken by decision block for the particular computer system used. The detection time increases as with the increase in the number of samples. For sensing, we don't always have a large number of samples. The input size can be adjusted to according to the performance required.

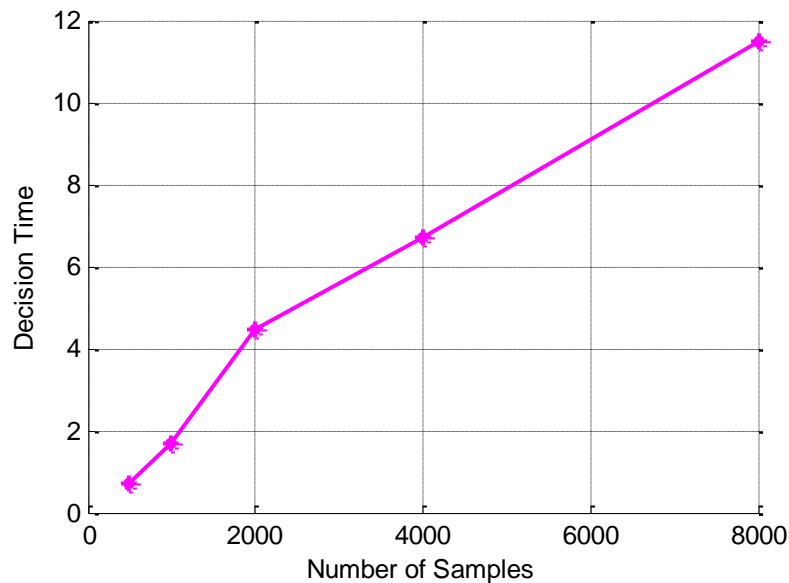


Figure 51 Detection Delay vs. Number of Samples

The probability of detection at -10dB for 500 samples was 90% and for 8000 samples was observed to be 100%. There are many parameters that can be adjusted for the algorithm such as number of samples, number of receivers and smoothing factor to set the ideal threshold for different conditions.

#### 3.2.5.8.1 Observations

The following observations were made:

- Decision blocks takes more time if the number of samples increases.

#### 3.2.5.9 Blind Sensing Scheme

This scheme [23][24] is designed for OFDM signals and is based on difference of energy of the sub-band carriers. The technique claims to outperform energy detection and correlation based detector in terms of probability of detection. The graph below shows the PD vs. SNR and PFA vs. SNR graph for the novel technique.

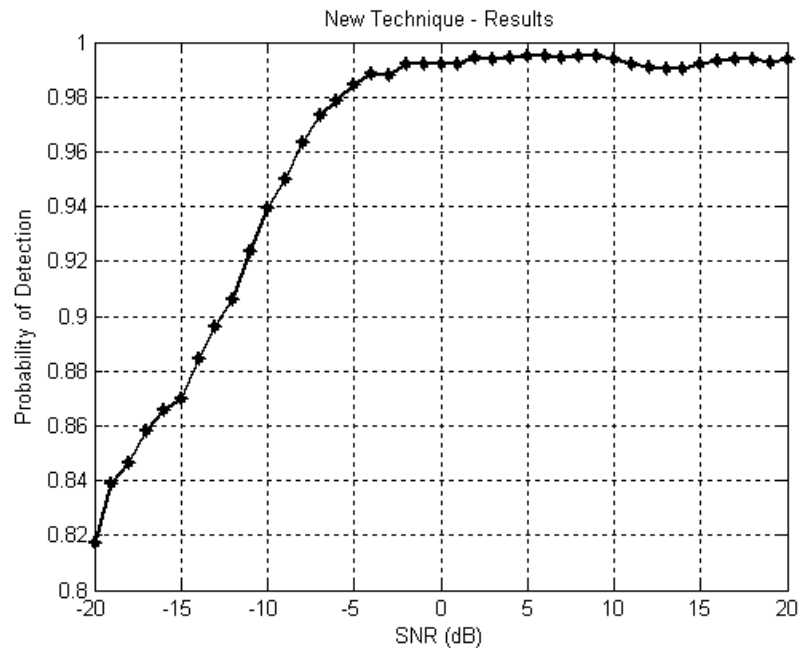


Figure 52 Blind Technique - PD vs. SNR

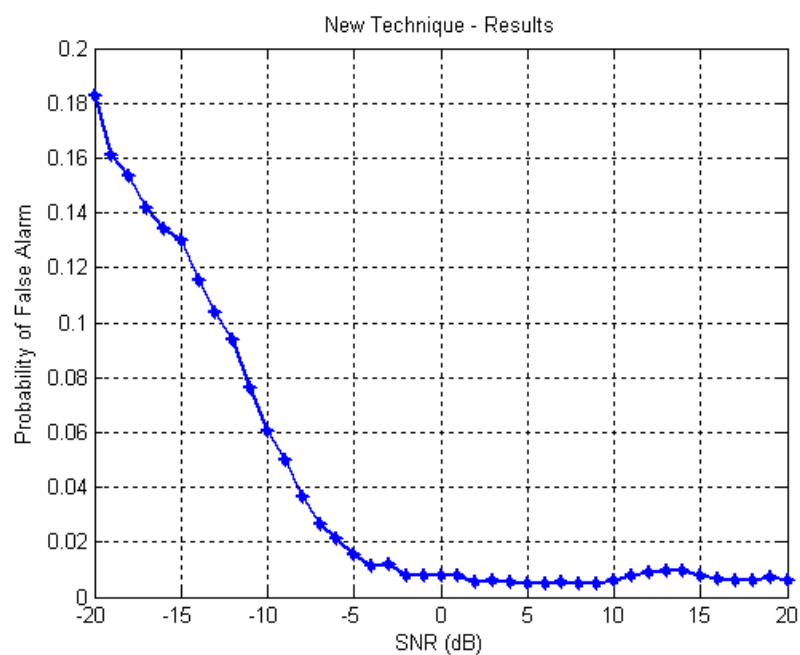


Figure 53 Blind Technique PFA vs. SNR

### 3.2.5.9.1 Observations

The following observations were made:

- Detection works on the sub-band level.
- Tests were carried out with the following recommended default settings i.e QPSK modulation with 2 frames (28672 complex samples, which are then reshaped in columns to perform post-processing), column size (defined by Num\_of\_QPSKmodData/Block\_Size) set to 28, block size set to 1024 and the emitting sub-carrier block (which is the first step of decision block) hard coded for block size 1024

- With the default settings above the proposed technique outperforms energy detection and cyclostationary detection at SNRs below -10dB.
- Experimentation with different set of configuration values also indicates superiority of proposed technique below -10dB but it needs minor adjustments to the threshold if it is to remain superior at higher SNR.

### **3.2.5.10 Performance Comparison of Spectrum Sensing Techniques**

The previous section discussed the performance evaluation of the spectrum sensing techniques. The following sections provide comparisons of the standalone spectrum sensing techniques using the WARP nodes.

#### **3.2.5.10.1 Statistical Comparison**

##### **3.2.5.10.2 Probability of Detection vs. SNR**

For a fair performance comparison, the sensing techniques were tested under same conditions. The first graph represents the probability of detection against signal to noise ratios of the five techniques namely energy detection, matched filter, cyclostationarity based detection, covariance based detection and minimum-maximum eigen-value based detection. The last technique which is the blind technique that is not incorporated into this comparison, as it works at a sub-band level for an OFDM system. Its comparison will be presented later in the section with energy detection in detail.

As it can be seen in Figure 54, energy detection and matched filter based detection work better than the other techniques. However it should not be ignored that energy detection is highly affected by noise uncertainty. There are two type of noise un-certainty:

- Receiver Noise Uncertainty
- Environment Noise Uncertainty

Additionally, there are several sources of receiver noise uncertainty:

- Non-linearity of the components
- Thermal noise in the components

The environmental noise is from the other transmissions in the air. Due to this it is difficult to estimate the noise power, which can lead to wrong threshold setting hence have an effect on the performance of the spectrum sensing technique [22]. QPSK scheme was used to modulate the random data stream. Number of samples are 800 for the first test and 2400 for the second test. Probability of the false alarm in both cases is 10%.

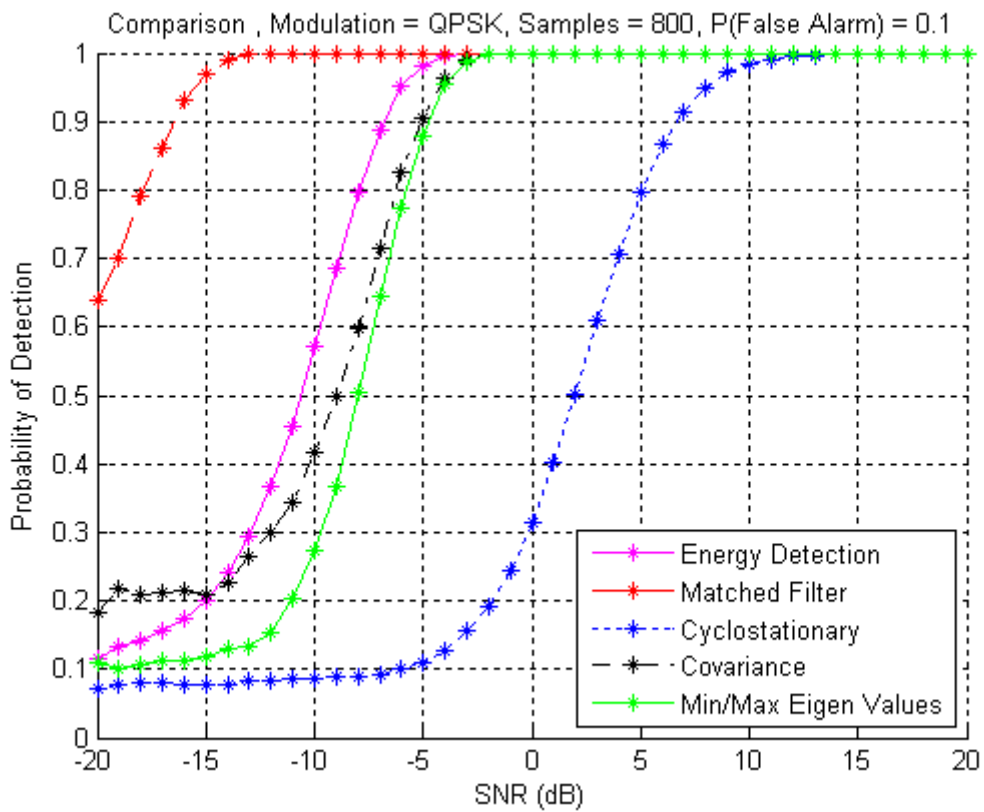


Figure 54 Comparison, PD vs. SNR

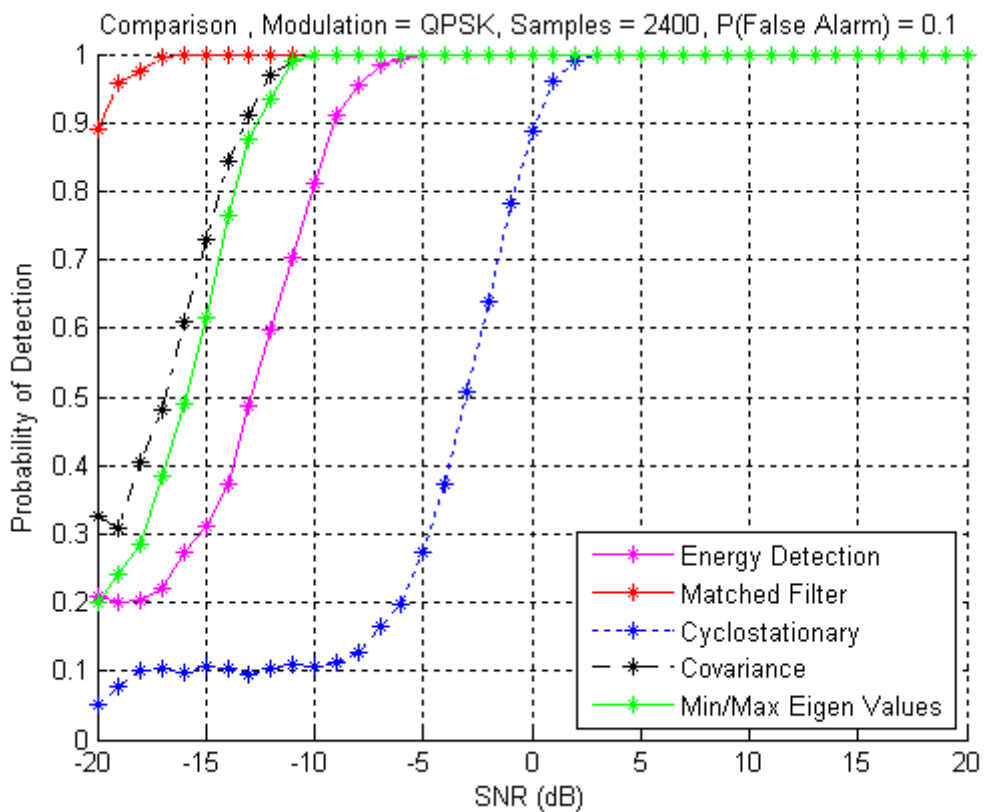


Figure 55 Comparison, PD vs. SNR

The performance of schemes was almost 99% at the following signal to noise ratios

Table 3 Sample and SNR of Sensing Techniques

Technique	800 samples	2400 samples
Matched Filter	-14 dB	-16 dB
Energy Detection	-5 dB	-6 dB
Covariance	-4 dB	-12 dB
Min/Max Eigen Value	-4 dB	-12 dB
Cyclostationarity	10 dB	0 dB

It was observed that covariance based detection schemes perform better than energy detection if the number of samples fed to the decision block is increased, but these techniques have a drawback of increased computational complexity and time.

Matched filter outperforms these techniques, but it requires prior knowledge of the channel and primary user's signal characteristics. This information is not voluntarily available and with the increasing number of systems that have a capability to change their baseband or passband signal processing with the changing channel characteristics, it is almost impossible to use matched filtering for signal detection. If the prior signal information is available then this technique can be used for signal detection and to distinguish between primary and secondary user signals.

The next test shows the scenario where probability of false alarm is reduced to 5%. This is done in practical systems to maximize the spectrum reutilization and to avoid collision with the primary user.

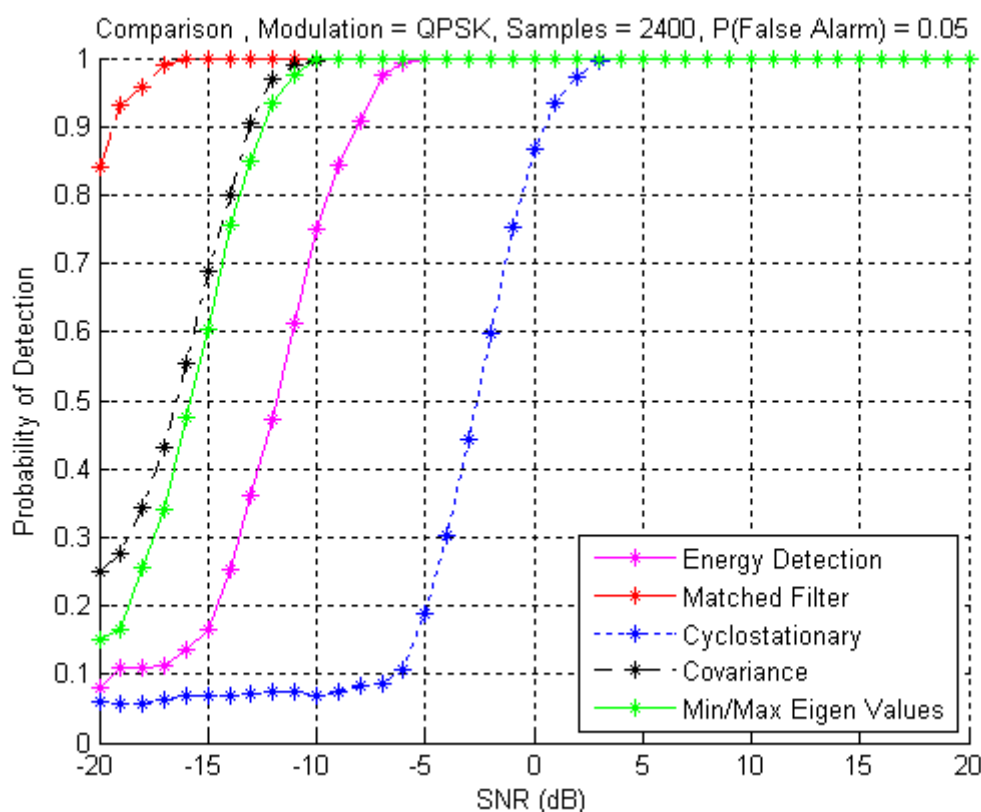


Figure 56 Comparison - 2400 Samples

The probability of detection remains almost the same, but now we will have half the number of false alarms. Hence increasing the performance of the decision block overall.

Next the performance comparison of the novel energy detection scheme with energy detection is presented.

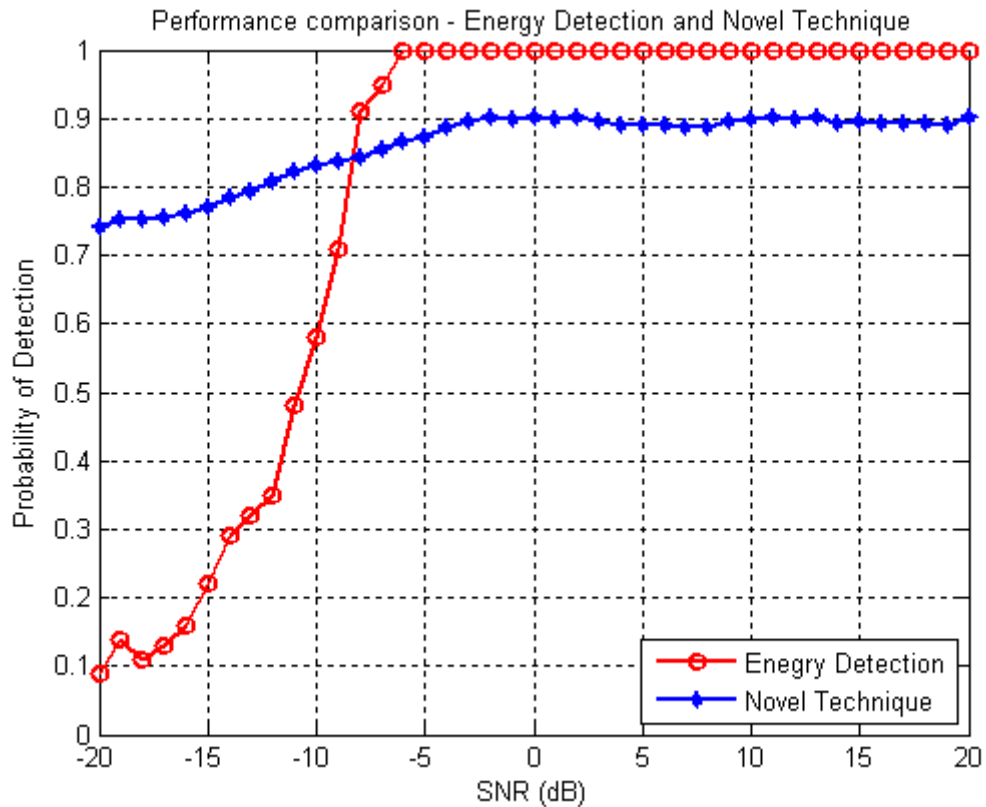


Figure 57 Performance Comparison ED vs. Blind Technique – 2 Frames

The number of frames for this set of experiments was 2, with block size = 1024. It is very clear that this novel technique outperforms energy detection in the region below -8dB with a big margin. If we increase the number of frames to 10, the performance of the novel technique outperforms energy detection for the full range.

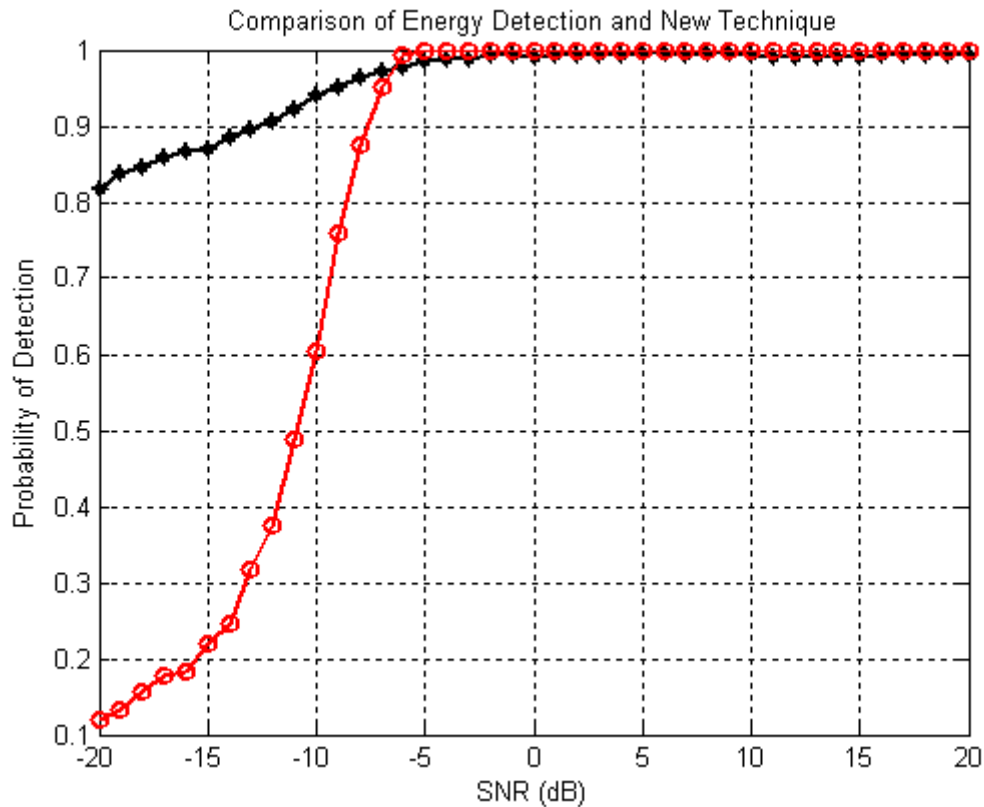


Figure 58 Comparison ED vs. Blind Technique - For 10 Frames

The red plot is energy detection and the black plot is the novel technique. At lower SNR values the probability of detection of the new technique is much better than conventional energy detection.

### 3.2.5.10.3 Probability of False Alarm

Probability of false alarm is a very important statistic. Consider a scenario where a primary user is using the spectrum band and a secondary user detects that the band is vacant (by mistake). The secondary user will start transmission resulting in collision with the primary user's signal.

The whole concept of spectrum reuse revolves around the usage of vacant spectrum. If the spectrum sensing technique is giving too many false alarms, the primary users will be affected and that whole network will suffer. The aim is to find a balance between under-utilization and collisions.

To demonstrate the importance of false alarm, consider the following figure:

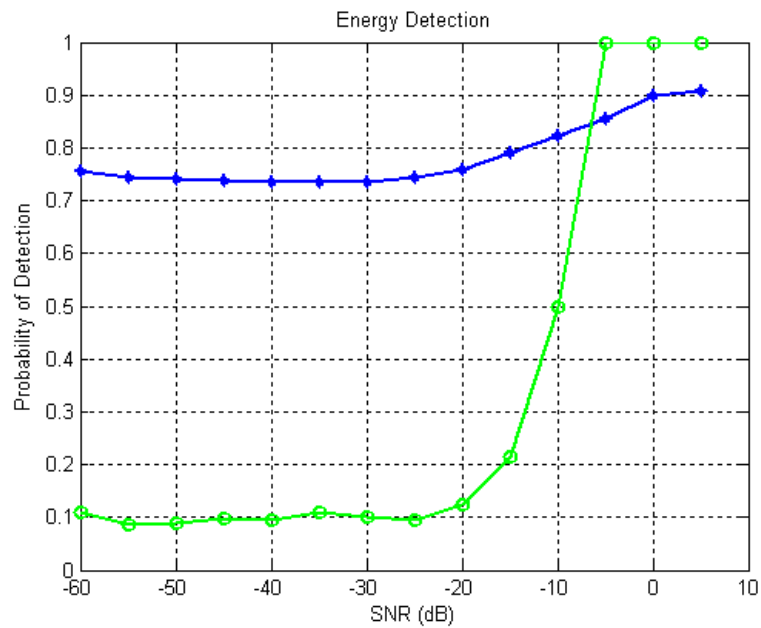


Figure 59 ED vs. Blind Technique - PD vs. SNR

The green plot shows the results of conventional energy detection and blue plot shows the result of novel/blind spectrum sensing technique. At first it looks like that the blue technique is performing very well on very low SNRs too. The probability of false alarm will give the complete picture.

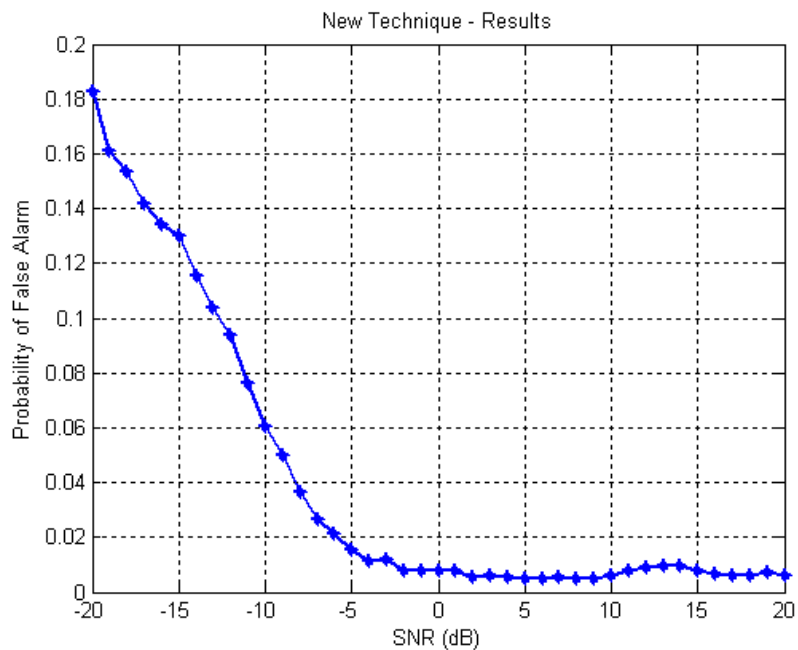


Figure 60 Blind Technique - Probability of False Alarm

As it can be seen that probability of false alarm is increasing at low SNR values, so high probability of detection will be of no use.



### 3.2.5.10.4 Probability of Missed Detection

Probability of missed detection is calculated to estimate the effective utilization of the spectrum that is not being used by the primary user. Probability of missed detection implies that a primary user is not using a spectrum band and the decision block gives a result that spectrum is being used. In this case secondary user cannot access the band and spectrum will be wasted.

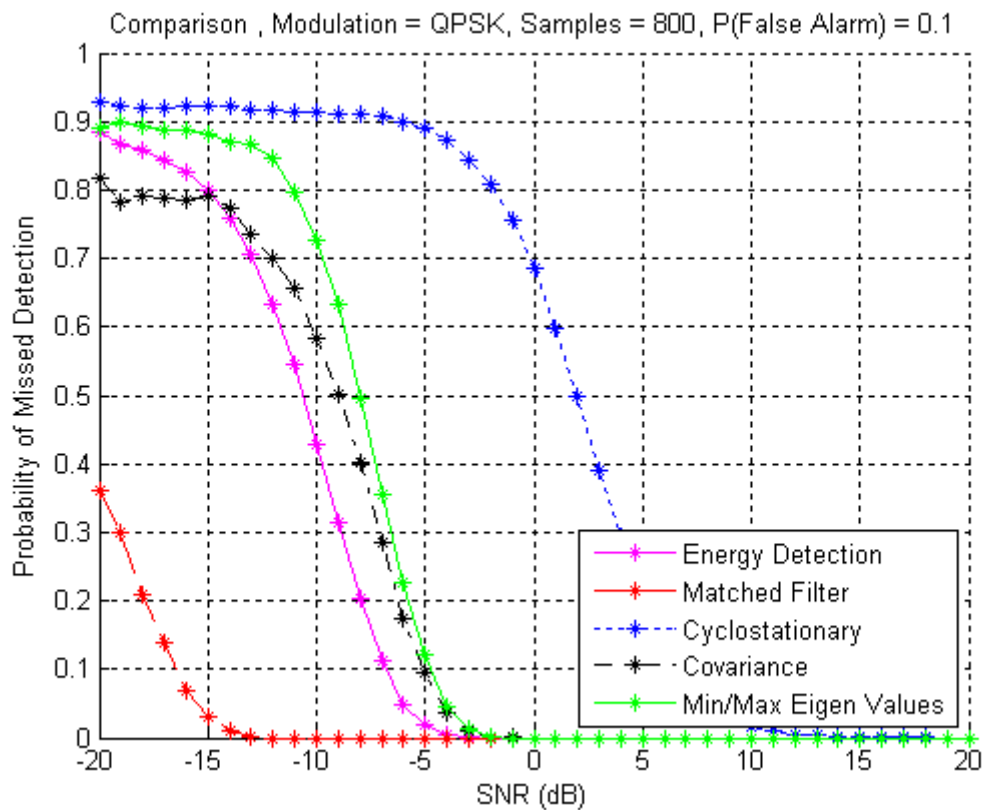


Figure 61 Probability of Missed Detection

### 3.2.5.10.5 Decision Time

This section presents a comparison of time taken by each decision block to process  $X$  number of samples. For clarification, this time calculation is purely based on processor time. It is not related to sensing time which is measured by number of samples in the literature. This test is only done by the motivation of finding out which technique can give the decision first if same number of samples is fed to all. This test does not account the performance of the decision block in terms of probability of detection and other statistical measures.

The motivation of this metric was very simple. Some of the techniques like energy detection took minutes to perform 10000 experiments for a certain number of samples, other like covariance based techniques needed one hour to perform 50 experiments for the same number of samples. Also note that the stated time is measured from the time data is fed to the decision block to the time where test statistic is compared to the threshold for decision. No extra processing, plotting graphs or printing variables was done during this time.

The graph below shows the average time taken for single run of decision block.

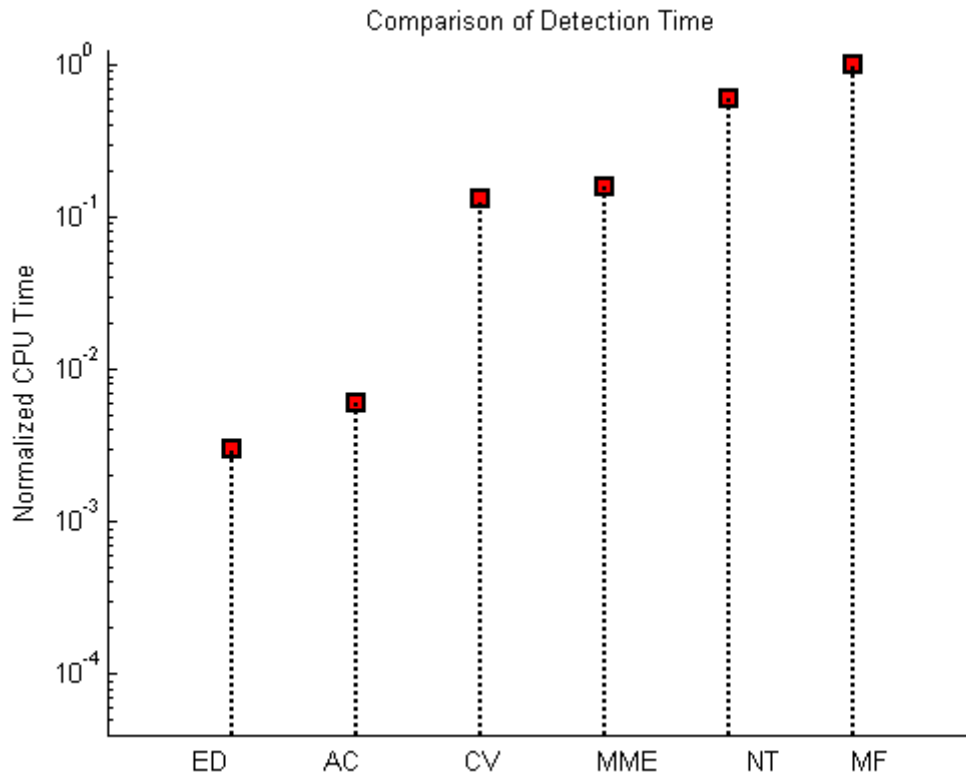


Figure 62 Decision Time

*ED = Energy Detection*

*AC = Cyclostationary Detection*

*CV = Covariance based Detection*

*MME = Minimum Maximum Eigen Values*

*NT = Novel Technique (Blind)*

*MF = Matched Filter*

The number of samples fed to each block was 30912, which is equivalent the length of OFDM data generated when number of frames = 2 and length is  $14 \times$  number of frames.

The measurements showed the energy detection block was the fastest and matched filter based detection took longest time.

### 3.2.5.11 Summary

In the first phase, the task of performance evaluation of spectrum sensing techniques was carried out. The methods evaluated included Energy Detection, Matched Filter based Detection, Cyclostationary feature based Detection, Covariance based Detection Minimum Maximum Eigen value based detection and a blind technique. These techniques can meet the requirements under specific conditions, but each has their own limitations and benefits. Energy detection requires knowledge of the noise power. Covariance based methods utilize correlation of samples with different delays. Maximum Minimum eigen value based technique is to some extent noise resistant. Matched filter can be used when we have knowledge of the signal and cyclostationarity is used when we don't. A blind technique discussed and evaluated which is designed for OFDM systems and works on the difference of energy at the sub-band level.

The theoretical ROCs for different SNR were plotted and verified with the experimental curves, it was seen that reported theoretical probability of detection from simulations was slightly higher than the experimentally observed values. The results were presented in terms of Probability of

Detection, Probability of False Alarm and Probability of Missed Detection. The summary of observations on all techniques is as follows:

- The number of samples (sample size) has a major impact on the performance of all techniques.
- The probability of false alarm had the least performance impact. Higher probability of false can lead to collision with the primary signal, so it needs to be set at reasonably low level e.g. 5%.

### ***3.3 Results analysis and conclusions***

Platforms related to Scenario 1 simulate/emulate conditions where terminals are out of infrastructure coverage and an operator-governed ON needs to be created in order to serve the out-of-coverage users. Results from various implementations show that as less ON nodes are used, then the duration of connections of the ON in terms of energy tends to decrease (since the ON nodes are more stressed in terms of load, as the same load passes through less nodes, so energy consumption of these few nodes is expected to be increase). Moreover, when using opportunistic networking, the direct connection is used in cases of good direct coverage; else a relaying device could be used in order to obtain always the best available connection from each situation.

In addition, according to obtained measurements for energy consumption of non-moving laptops, it is shown that there is no substantial difference in terms of power consumption between LAN, WLAN (with one user having all resources, two users sharing the available resources, etc.) and 3G (Macro BS based connection). On the other hand, a notable difference is identified for Femto BS i.e., whenever a highly efficient Femto BS network is available, it should be preferred over standard WLAN and 3G (Macro BS) connections. Finally, the performance comparison of spectrum sensing techniques has been evaluated. The methods evaluated included Energy Detection, Matched Filter based Detection, Cyclostationary feature based Detection, Covariance based Detection, Minimum Maximum Eigen value based detection and a blind technique. Specific result sets on all these methods are included in section 3.2.5.

In general, the prototypes created for the scenario 1 have successfully focused on opportunistic coverage extension and prove that the proposed coverage extension techniques can be beneficial for the operator's infrastructure in order to be able to satisfy users who cannot connect directly to the operator's infrastructure. Also, techniques for the detection of spectrum opportunities have been extensively evaluated in order to tackle issues of topology creation (which nodes are able to participate in an ON) and spectrum assignment. Also, energy consumption of connected terminals has been measured with live prototypes and simulations.

## 4. Validation of Scenario 2 “Opp. capacity extension”

### 4.1 Set-up of test platforms

#### 4.1.1 Platform 1 “Prototyping platform for the management of opportunistic networks”

##### 4.1.1.1 Capacity extension through neighbouring terminals

###### 4.1.1.1.1 Configuration

According to the provided implementation, a configurable number of infrastructure elements (e.g. base stations) and terminals are available in the environment. Terminals have two available interfaces (namely a 3GPP-based interface to connect to the infrastructure elements of the cellular network and a short-range interface in order to be able to connect between each other). Moreover, the mobility level of each terminal and the traffic/message generation from each terminal are configurable.

###### 4.1.1.1.2 Test plan

Regarding the scenario 2-capacity extension through neighbouring terminals, initially simulated base stations are not-congested and ONs are not needed yet, since terminals are connected directly to the infrastructure. As soon as a base station experiences congestion, due to high traffic, terminals which have the ability to connect to neighbouring terminals will connect to each other in order to gain to a nearby, non-congested base station. To that respect, the previously congested base station will be offloaded and also terminals will be served with better quality of communication by neighbouring, available base stations. The aforementioned approach is visually represented in the figure that follows. Figure 63a shows the situation before the congestion and therefore before the ON creation, while Figure 63b depicts the created ONs after the solution enforcement.

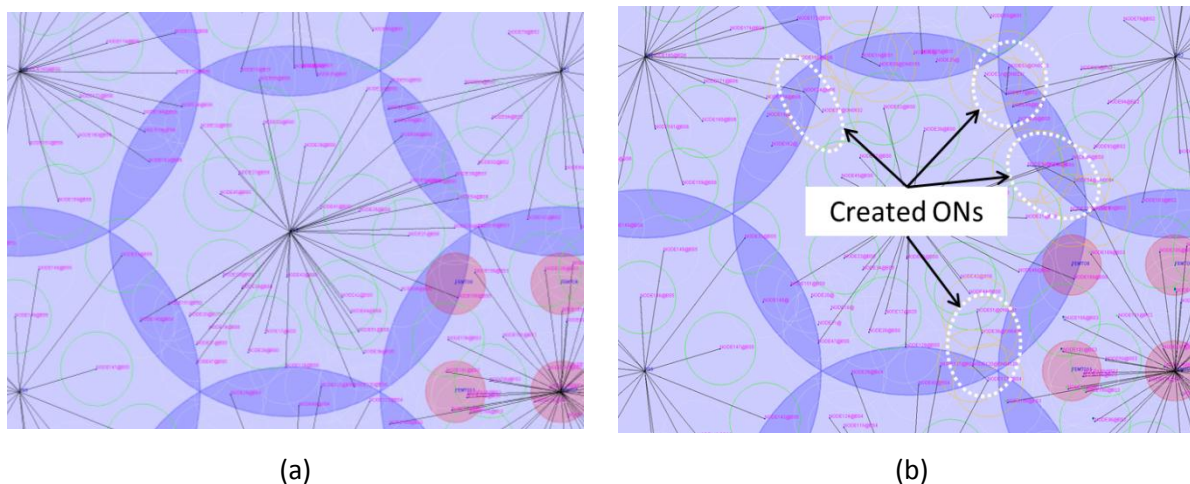


Figure 63: Implementation of capacity extension through neighbouring terminals

##### 4.1.1.2 Capacity extension through femtocells

###### 4.1.1.2.1 Configuration

According to the provided implementation, a configurable number of infrastructure elements (e.g. base stations) and terminals are available in the environment. The mobility level of each terminal and the traffic/message generation from each terminal are configurable. Moreover, each terminal has the ability to connect via a 3GPP-based interface to a base station or an available femtocell.

#### 4.1.1.2.2 Test plan

Regarding the scenario 2-capacity extension through femtocells, initially simulated base stations are not-congested and offloading to femtocells is not necessary yet, since terminals are connected directly to the infrastructure. As soon as a base station experiences congestion, due to high traffic, terminals which have the ability to connect to nearby, available femtocells will do so. To that respect, the previously congested base station will be offloaded and also terminals will be served with better quality of communication by nearby, available femtocells. Furthermore, according to the proposed algorithm (energy-efficient resource allocation [19]), the power level of each femtocell which acquires traffic, is adjusted in order to consume as low energy as possible (by covering at the same time the offloaded terminals).

The aforementioned approach is visually represented in the figure that follows. Figure 64a shows the problematic situation where all terminals are served through the base station, while Figure 64b depicts the created ONs after the assignment of terminals and power levels to femtocells.

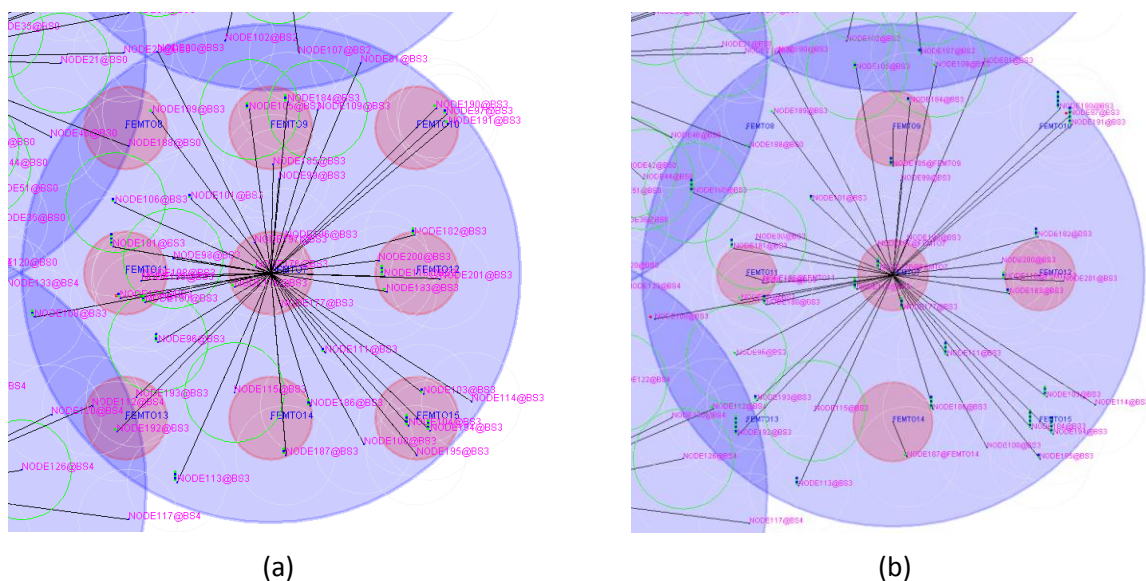


Figure 64: Implementation of capacity extension through femtocells

### 4.1.2 Platform 2 “Opportunistic networking demonstrator”

#### 4.1.2.1 Configuration

The opportunistic networking demonstrator will be used in the same configuration as described in scenario 1, see section 3.1.2.1.

#### 4.1.2.2 Test plan

The tests will be executed similarly as described in scenario 1, see section 3.1.2.2.

In difference to scenario 1 (coverage extension), the focus of this test is to compare the throughput at the cell edge between the standard case (direct coverage, ON disabled) with the case where the ON is enabled and a relaying device is used to improve throughput at the edge of the cell.

### 4.1.3 Platform 4 “Opportunistic ad-hoc network demonstrator”

#### 4.1.3.1 Configuration

The opportunistic networking demonstrator will be used in the same configuration as described in scenario 1, see section 3.1.2.1. Indeed, the scenario 2 deals with opportunity capacity extension. As the algorithm tackles the maintenance of the routing path and flows establishment of the already

created ad-hoc part of the opportunistic network, generic results of scenario 1 are applied on scenario 2 with no particular specificities of the application on this scenario.

#### 4.1.3.2 Test plan

The opportunistic networking demonstrator will be used in the same configuration as described in scenario 1, see section 3.1.3.2.

## 4.2 Obtained results

### 4.2.1 Results from platform 1 “Prototyping platform for the management of opportunistic networks”

#### 4.2.1.1 Capacity extension through neighbouring terminals

The platform has the ability to collect results related to energy consumption in the congested BS, in the non-congested BSs (which acquire terminals), in the terminals which switch to ON and in the terminals which act as intermediate nodes. Specifically, Figure 65a shows a reduction of the average energy consumption in the congested BS, since users have switched to alternative BSs through ONs. Also, Figure 65b shows a slight increase in the average energy consumption of the non-congested BSs, since they have acquired traffic from the congested one and Figure 65c provides an indication of the energy consumption in terminals where the intermediate experience a slight increase since they serve other users as well (through the ON), while terminals which switch to ON experience a decrease in energy consumption since they operate in a short-range interface.

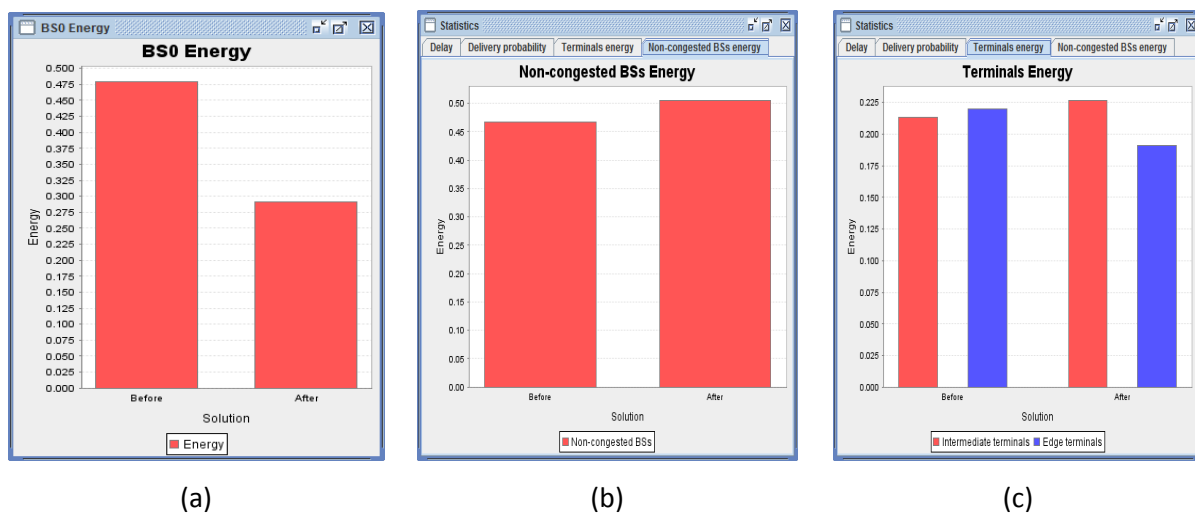


Figure 65: Indicative results from capacity extension through neighboring terminals (no mobility)

Respectively, Figure 66 a, b and c illustrate the same attributes by taking into account the impact of mobility (e.g. the case of 2m/s is visualized).

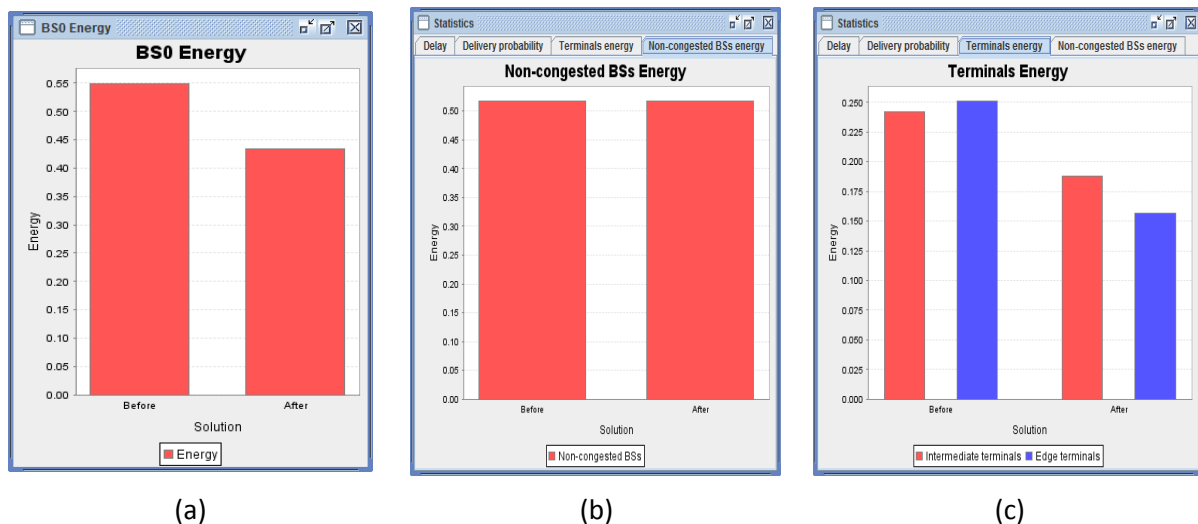


Figure 66: Indicative results from capacity extension through neighboring terminals (mobility level of 2m/s)

#### 4.2.1.2 Capacity extension through femtocells

The platform has the ability to collect results related to energy consumption and network performance in the congested BS and the terminals which switch to femtocells. Specifically, Figure 67a shows a reduction of the average energy consumption in the congested BS, since users have switched to available femtocells which can handle the additional traffic. Also, Figure 67b shows a reduction in the energy consumption of a terminal (e.g. Node181) after the attachment of the terminal to a nearby femtocell. This is also justified by the fact that less energy is needed in order to communicate with a nearby serving AP (in this case the femtocell), compared to a distant base station.



Figure 67: Indicative results from capacity extension through femtocells

Moreover, as Figure 68a suggests, the delivery delay (from the source to the destination), tends to slightly drop after the solution, while the delivery probability (i.e., the percentage of successfully transmitter messages to their destination) that is depicted in Figure 68b, tends to increase after the solution enforcement and the attachment of terminals to femtocells.



Figure 68: Indicative results from capacity extension through femtocells

#### 4.2.2 Results from platform 2 “Opportunistic networking demonstrator”

Figure 69 shows the measured throughput for the capacity extension scenario. The measurements have been performed by downloading large files with ftp from the infrastructure.

The solid blue curve shows the throughput at different locations as described in section 3.2.2.3 for the case that the cell carries no other traffic, this means, the download uses 100% of the cell capacity. When the device is located closer to the cell edge, e.g. beyond location 8, the throughput gets worse.

When an ON is created by using a relaying device similarly to the coverage extension scenario, the throughput at the cell edge can be improved as shown in the orange curve in Figure 69. For example, at location 9, the throughput can be increased from 30% to 55% when using an ON with a relaying device at location 5.



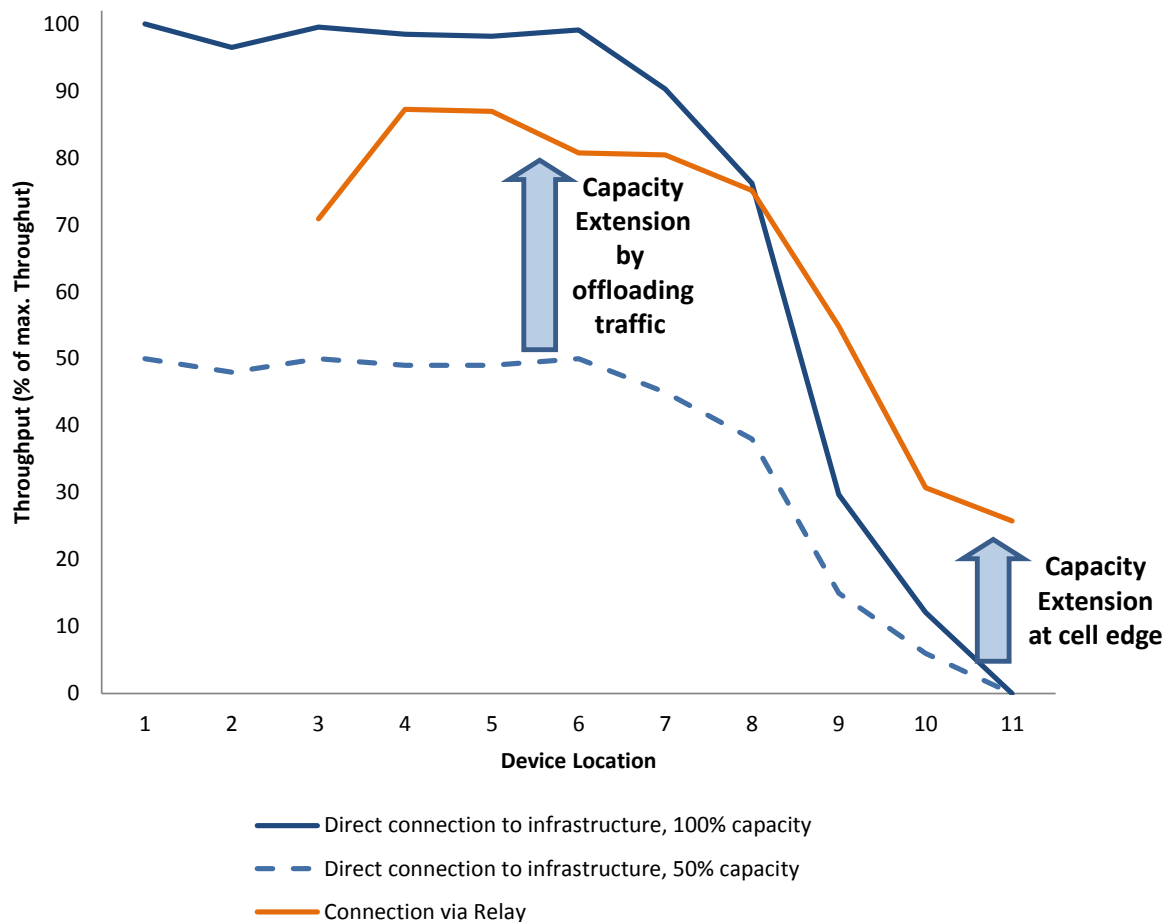


Figure 69: Throughput in the capacity extension scenario

The main target of the capacity extension scenario is a case where a cell is congested due to the demand of several users. In the prototype, this scenario was simplified by making a large file download from two devices in parallel so that the throughput is only 50% of the original throughput. This is shown in the blue dashed curve in Figure 69. When an ON is created for offloading the traffic via a relaying device towards another, less loaded cell, a throughput as shown in the orange curve can be achieved. As an example, at location 5, the throughput can be improved from 49% to 87% by using an ON.

#### 4.2.3 Results from platform 4 “Opportunistic ad-hoc network demonstrator”

As indicated in section 4.1.3, the algorithm tackles the maintenance of the routing path and flows establishment of the already created ad-hoc part of the opportunistic network, generic results of scenario 1 are applied on scenario 2 with no particular specificities of the application on this scenario. The opportunistic networking demonstrator will be used in the same configuration as described in scenario 1, see section 3.1.2.1. Results are described in section 3.2.3.

### 4.3 Results analysis and conclusions

Platforms related to Scenario 2 simulate/emulate conditions where more capacity is needed in the operator’s infrastructure (e.g. due to congestion) and an operator-governed ON is created in order to provide extra capacity to the users (e.g. by redirecting traffic from congested base stations to neighbouring non-congested or by allocating terminals to nearby femtocells). Results from various implementations show that the average end-to-end delay for the delivery of whole messages (ranging from 64KB to 1024B) tends to drop, as the terminals switch from the congested macro BS to

the ONs. At the same time the average delivery probability tends to increase since users are re-directed to non-congested infrastructure elements (or nearby femtocells), by exploiting the opportunity of closely located nodes. In addition, when an ON is created for offloading the traffic via a relaying device towards another, less loaded cell, a throughput improvement can be achieved (e.g. an increase from 49% to 87%).

In general, the prototypes created for the scenario 2 have successfully focused on opportunistic capacity extension and prove that the proposed capacity extension techniques can be beneficial for the operator's infrastructure in order to satisfy temporary demand surge, in a specific location for a given timeframe. Of course, in cases where the problem of congestion persists, new infrastructure elements have to be installed in order to cover efficiently the permanent increased demand. In addition, energy consumption of connected terminals has been measured with simulations, in order to be able to show the benefits also in the field of energy.

## **5. Validation of Scenario 3 “Infrastructure supported D2D networking”**

### ***5.1 Set-up of test platforms***

#### **5.1.1 Platform 2 “Opportunistic networking demonstrator”**

##### **5.1.1.1 Configuration**

The opportunistic networking demonstrator will be used in the same configuration as described in scenario 1, see section 3.1.2.1.

##### **5.1.1.2 Test plan**

The tests will be executed similarly as described in scenario 1, see section 3.1.2.2.

The focus of this test is to compare the throughput of a direct D2D connection with the case where the traffic is routed via the infrastructure.

#### **5.1.2 Platform 3 “Opportunistic service provision demonstrator”**

##### **5.1.2.1 Configuration**

As described in section 2.2.3, the objective of this platform is to evaluate the performance of a final service designed to run over (and capitalize on) an ON-enabled mobile network. The selected service is intended to collect the pollution emission data from sensors aboard the motor vehicles present on a certain target area. The vehicles are supposed to have one or more radio interfaces available, so that they can organise themselves into Opportunistic Networks when some situation triggers the execution of the service (e.g. when a traffic jam is detected in the area). The advantages of using an ON approach to deploy such service are:

- **Better accuracy:** The information from sensors on vehicles with no 3G interface can be collected through a different RAT and routing via neighbouring vehicles. Therefore, as more users are reached, the measures on the pollution levels will become more accurate.

The following figure shows a screenshot of the difference between the measurements when only 3G mobile nodes are reporting and when the ON is alive and more nodes send their reports:



Figure 70: Sensor reporting when the ON is off (above) and when it is established (below)

- Better radio efficiency: Data collection from all vehicles can be performed in a single infrastructure-vehicle link, as the ON will route all data towards the linked node.

To test this service, a traffic simulator is used, so that high-mobility conditions and updated cartography can be simulated. This allows testing the resilience of the service in a realistic situation where a number of vehicles enter and leave the ON as they move along the streets of the target city.

The target area selected to test the service is the crossing between two major avenues in Madrid centre, where traffic jams are usually expected at rush hours. The following picture shows the

simulator interface centred in the target area and an infrastructure node placed at the same spot where a Telefonica's 3G eNB is located.

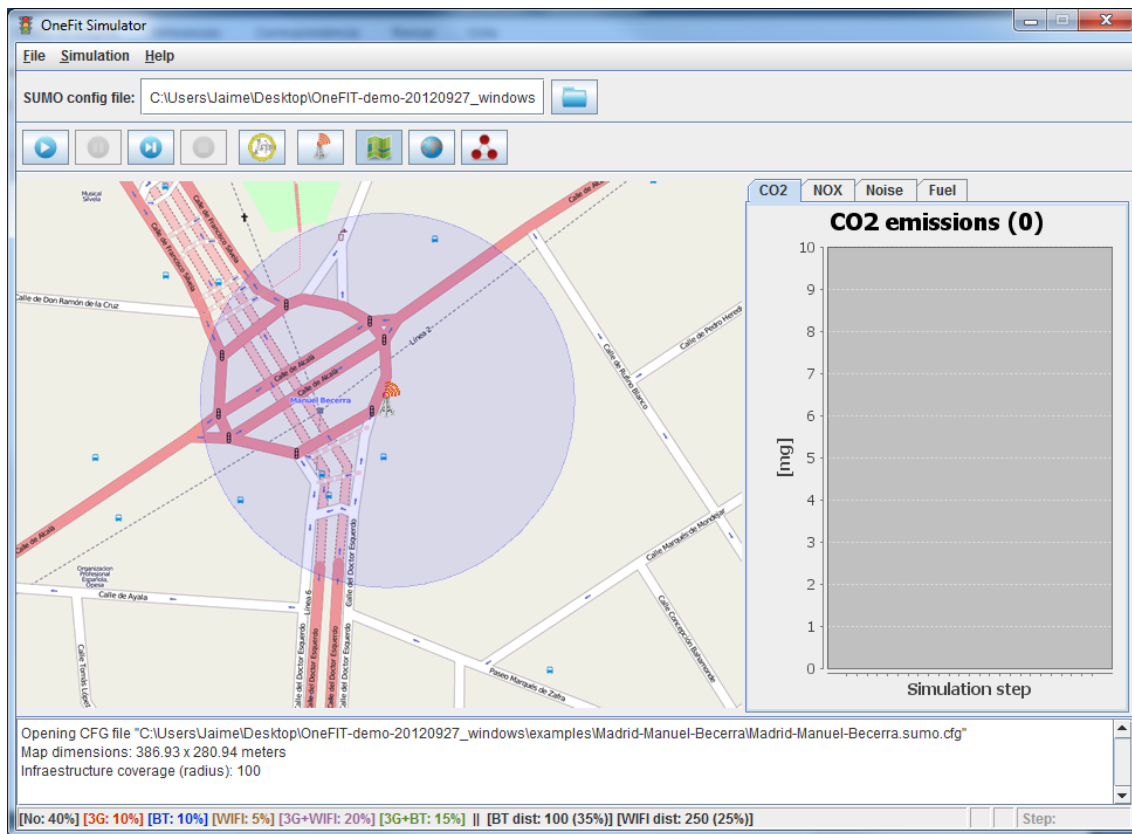


Figure 71: Target simulation area

In order to realistically simulate the traffic conditions in the target area, some demographic information (e.g. total population, age ranges and daily vehicle rates) has been collected from Madrid Council public data and properly included in the simulator.

The "Load OSM" dialog box contains the following configuration parameters:

Population	146425
Childre Age Limit	18
Retirement Age Limit	67
Car Rate	0.9
Incoming Traffic	32909
Outgoing Traffic	30000
Simulation Lenght	3600
Vehicle Types	1

At the bottom of the dialog is a "Load OSM" button.

Figure 72: Demographic configuration

Further configuration parameters are related to the simulated vehicles. For what concerns of this project, all vehicles are considered equal (they use the same consumption, pollution and noise data) and their routes through the map follow strict traffic rules.

Only one infrastructure node is considered in the simulation (a 3G-enabled node) and several mobile nodes are located on board of some of the vehicles. Mobile node interfaces are 3G, WiFi and Bluetooth; one node can have just one of these interfaces or use both 3G and one of the others.

Once the simulator has been tuned to fit the requirements of the scenario, some test have been planned, as described below.

### 5.1.2.2 Test plan

The validation of the service relies on two performance tests:

#### Low-connectivity test

In the first test, only 60% of the vehicles carry a mobile node and just half of them use double interface, which complicates the creation of dense opportunistic networks. The distribution of mobile interfaces on board the vehicles is the following:

Table 4: Test case 1 node distribution

Mobile interfaces	Proportion
3G only	10%
WiFi only	5%
BT only	10%
3G and WiFi	20%
3G and BT	15%
None	40%

This test tries to replicate a scenario where a significant amount of nodes cannot be connected to the ON, so the measurements collected by the application should not be very reliable compared to real values, and the enhancement produced by the ON should be low.

Tests on this scenario will comprise retrieving measurement data from nodes and performing a benchmarking analysis for several of the parameters collected by the application.

#### High-connectivity test

In the second test, only 10% of the vehicles are connectionless, and most of the rest carry double interface nodes, so that ONs are more easily created. The distribution of mobile nodes is the following:

Table 5: Test case 2 node distribution

Mobile interfaces	Proportion
3G only	15%
WiFi only	5%
BT only	10%
3G and WiFi	30%
3G and BT	30%
None	10%

This test mimics a scenario in which most of the nodes will be reachable by the ON, so measurements collected by the application are expected to be quite accurate after the ON is created.

Tests on this scenario will comprise retrieving measurement data from nodes and performing a benchmarking analysis for several of the parameters collected by the application.

### 5.1.3 Platform 4 “Opportunistic ad-hoc network demonstrator”

#### 5.1.3.1 Configuration

The opportunistic networking demonstrator will be used in the same configuration as described in scenario 1, see section 3.1.2.1. Indeed, the scenario 2 deals with Infrastructure supported ad-hoc networking, with direct device to device links. As the algorithm tackles the maintenance of the routing path and flows establishment of the already created ad-hoc part of the opportunistic network, generic results of scenario 1 are applied on scenario 3 with no particular specificities of the application on this scenario.

#### 5.1.3.2 Test plan

The opportunistic networking demonstrator will be used in the same configuration as described in scenario 1, see section 3.1.3.2.

### 5.1.4 Platform 6 “Direct D2D communication test-bed”

#### 5.1.4.1 Configuration

The topology of the demonstration is depicted in Figure 77. The three PCs, called UE/STA1, UE/STA2 and UE/STA3 are located in different places within an office. The distance between UE/STA1 and UE/STA2 is 3.5 m, the distance between UE/STA1 and UE/STA3 is 15m, and UE/STA2 is located 15.5m far from UE/STA3. The office contains many obstacles (persons, tables, computers, desks, walls etc.) affecting the wave propagation and inducing shadow fading in addition to multipath induced fading which is due to multipath propagation. On each UE/STA are installed “Chanalyzer Pro”, “CommView for Wi-Fi” and “Ping Test Easy”. Before the WLAN configuration algorithms run from the WLAN manager, we make measurements in Wi-Fi channels using “Chanalyzer Pro”. We consider only Wi-Fi channel 3 and channel 11 for the demonstration. The goal of the demonstration is to perform the proposed WLAN configuration algorithms (Cf. OneFit D4.3 for more detail) in order to select a compliant couple (AP, channel) configuration that fulfils given 3GPP QCI requirements. We assume that the QCI conditions imply per-link PER requirement of 1%, that is, the chosen configuration must ensure 1.00% PER for each link in the network. In order to estimate the performance of the proposed algorithms, we estimate the PER for each link for each possible couple (AP, channel) configuration. We then compare the different configurations by expecting that the compliant configuration returned by our algorithms is among the best configurations in the per-link PER point of view.

Next, we describe the software used for the measurements: “Chanalyzer Pro”, “CommView for Wi-Fi” and “Ping Test Easy”.

##### 5.1.4.1.1 “Chanalyzer Pro” from METAGEEK

“Chanalyzer Pro” allows monitoring and visualizing Wi-Fi channels. A screenshot is represented in Figure 73. It also provides Channel Table which gives the occupancy of the various Wi-Fi channels.

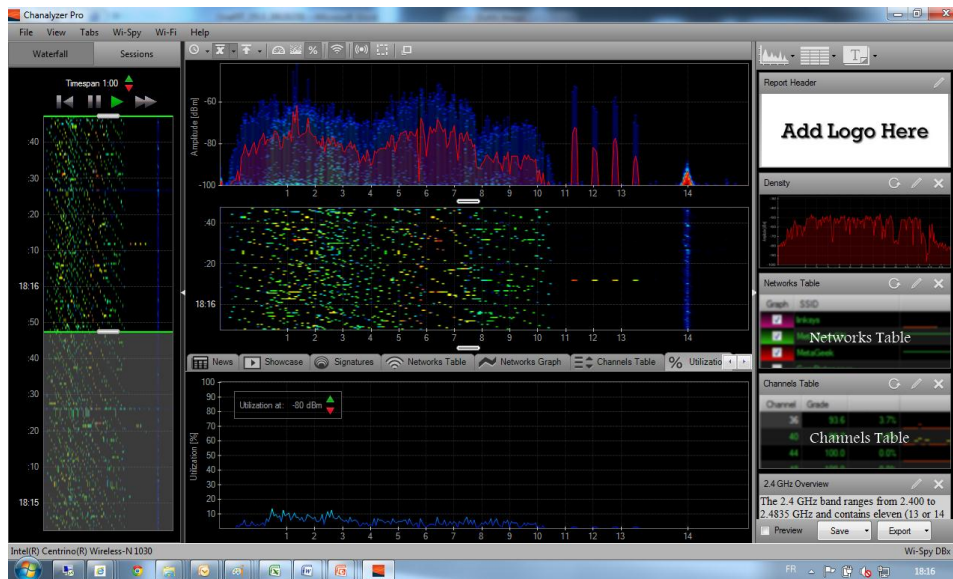


Figure 73: Screenshot of Chanalyzer Pro.

The Channel Table grades each Wi-Fi channel based on the RF activity within its given time span. This table is used in pre-deployment of the WLAN because it considers all RF noise occurring within Wi-Fi channels whether it is Wi-Fi or non-Wi-Fi. The Channel Grade is a weight for each freq/amp point based on how close it is to the center of the channel and its amplitude. The utilization is a relative score to help determine if a channel is usable or not. It measures how much RF activity is affecting the channel. It is weighted so that signals near the center of the channel have a greater effect on the utilization score. The average is a measurement of the average power within the channel frequency range. The max value is the highest amplitude point captured within the Wi-Fi channel frequency range. An example of Channel Table from “Chanalyzer Pro” is depicted below.

Table 6: Example of Channel Table from Chanalyzer Pro

Channel	Grade	Utilization	Average	Current	Max	Noise Floor	Access Points
1	83.5	7.9%	-72.0	-72	-55.5	-99.5	0
2	81.5	8.7%	-70.5	-72	-54.0	-99.5	0
3	82.3	8.6%	-71.0	-73	-54.5	-99.5	0
4	86.0	6.8%	-72.5	-74	-56.0	-100.5	0
5	91.6	4.0%	-74.5	-76	-58.0	-101.5	0
6	94.9	2.7%	-77.0	-76	-58.0	-102.0	0
7	97.9	1.1%	-79.0	-80	-59.0	-102.5	0
8	99.4	0.2%	-76.5	-102	-56.5	-103.0	0
9	99.4	0.2%	-76.5	-102	-56.5	-103.0	0
10	99.4	0.2%	-79.5	-102	-59.5	-103.0	0
11	99.6	0.2%	-79.5	-102	-59.5	-103.0	0
12	99.7	0.1%	-82.0	-102	-62.0	-103.0	0

#### 5.1.4.1.2 “Ping Test Easy”

Ping Test Easy is used to ping a device using its IP address to check network connection. It can save IP address and hosts name. Intuitive interface shows the route, hosts, packet loss percentage (that we assume to be an estimation of the PER), and min/max/average response times. The ping results can be copy to the clipboard or export to a text file. We use “Ping Test Easy” in order to estimate the PER. A screenshot of Ping Test Easy is represented in Figure 74.



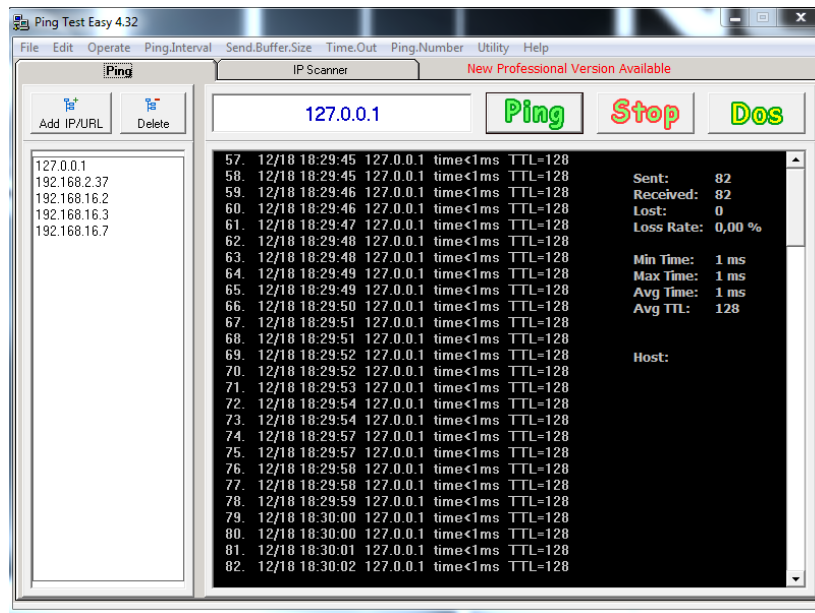


Figure 74: Screenshot of Ping Test Easy.

#### 5.1.4.1.3 “CommView for Wi-Fi” from TAMOSOFT

CommView for Wi-Fi is a powerful wireless network analyzer for 802.11 a/b/g/n networks. It allow capturing every packet on the air to display important information such as the list of access points and stations, per-node and per-channel statistics, signal strength, a list of packets and network connections, protocol distribution charts, etc. By providing this information, CommView for Wi-Fi can help to view and examine packets. For our demonstration, we use CommView for Wi-Fi only to estimate the transmit power of the UE/STA. It also allowed us to visualize the packets exchanged between the UE/STA. Figure 75 depicts a screenshot of nodes statistics measurements.

MAC Address	Channel	Type	SSID	Encryption	Signal	Rate	Bytes	Packets	Retry	ICV Err...
AP_DLINK	11	AP	PINO...	WPA-CCMP	51/69/81	1/5.78/54	122,801	1,249	66	0
LinksysGro:60:89:D5	11	STA		WPA	1/69/78	1/32.44/48	27,549	377	0	0
AP_DLINK	161	AP	PINO...	WEP	23/50/63	6/46.41/54	2,299,698	53,090	551	0
Proxim	161	STA		WEP	41/61/80	6/53.2/54	1,907,059	25,669	124	0

Figure 75: Screenshot of CommView for nodes transmit power measurements.

#### 5.1.4.2 Test plan

The test consists in measuring the PER of each link for each couple (AP assumption, channel) configuration. Having 3 UE/STA and considering 2 channels, we then have 6 possible configurations

for the test: configuration 1 = (AP= UE/STA1, channel # 3), configuration 2 = (AP= UE/STA1, channel # 11), configuration 3 = (AP= UE/STA2, channel # 3), configuration 4 = (AP= UE/STA2, channel # 11), configuration 5 = (AP= UE/STA3, channel # 3) and configuration 6 = (AP= UE/STA3, channel # 11) . For each configuration, there are 4 links as shown in Figure 76.

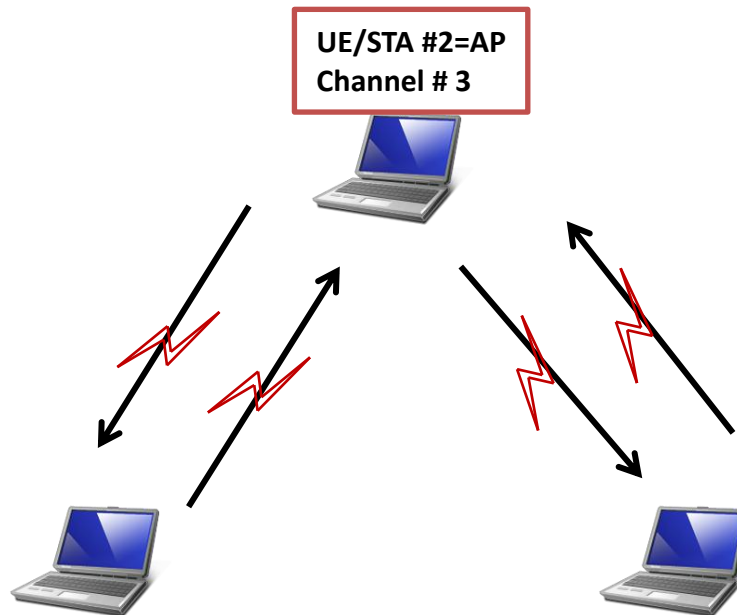


Figure 76: Example of configuration with UE/STA2=AP assumption operating in channel 3.

For each configuration, Ping Test is made between the UE/STA using the free software “Ping Test Easy” in order to estimate the per-link PER. The per-link PER is estimated by measuring the ratio between the lost response packets and the number of sent pings to a given device. At the end, we plot the PER in function of the configuration id, then we seek for the configuration(s) where all the per-link PER are lower than the threshold of 1%.

### 5.1.5 Platform 8 “Spectrum opportunity identification and spectrum selection test-bed”

In order to illustrate the testbed operation, some validation and performance results of spectrum opportunity identification and spectrum selection functionalities are presented in the following.

#### 5.1.5.1 Configuration

##### a) Configuration for evaluating the spectrum opportunity identification

The indoor office scenario illustrated in Figure 77 is considered. The environment where the testbed operates includes the presence of two WiFi access points (AP5 and AP6) that occupy channels at 2.412 GHz and 2.432 GHz. The testbed with the ON is located in room R1.

To test the spectrum opportunity identification algorithm, the measurement procedure considered the total band from 2.4 GHz to 2.5 GHz subdivided in 1000 portions of 100 kHz. Energy detection sensing was performed for each portion during 100 ms. The threshold to detect that a portion is available is set using the following procedure: (i) the USRP antenna was replaced with a matched load (i.e., a 50 ohm resistor); (ii) the Cumulative Distribution Function (CDF) of the thermal noise was calculated; (iii) a threshold between thermal noise and signal energy was selected considering a false alarm probability equal to 1%.

The maximum number of spectrum portions of a block has been set to  $P_{max}=290$ .

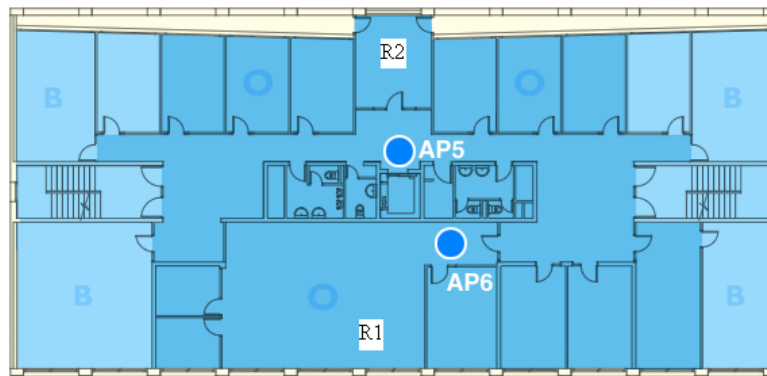


Figure 77: Considered scenario for testing the spectrum opportunity identification functionality

### b) Configuration for evaluating the spectrum selection

In the scenario illustrated in Figure 13 and Figure 14, the two terminals forming the ON (i.e., USRP#2 and USRP#3) need a spectrum block to transmit data under the infrastructure (i.e., USRP#1) control. Following the ON creation procedure, the allocated spectrum block is decided by the infrastructure during the ON-Negotiation procedure based on the spectrum opportunity identification executed by USRP#1 in the ISM 2.4 GHz band. The identification procedure is the same explained above, but now averaging the measurements during a period of 10s and with  $P_{max}=200$ . Once the spectrum is assigned, USRP#2 is the data transmitter and USRP#3 the receiver. The experiment assumptions for the communication between terminals are given in Table 7.

In the considered experiment, an additional AP has been set-up as an interference source that can be manually configured in the spectrum block allocated to the link between USRP#2 and USRP#3, as seen in Figure 78.

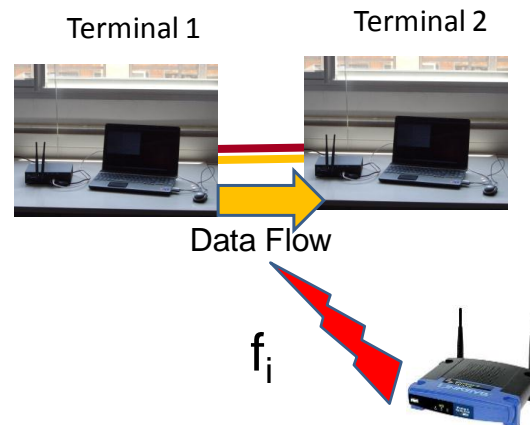


Figure 78: Set-up of an external interference source

USRP#2 periodically monitors the efficiency in the data transmission as the ratio between successfully transmitted data packets and total number of transmitted data packets including retransmissions. This is computed based on the received acknowledgements for each packet. When degradation in the communication is detected (i.e., efficiency is below the threshold of 80%), USRP#2 triggers the ON modification procedure, requesting a new spectrum block.

Table 7: Experiment assumptions

Parameter	Value
Modulation	GMSK
Data Rate	256 kbps
Packet Size	1500 byte
Minimum Efficiency threshold	80%
Experiment Time	20 minutes

### 5.1.5.2 Test plan

The following two tests are envisaged, based on the configurations presented in sub-section 5.1.5.1.

#### Test 1: Spectrum opportunity identification

The purpose of this test is to evaluate the behavior of the spectrum opportunity identification algorithm. For that purpose, the test will focus on the following metrics/outputs:

- Spectrum Opportunity Index (SOI): It is defined as the fraction of measurements in which a given spectrum portion has been detected as available.
- Identified spectrum blocks: It is the output of the algorithm that presents a list with the different spectrum blocks, represented by the central frequency and the bandwidth of each one.

The objective of the test will be two-fold. On the one hand the test intends to verify that the obtained SOI properly captures the actual conditions of the ISM spectrum band in the scenario under test, where a number of WiFi APs exists. On the other hand the test intends to demonstrate that the identified spectrum blocks are in accordance with the measured SOI in each spectrum portion.

#### Test 2: Adaptation of spectrum selection algorithm to interference variations

The purpose of this test is to demonstrate the capability of the spectrum selection algorithm to dynamically adapt to interference variations in the scenario under test.

For that purpose, an external interferer source will be activated in different time instants using the same frequency that the ON link. The target of the test is to show that the spectrum selection algorithm (supported by the spectrum opportunity identification algorithm) is able to reconfigure the allocated spectrum and to continue the communication between the two terminals.

The main metric considered in this test is:

- Efficiency in the data transmission: It is defined as the ratio between successfully transmitted data packets and total number of transmitted data packets including retransmissions.

It should be observed that, whenever the efficiency falls below a specific threshold the algorithm reconfigures the allocated spectrum and the efficiency increases again.

#### Test 3: Performance of spectrum selection algorithm

The purpose of this test is to evaluate the performance of the proposed fitness factor spectrum selection algorithm in relation to the random spectrum selection scheme.

In this test the ON link is configured to generate sessions with a certain average duration and an inactivity time between them, in accordance to Table 8. The required bit rate is 512 kb/s with modulation GMSK.

Moreover, the external interference is configured to operate on a specific spectrum block centred at 2.472 GHz. The activity of this external interference is automatically adjusted following the transmission patterns indicated in Table 8, considering 4 different experiments.

There is another spectrum block available centred at frequency 2.484 GHz. No external interference is configured in this spectrum block during the experiment. However, it is subject to some spurious uncontrolled interference existing in the environment. Statistics obtained in this spectrum block indicate that it is free of interference during 99.92% of the time.

Table 8: Activity patterns of the external interference and the ON link

Experiment	Average inactivity time interferer	Average activity time interferer	Average inactivity time ON link	Average session duration ON link
1	300s	300s	30s	60s
2	300s	60s	30s	60s
3	60s	300s	30s	60s
4	300s	300s	90s	120s

The test compares the performance of the following two algorithms:

- Random spectrum selection: It chooses a spectrum block randomly among the available ones.
- Fittingness factor-based spectrum selection: It chooses a spectrum block in accordance with the fittingness factor algorithm and statistics previously generated and stored about the interference behaviour in the existing spectrum blocks.

The duration of each experiment is 10 min.

Spectrum handover procedure is executed whenever the efficiency falls below 80%.

The main metrics considered in this test are:

- Efficiency in the data transmission: It is defined as the ratio between successfully transmitted data packets in the ON link and total number of transmitted data packets including retransmissions.
- Spectrum HO rate: It is defined as the ratio of spectrum handovers per unit of time that have occurred during the experiment in the ON link.

## 5.2 Obtained results

### 5.2.1 Results from platform 2 “Opportunistic networking demonstrator”

In addition to the more detailed evaluations for scenarios 1 and 2, the opportunistic networking demonstrator is also used to evaluate different cases for the data transfer between two devices.

As shown in Figure 79, four different cases are evaluated. In each case, WLAN is used and one device is downloading a large file from an FTP-Server running on the other device.

- Case 1: The two devices are in proximity of each other. A direct Device-to- Device (D2D) link is used for the file transfer.
- Case 2: The two devices are in proximity of each other, but they are not using a D2D connection. Both devices are connected to the same access point in the infrastructure. Both devices use the same WLAN channel for the connection to the access point.

- Case 3: The two devices are in proximity of each other, but they are not using a D2D connection. Both devices are connected to the same access point in the infrastructure. The devices use different WLAN channels for the connection to the access point.
- Case 4: The two devices are not in proximity of each other. Each device is connected to an access point in the infrastructure and the access points are connected via a fixed link. The access points are operated on different WLAN channels.

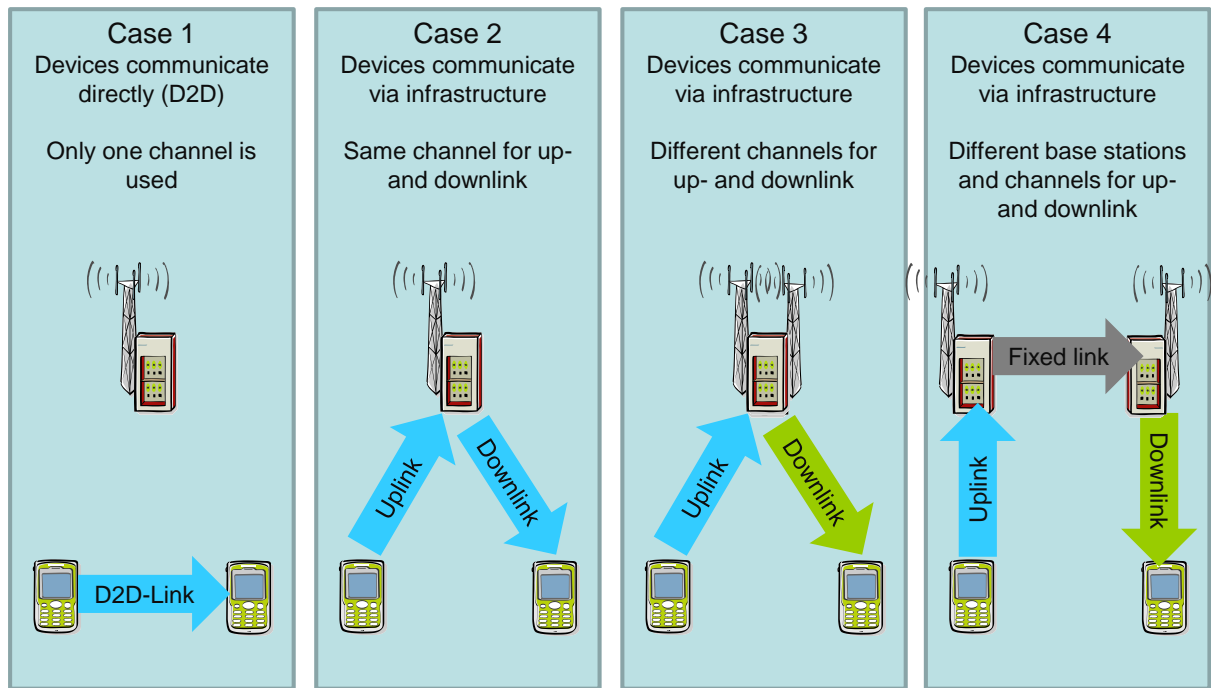


Figure 79: Different cases for transferring data between two devices

As shown in the throughput measurements in Figure 80, the throughput for the cases 1, 3 and 4 are nearly on the same level while case 2 provides only about 50% throughput.

The best result was achieved in the case 4 which is used as a reference case (100% Throughput). There the devices are out of proximity and there is no interference between the radio channels.

The direct D2D link (Case 1) has achieved 93% of the throughput of the reference case. The different throughput compared to case 4 can be caused by the fact that the access points use different hardware and larger antennas than the user devices.

Case 3 has achieved 90% of the throughput of the reference case. This reduced throughput may be caused by some interference due to a small overlap between the used WLAN channels (Channel 5 and 9).

Case 2 provides with 50% throughput of the reference case the smallest throughput. This is caused by the fact that the same channel is used for the uplink and the downlink and thus, the data has to be transferred twice on the same channel.

These results show that a direct D2D connection between two devices in proximity can either

- provide the same throughput with half the amount of radio resources (one channel instead of two channels) when comparing with Case 3 and Case 4 where different channels towards the infrastructure are used, or
- provide twice the throughput with the same amount of radio resources when comparing with Case 2 where the same channel is used for the up- and downlink.

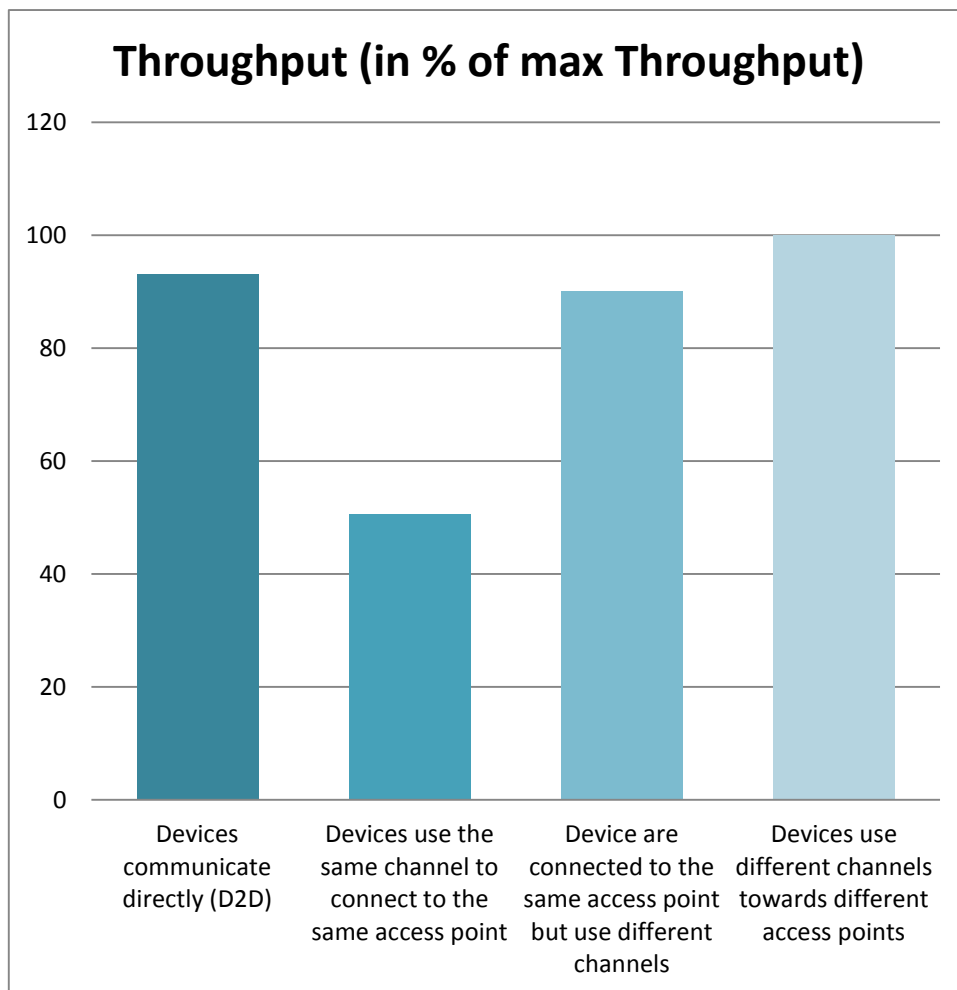


Figure 80: Throughput Measurements

## 5.2.2 Results from platform 3 “Opportunistic service provision demonstrator”

### Low-connectivity test

In this test, the number of simulated vehicles grows according to the demographic and traffic rules, reaching close to 350 vehicles in the whole area by the end of the simulation. The evolution of the number of nodes connected to the infrastructure and to the ON is the following:

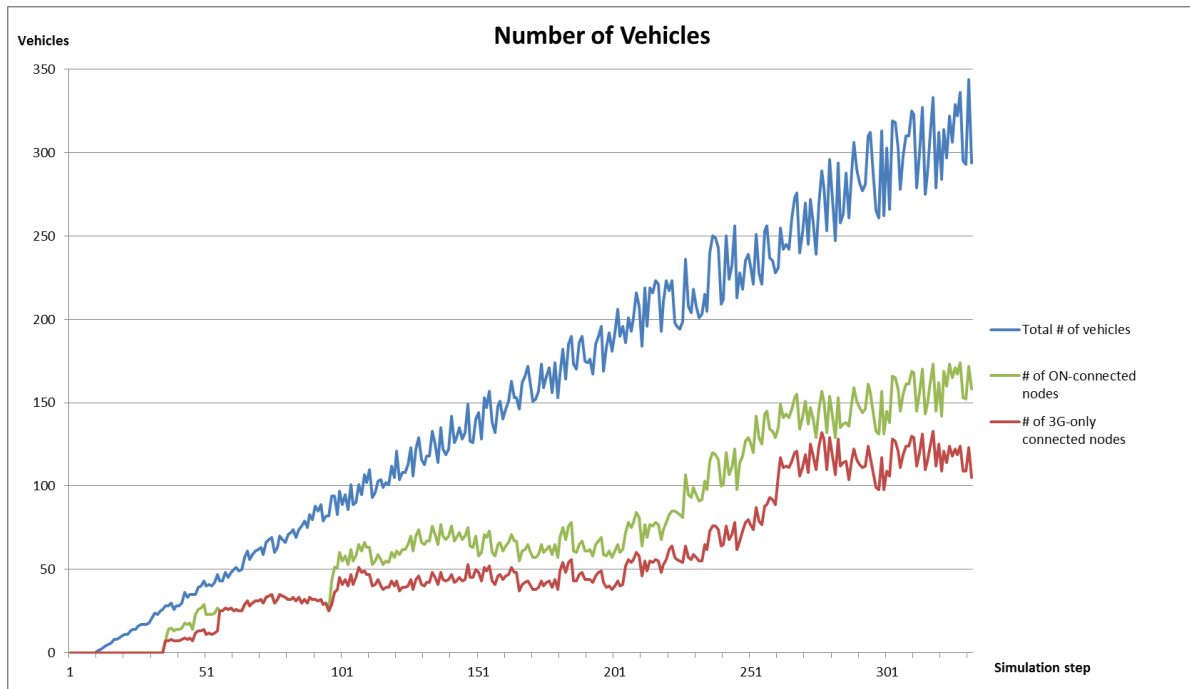


Figure 81: Number of connected nodes

Average and maximum values from this graph are the following.

Table 9: Statistics on connected nodes

	Average	Max
Total number of vehicles	160	344
Number of nodes connected to infrastructure	57	133
Number of extra nodes reached by the ON	21	56
Total number of connected nodes	77	189

The simulations show that the presence of the ON makes the number of connected nodes grow from about one-third to more than half of the existing vehicles. These figures are consistent with the mobile interface distribution of this test case shown in Table 4.

The presence of a higher number of connected nodes due to the existence of the ON helps the service obtaining more accurate measurements of the instantaneous pollution emissions in the area. The following figures depict how pollution measurements are enhanced when the ON is established:



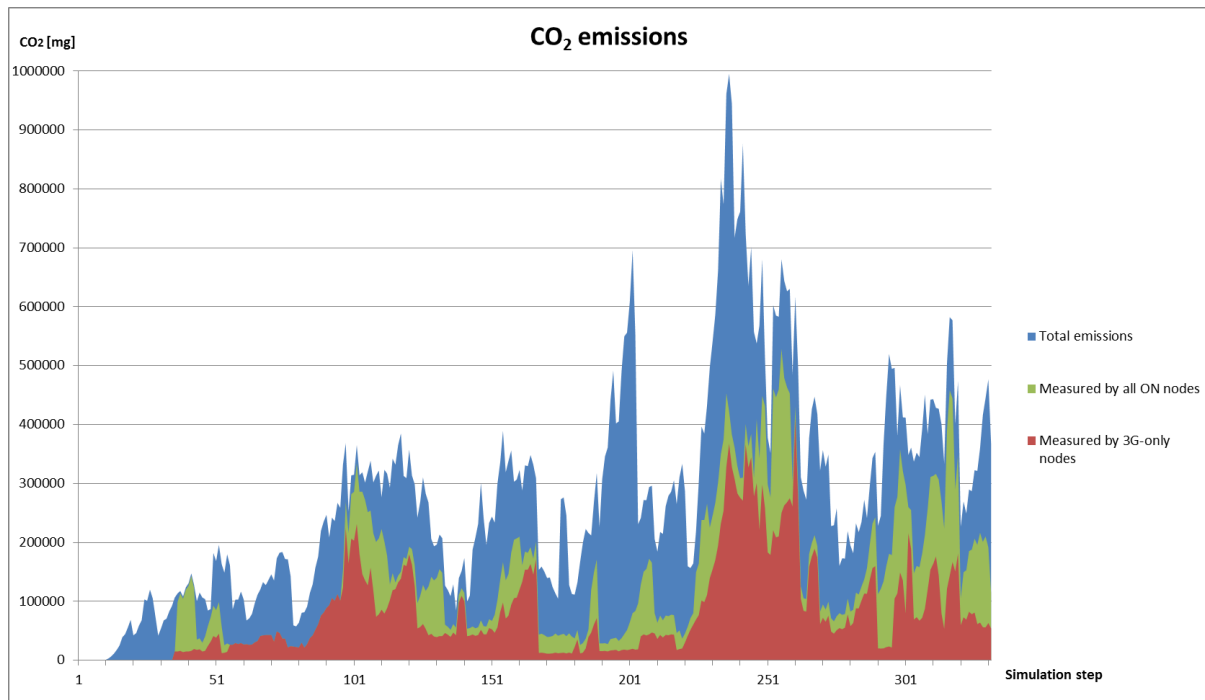


Figure 82: CO<sub>2</sub> emission measurement

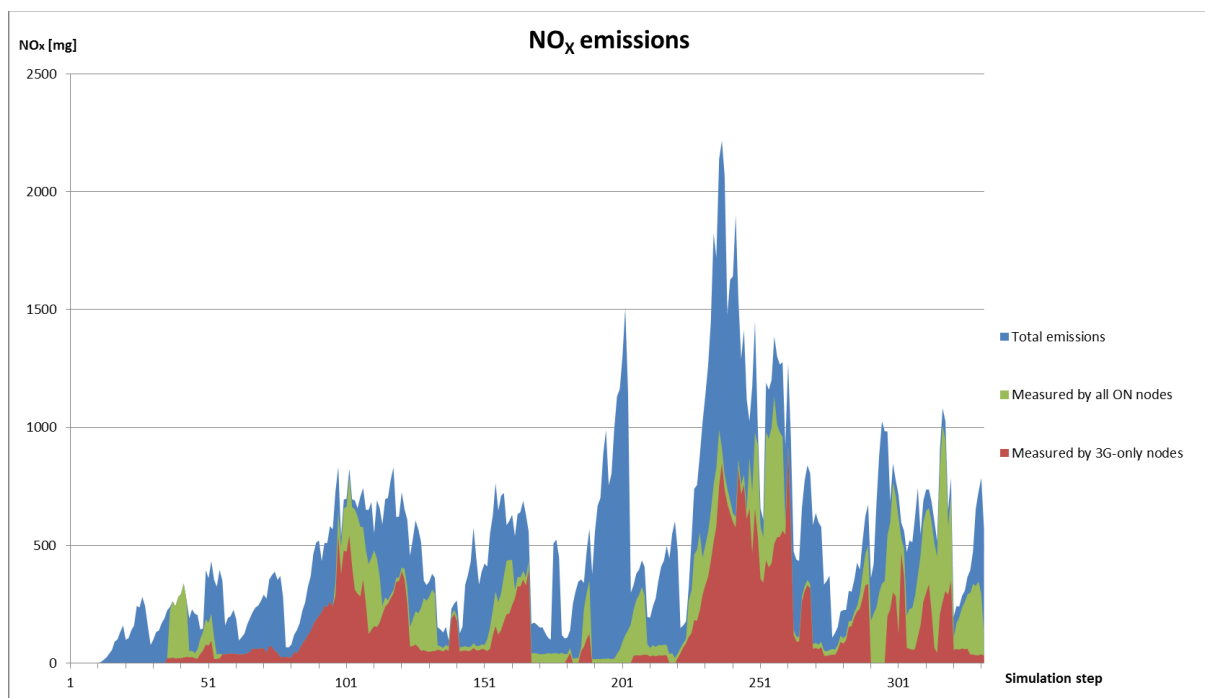


Figure 83: NO<sub>x</sub> emission measurement

The values extracted from previous figures are:

Table 10: Statistics on pollution measurements

	CO <sub>2</sub>		NO <sub>x</sub>	
	Average	Max	Average	Max
Total emissions (mg)	287006	995043	532	2217
Measurement via 3G-only nodes	89767	410670	163	905
Measurement via the ON	150506	528528	285	1133
Accuracy without the ON	31.28%	41.27%	30.59%	40.82%
Accuracy with the ON	52.44%	53.12%	53.66%	51.11%

Results show an interesting increase in the accuracy of the measurements, averaging over 20% in the whole simulation.

The application also allows measuring other traffic-related parameters with different time evolution. For example, the fuel instantaneously consumed by the vehicles, which shows a bursty behaviour, gets a similar enhancement due to the presence of the ON:

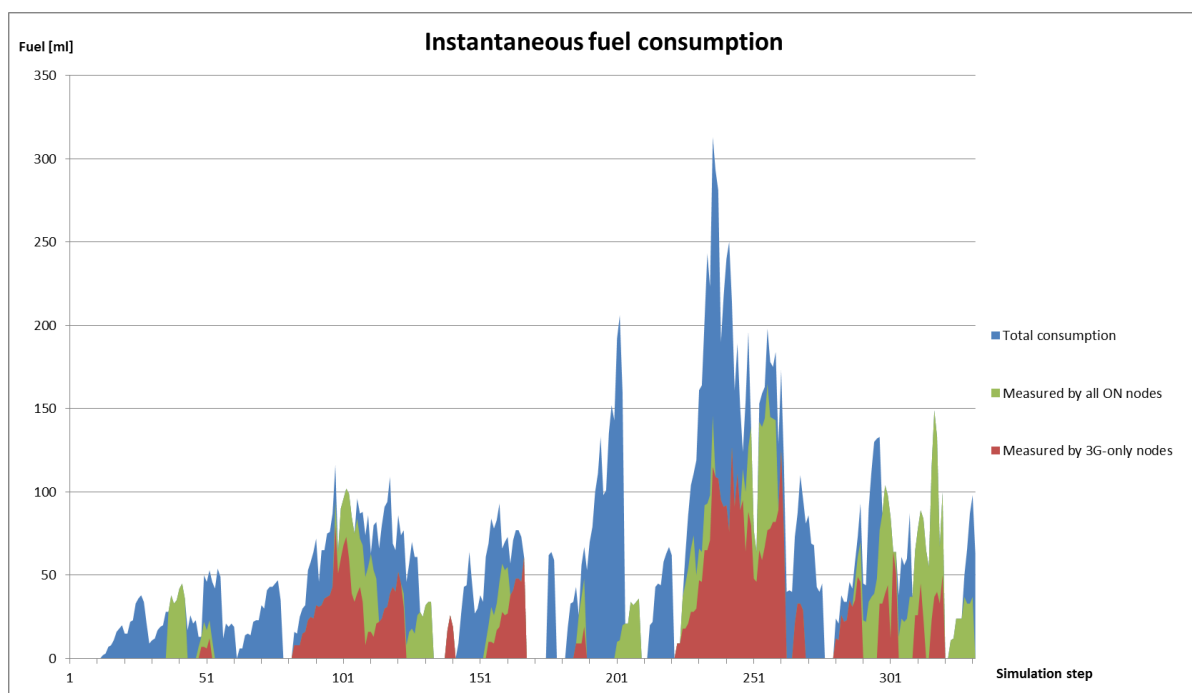


Figure 84: Fuel consumption measurement

Table 11: Statistics on fuel consumption measurements

	Fuel consumed	
	Average	Max
Total instantaneous consumption (ml)	63	313
Measurement via 3G-only nodes	19	127
Measurement via the ON	34	165
Accuracy without the ON	30.70%	40.58%
Accuracy with the ON	53.62%	52.72%

Another example: the ambient noise generated by the engines of the vehicles show a more stable behaviour, as it is measured in logarithmic units. In this case, measurements are quite accurate initially, so no great enhancement is obtained from the ON:

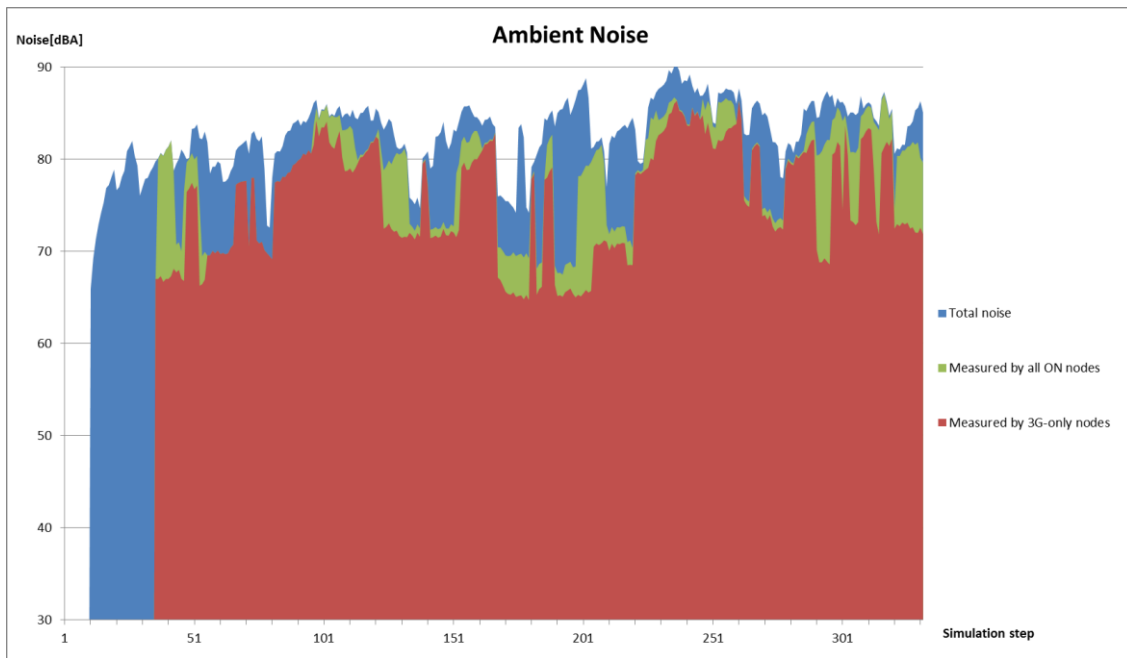


Figure 85: Generated noise measurement

Table 12: Statistics on generated noise measurements

	Generated noise	
	Average	Max
Total ambient noise (dBA)	84	90
Measurement via 3G-only nodes	79	86
Measurement via the ON	81	87
Accuracy without the ON	93.44%	95.69%
Accuracy with the ON	96.25%	96.52%

### High-connectivity test

In this test, the number of simulated vehicles grows according to the demographic and traffic rules, reaching over 300 vehicles in the whole area by the end of the simulation. The evolution of the number of nodes connected to the infrastructure and to the ON is the following:

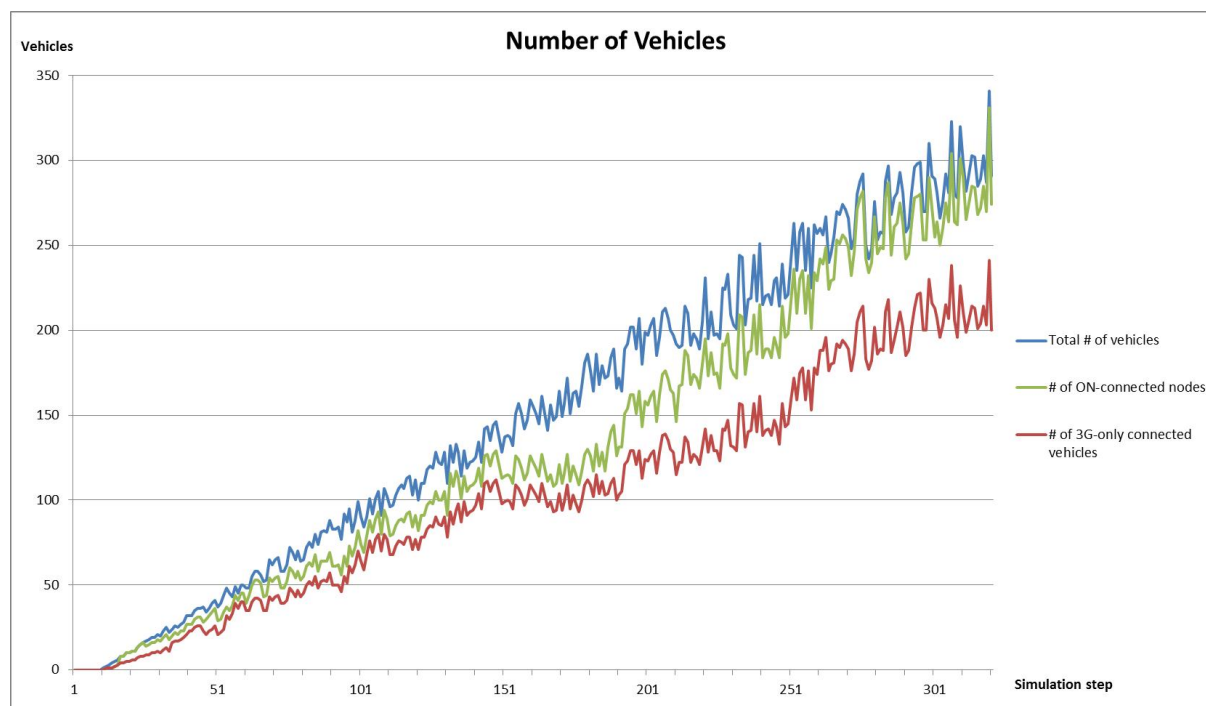


Figure 86: Number of connected nodes

Average and maximum values from this graph are the following.

Table 13: Statistics on connected nodes

	Average	Max
Total number of vehicles	155	341
Number of nodes connected to infrastructure	106	241
Number of extra nodes reached by the ON	29	90
Total number of connected nodes	135	331

As opposed to the previous test, in these simulations there is a majority of connected nodes, and once the ON is established, less than 10% of them are unreachable. These figures are consistent with the mobile interface distribution of this test case shown in Table 5.

With such a high number of connected nodes, the measurements retrieved by the application are quite accurate, but the presence of the ON greatly enhances these values as most of the nodes are reached. The following figures depict how instantaneous pollution measurements are enhanced when the ON is established in the target area:

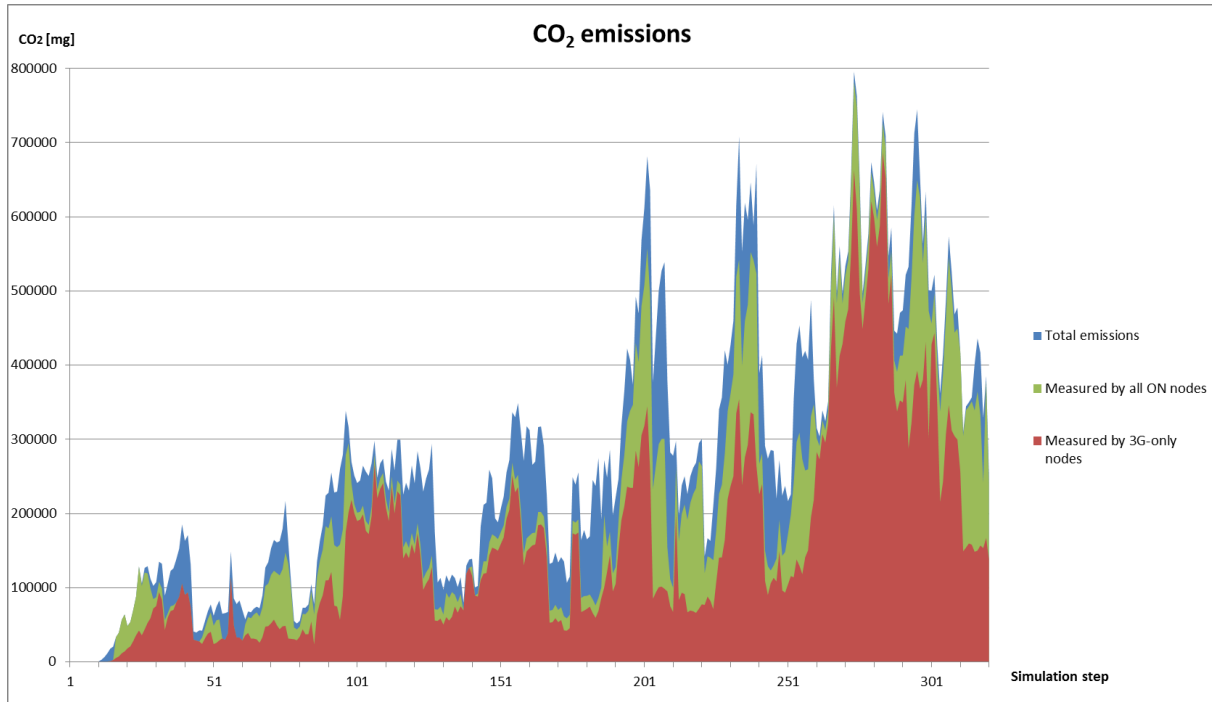


Figure 87: CO<sub>2</sub> emission measurement

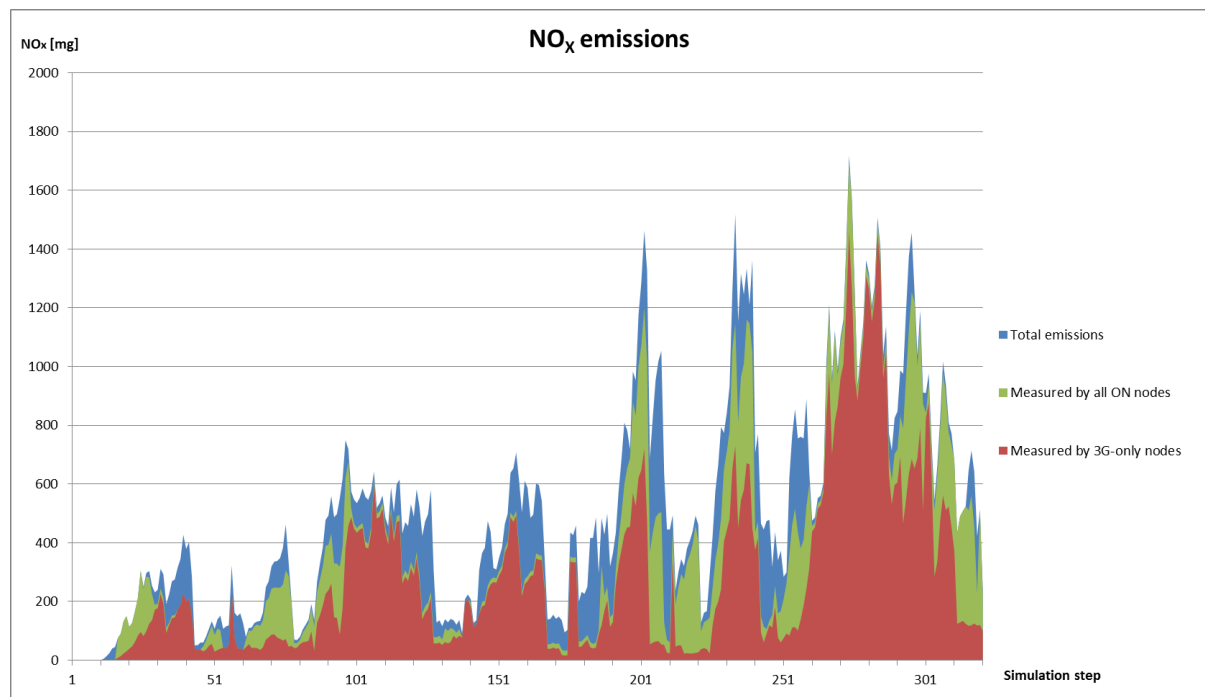


Figure 88: NO<sub>x</sub> emission measurement

The values extracted from previous figures are:

Table 14: Statistics on pollution measurements

	CO <sub>2</sub>		NO <sub>x</sub>	
	Average	Max	Average	Max
Total emissions (mg)	287006	995043	522	1717
Measurement via 3G-only nodes	89767	410670	304	1456
Measurement via the ON	240593	781751	432	1699
Accuracy without the ON	58,20%	86,23%	58,15%	84,80%
Accuracy with the ON	85,27%	98,24%	82,59%	98,95%

Results show an important increase in the accuracy of the measurements, averaging between 25%-30% in the whole simulation.

Similar enhancement values can be found on the fuel consumption measurement:

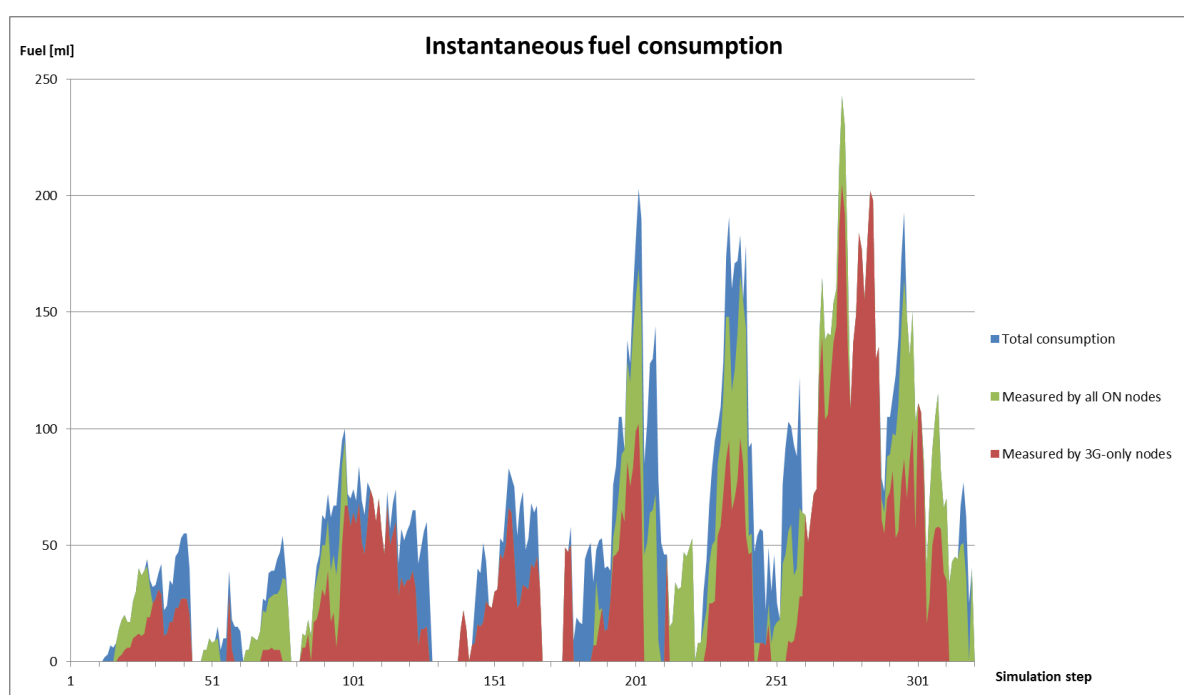


Figure 89: Fuel consumption measurement

Table 15: Statistics on fuel consumption measurements

	Fuel consumed	
	Average	Max
Total instantaneous consumption (ml)	62	243
Measurement via 3G-only nodes	36	205
Measurement via the ON	51	243
Accuracy without the ON	58,37%	84,36%
Accuracy with the ON	83,37%	100,00%

Finally, the results on a logarithmically-measured parameter are particularly good, so the effect of the ON is almost negligible:

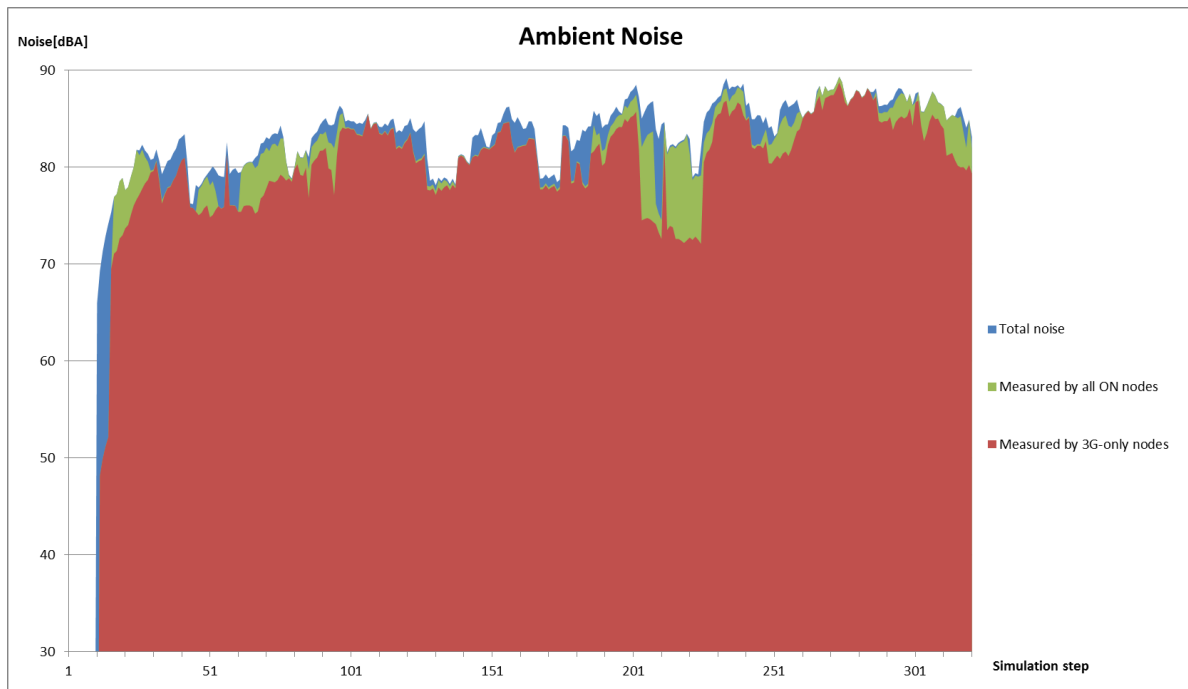


Figure 90: Generated noise measurement

Table 16: Statistics on generated noise measurements

	Generated noise	
	Average	Max
Total ambient noise (dBA)	84	89
Measurement via 3G-only nodes	82	89
Measurement via the ON	84	89
Accuracy without the ON	97,40%	99,33%
Accuracy with the ON	98,92%	99,98%

### 5.2.3 Results from platform 4 “Opportunistic ad-hoc network demonstrator”

As indicated in section 5.1.3, the algorithm tackles the maintenance of the routing path and flows establishment of the already created ad-hoc part of the opportunistic network, generic results of scenario 1 are applied on scenario 3 with no particular specificities of the application on this scenario. The opportunistic networking demonstrator will be used in the same configuration as described in scenario 1, see section 3.1.2.1. Results are described in section 3.2.3.

### 5.2.4 Results from platform 6 “Direct D2D communication test-bed”

We consider the topology depicted in Figure 91 with initial measurements in channel 3 and 11. Having 3 UE/STA, therefore there are three possible AP assumptions as shown in Figure 92, Figure 93 and Figure 94. For each AP assumption, we estimate the per-link PER in channels 3 and 11.

On the one hand, the results obtained for the test are given in table 14 and illustrated in Figure 95; we note that only the configuration 1 (UE/STA1=AP, channel 3) allows having all the per-link PER lower than the threshold 1%. On the other hand, the proposed AP and channel selection algorithm is performed with the following inputs (table 13) in order to find one configuration which meets the per-link PER requirement of 1%. The inputs “initial average signal power in channels” are measured with “Chanalyzer Pro”, while the mean transmit power of the UE/STA are measured using “CommView for Wi-Fi”. The Path loss exponent is set to 2 to reflect the fact that the environment during the measurements seems close to free space. The antenna gain of the UE/STA is set to 0 dBi.

We assume that the UE/STA use IEEE 802.11b with CCK (Complementary Code Keying) modulation and 11 Mb/s rate. For the per-link PER threshold of 1% as input, the algorithm returns the configuration 1 as the sole configuration that allows meeting the per-link PER requirements. This result is in concordance with the measurements (see Figure 95) with an error of 0.2% PER. The estimation error on the PER is due to the fact that the proposed algorithms do not take into account the channel conditions in the network, and also the algorithms assume free space condition that is far from Wi-Fi environment. Furthermore, performing the proposed power efficient WLAN AP and channel selection algorithm, it returns the configuration 2 (UE/STA1=AP, channel 11) as the most power efficient configuration, that is, the power efficiency is higher in configuration 2 than in the others. This result is in concordance with the initial channel measurements (Figure 91) where we can note that the channel 11 was the lowest occupancy channel with -79.5 dBm signal level at the position of UE/STA 1, -57.5 dBm signal level at the position of UE/STA 2 and -61 dBm signal level at the position of UE/STA 3.

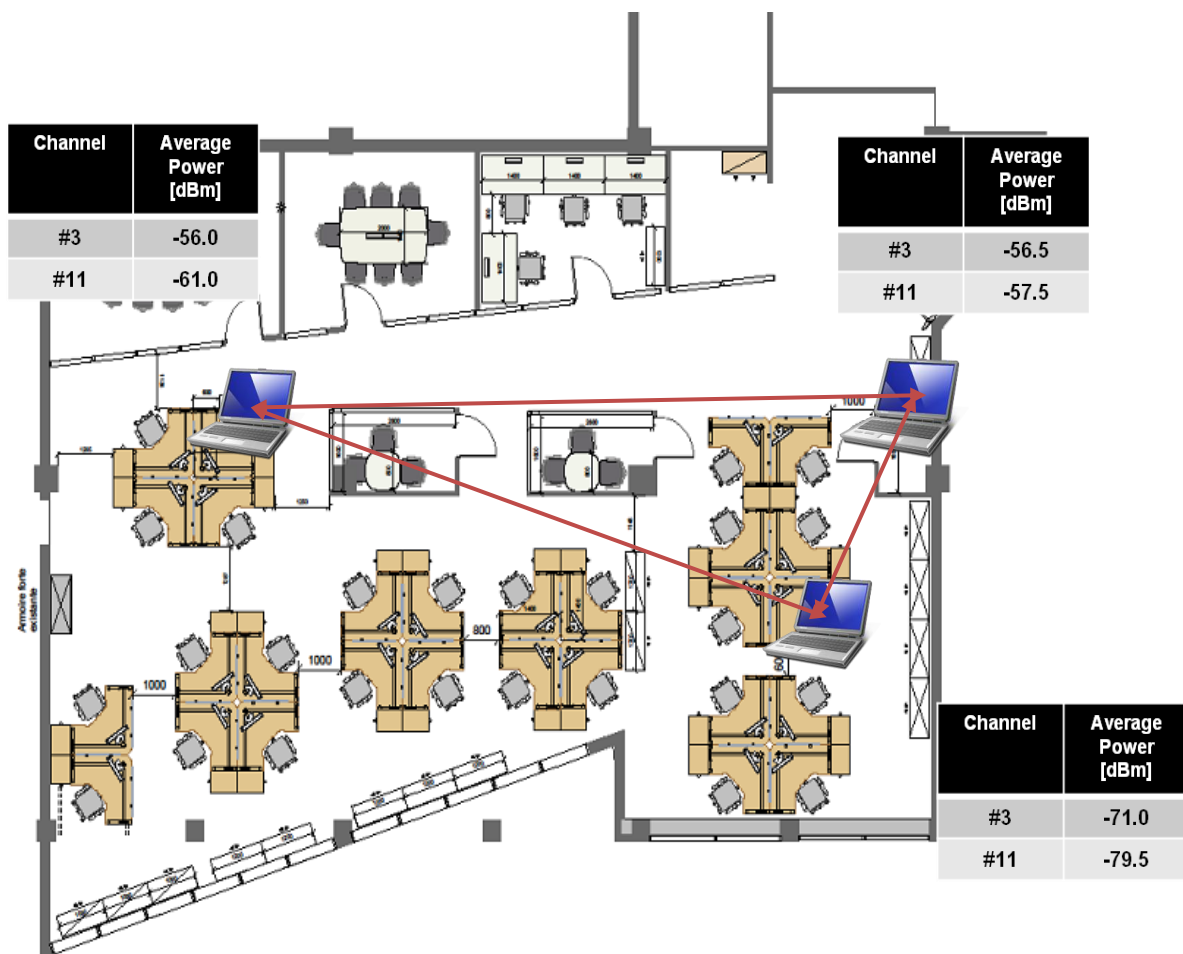


Figure 91: Initial Topology for WLAN establishment



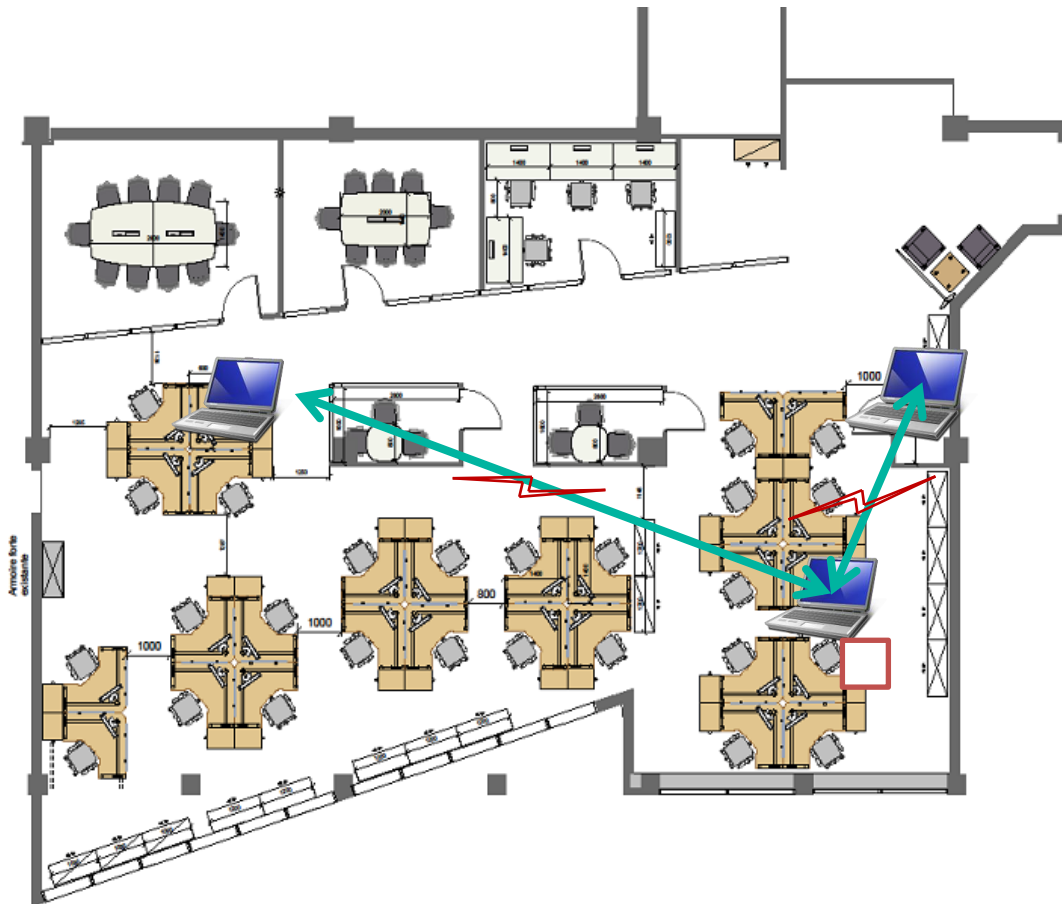


Figure 92: Configuration for UE/STA#1=AP assumption

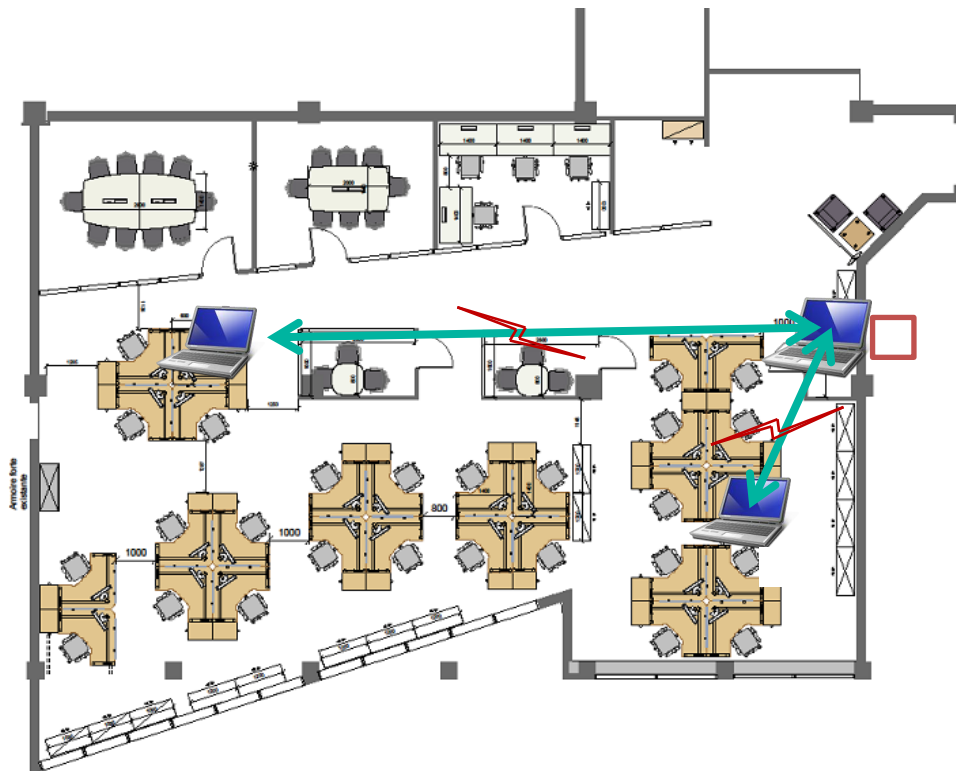


Figure 93: Configuration for UE/STA#2=AP assumption

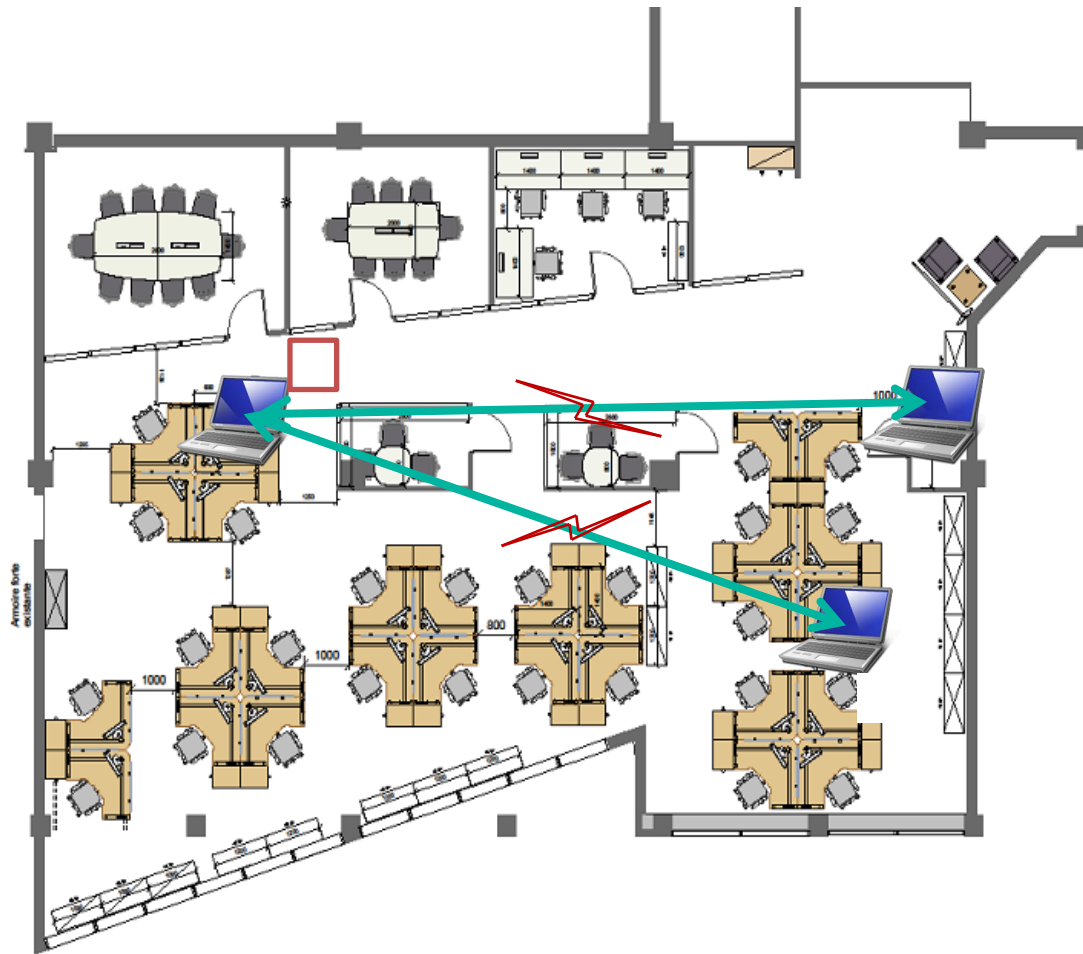


Figure 94: Configuration for UE/STA#3=AP assumption

Table 17: Inputs for proposed AP and Channel selection algorithms.

Parameter		Value
Number of UE/STA		3
Number of Channel		2
Distance between UE/STA	$d(\text{UE/STA1—UE/STA2})$	3.5 m
	$d(\text{UE/STA1—UE/STA3})$	15 m
	$d(\text{UE/STA2—UE/STA3})$	15.5 m
Initial Average Signal Power in channel #3	Position UE/STA1	-71 dBm
	Position UE/STA2	-56.5 dBm
	Position UE/STA3	-56 dBm
Initial Average Signal Power in channel #11	Position UE/STA1	-79.5 dBm
	Position UE/STA2	-57.5 dBm
	Position UE/STA3	-56 dBm
Path Loss Exponent		2
Antenna Gain		0 dBi
Channel width		22 MHz
Per-link PER Threshold		1.00%
Technology		IEEE 802.11b, CCK modulation, 11 Mbits/s rate
Mean Transmit power for UE/STA 1= AP assumption	$P_{tx}(\text{AP} \rightarrow \text{UE2})$	-24 dBm
	$P_{tx}(\text{AP} \rightarrow \text{UE3})$	-21 dBm
	$P_{tx}(\text{UE2} \rightarrow \text{AP})$	-27 dBm
	$P_{tx}(\text{UE3} \rightarrow \text{AP})$	-29 dBm
Mean Transmit power for UE/STA 2= AP assumption	$P_{tx}(\text{AP} \rightarrow \text{UE1})$	-26 dBm
	$P_{tx}(\text{AP} \rightarrow \text{UE3})$	-22 dBm
	$P_{tx}(\text{UE1} \rightarrow \text{AP})$	-24 dBm
	$P_{tx}(\text{UE3} \rightarrow \text{AP})$	-28 dBm
Mean Transmit power for UE/STA 3= AP assumption	$P_{tx}(\text{AP} \rightarrow \text{UE1})$	-25 dBm
	$P_{tx}(\text{AP} \rightarrow \text{UE2})$	-24 dBm
	$P_{tx}(\text{UE1} \rightarrow \text{AP})$	-23 dBm
	$P_{tx}(\text{UE2} \rightarrow \text{AP})$	-26 dBm

In the previous table, " $d(\text{UE/STAx—UE/STAy})$ " means the distance between UE/STAx and UE/STAy and " $P_{tx}(\text{AP} \rightarrow \text{UEx})$ " means the transmit power of AP when communicating to UEx.

Table 18: Per-link PER estimation for the various configurations

Configuration #	Detail	PER estimation
1	UE/STA #1=AP Channel #3	PER(AP→UE2) =0.87% PER(UE2→AP) =1.15% PER(AP→UE3) =1.11% PER(UE3→AP) =1.03%
2	UE/STA #1=AP Channel #11	PER(AP→UE2) =0.91% PER(UE2→AP) =1.35% PER(AP→UE3) =1.12% PER(UE3→AP) =1.21%
3	UE/STA #2=AP Channel #3	PER(AP→UE1) =1.08% PER(UE1→AP) =1.29% PER(AP→UE3) =1.00% PER(UE3→AP) =0.94%
4	UE/STA #2=AP Channel #11	PER(AP→UE1) =0.65% PER(UE1→AP) =0.90% PER(AP→UE3) =1.37% PER(UE3→AP) =1.15%
5	UE/STA #3=AP Channel #3	PER(AP→UE1) =1.03% PER(UE1→AP) =1.37% PER(AP→UE2) =0.89% PER(UE2→AP) =1.09%
6	UE/STA #3=AP Channel #11	PER(AP→UE1) =1.01% PER(UE1→AP) =0.9% PER(AP→UE2) =1.32% PER(UE2→AP) =1.11%

In the previous table, **PER(AP→UE<sub>x</sub>)** means Packet Error Rate on the link AP to UE<sub>x</sub>.

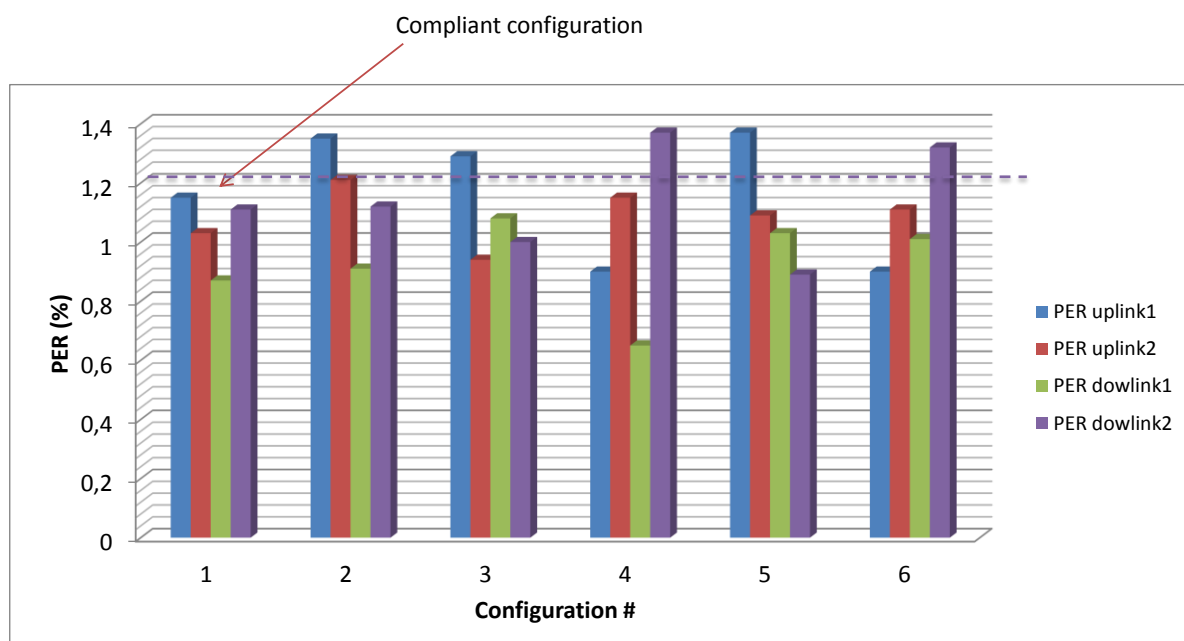


Figure 95: Per-link PER for the various configurations

To conclude, one can note that the results from the proposed algorithms are in concordance with the observations. However, one can note also that in practise, the PER is a little higher (0.2% in our demonstration) than expected due to the fact that the proposed algorithms do not take into account multipath fading and environment shadowing. One challenge from our demonstration is how to pre-estimate the real channel conditions in order to make the configuration algorithms able to predict the per-link PER.

### 5.2.5 Results from platform 8 “Spectrum opportunity identification and spectrum selection test-bed”

This section presents the results of the tests described in section 5.1.5 dealing with spectrum opportunity identification and spectrum selection functionalities.

#### 5.2.5.1 Test 1: Spectrum opportunity identification

Under the configuration presented in sub-section 5.1.5.1a, Figure 96 shows the obtained SOI for all the 1000 portions of 100 kHz averaged during a 10 minutes period. It can be observed that: (i) the spectrum portions in the ISM channels occupied by AP5 and AP6 at 2.412 GHz and 2.432 GHz, have a SOI equal to 0%; (ii) there are three groups of consecutive 100 kHz blocks with a high opportunistic index value (i.e. greater than 80%).

As a result, the spectrum blocks provided as output by the spectrum opportunity identification algorithm are those indicated in Table 19, considering that the maximum number of portions of a block has been set to  $P_{max}=290$ . Correspondingly, the available set of portions between 2442 to 2500 MHz with a total of 58 MHz has been split into 2 blocks.

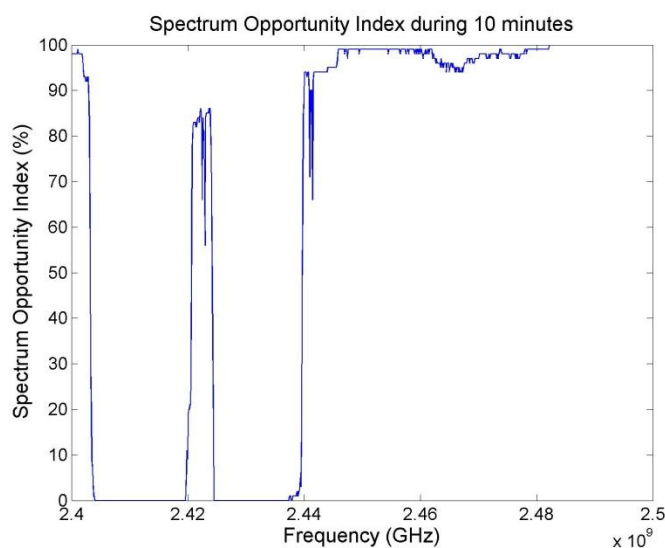


Figure 96: Measured Spectrum Opportunity Index

Table 19: Spectrum blocks obtained as a result of the spectrum opportunity identification algorithm

Index	Central Frequency (MHz)	Bandwidth (MHz)
1	2401.500	3
2	2422.000	4
3	2456.500	29
4	2485.500	29

As a result of the above, it can be concluded that the spectrum opportunity selection algorithm is able to properly identify the available spectrum blocks in the considered scenario.

### 5.2.5.2 Test 2: Adaptation of spectrum selection to interference variations

Under the test configuration discussed in sub-section 5.1.5.1b, Figure 97 depicts the obtained results in one experiment. Specifically, the figure reflects the evolution of the efficiency in the communication between the two terminals as a function of time, measured in periods of 30 s. The interferer source has been activated 3 times during the experiment, leading to efficiency degradations below the threshold of 80% as can be seen in the figure. After each one of these degradations the ON modification is executed and a new spectrum block is assigned. The figure indicates the spectrum assigned to the ON link in each period of time.

For a better understanding of the process some screenshots of the different laptops controlling the USRPs are presented reflecting some instants of the demonstration, related to the message sequence charts of the ON creation and ON maintenance procedures (see deliverable D5.2 [3] for details).

Figure 98 presents a screenshot of the terminal 1 when the ON creation procedure starts. As it can be observed in the right side of the screen, the terminal has sent the ONN.request message to request the support of the infrastructure to create the ON. Transmission has not started yet, waiting for the response of the infrastructure indicating the spectrum block to use. Figure 99 presents the screenshot of the infrastructure node at this time. After receiving the ONN.request message from terminal 1 and contacting terminal 2 to confirm its availability to create the ON, it executes the spectrum opportunity identification. At the right side of the figure the list of available spectrum blocks can be observed. The spectrum selection has chosen the spectrum block centred at 2.447 GHz. This information is communicated to terminal 1 in the ONN.response message. This triggers the ONC.request message to finalise the ON creation. At this stage, it can be seen in the screenshot of terminal 1 in Figure 100 that, after the ON has been created the transmission has started in this spectrum block. At the left side of the figure the on-line evolution of the efficiency is shown (each point corresponds to 30s), reflecting a high level of efficiency. This corresponds to the first part of the overall evolution shown in Figure 97.

Looking at Figure 97, it can be observed that the efficiency monitored by terminal 1 is above 80% until minute 9, when the interferer source is activated in the same frequency of the link. As a consequence, terminal 1 detects a degradation of the efficiency down to 60%. At this point, the screenshot of terminal 1 is shown in Figure 101. At the left side the degradation below the 80% level has been detected and correspondingly an ONN.request message is sent to the infrastructure starting the ON reconfiguration procedure. This can be seen in the screenshot of the infrastructure node shown in Figure 102. At this stage, the spectrum opportunity identification is executed again and a new spectrum selection is performed, selecting spectrum block centred at 2.442 GHz. This is notified to terminal 1 in the ONN.response message. After receiving this response, in Figure 103 the left side of the screenshot in terminal 1 reflects that the ONM.request message has been sent to terminal 2 to reconfigure the link in the new spectrum block. The completion of the reconfiguration is observed in Figure 104, corresponding to the screenshot of terminal 2. In the right side of Figure 103, as well as in Figure 97, it can be observed how the communication has continued, reaching again high efficiency levels.

This process is repeated during 20 minutes demonstrating how the testbed is able to automatically reconfigure the assigned resources during changes in the interference conditions, as seen in Figure 97.

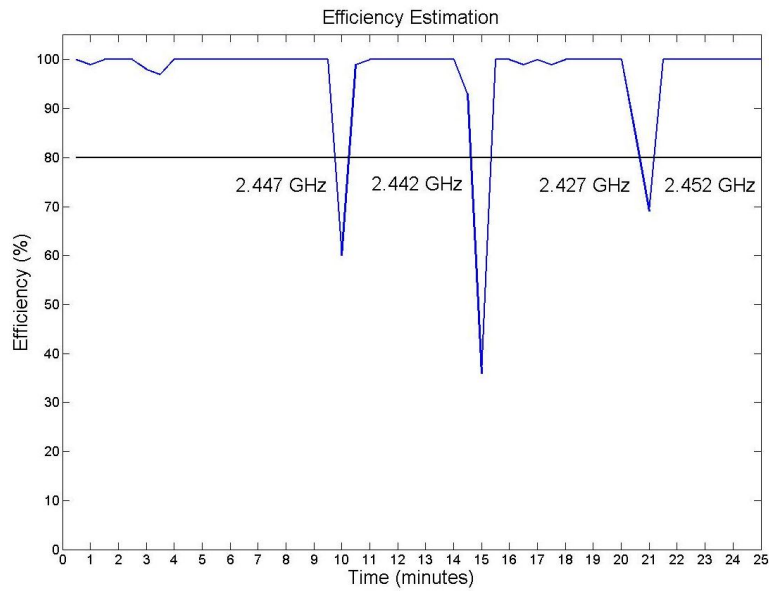


Figure 97: Spectrum Selection under changes in the interference conditions

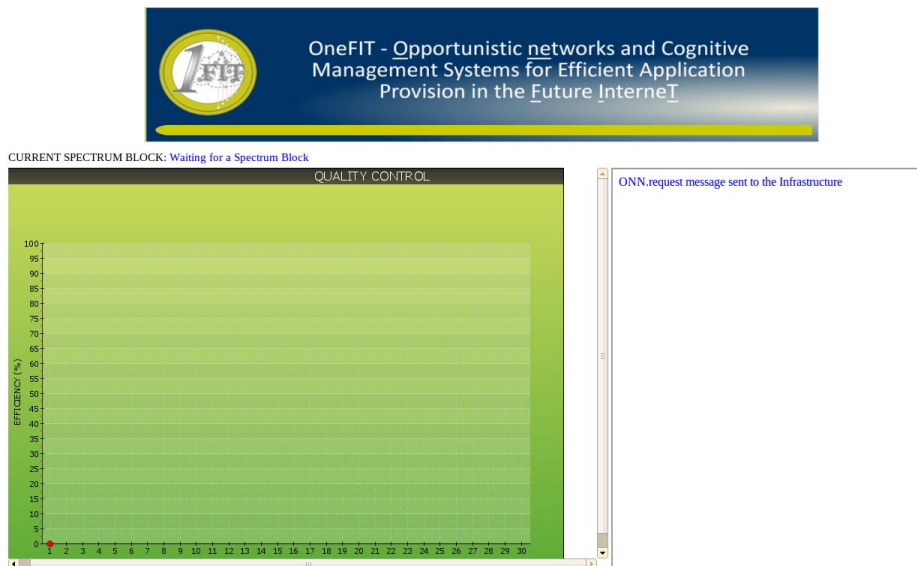


Figure 98: Screenshot of Terminal 1 at the start of the ON creation

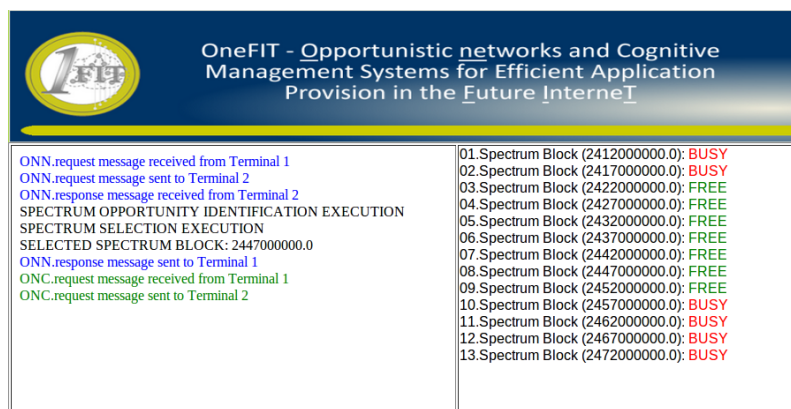


Figure 99: Screenshot of the Infrastructure Node at the start of the ON creation

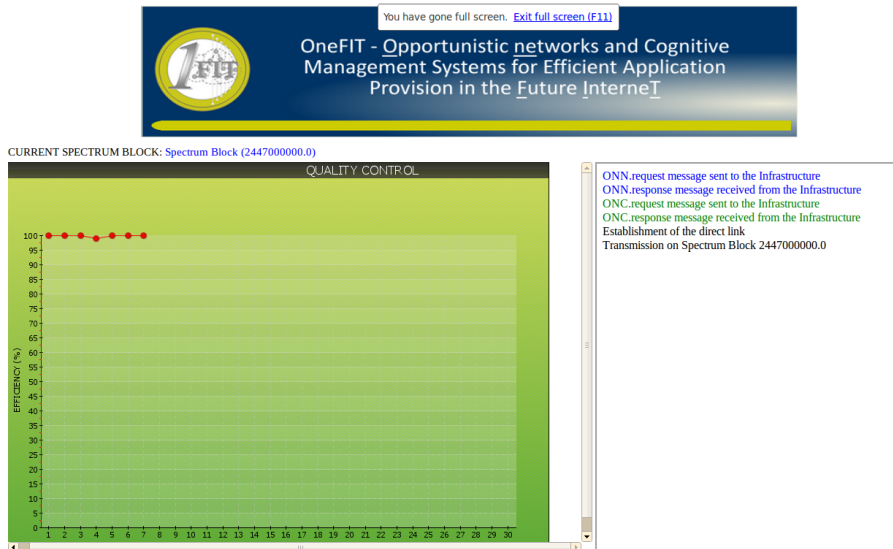


Figure 100: Screenshot of Terminal 1 after the ON link has been established

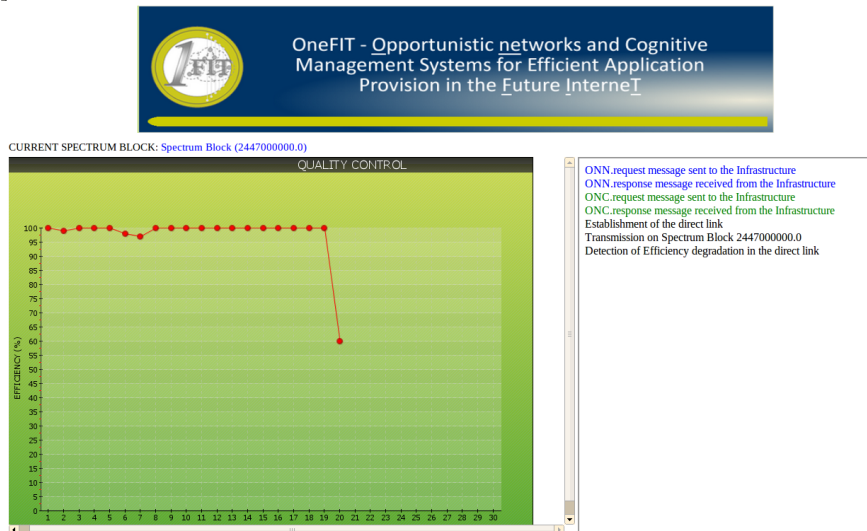


Figure 101: Screenshot of Terminal 1 after switching on the external interferer

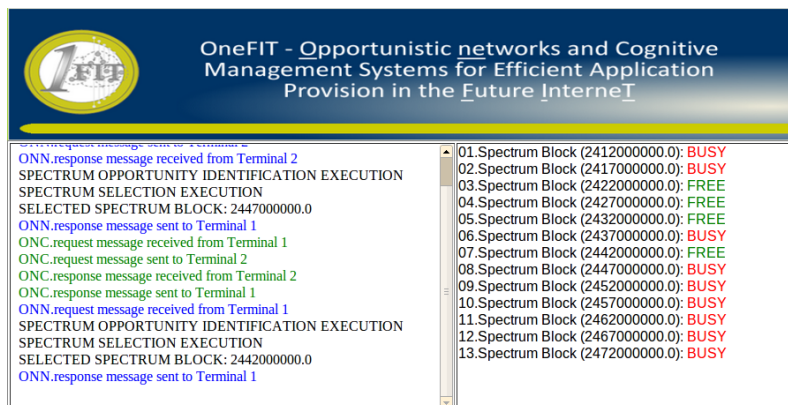


Figure 102: Screenshot of the Infrastructure Node at ON reconfiguration



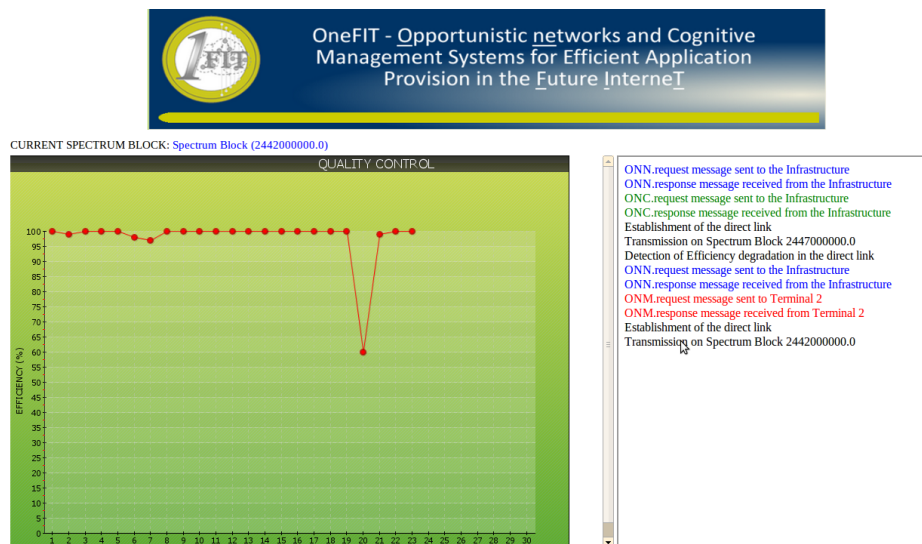


Figure 103: Screenshot of Terminal 1 after the ON reconfiguration



Figure 104: Screenshot of Terminal 2 after the ON reconfiguration

As a result of the above, it can be concluded that the spectrum selection algorithm is able to properly choose the adequate spectrum block for the communication and to dynamically adapt to the appearance of interference sources in the allocated blocks.

### 5.2.5.3 Test 3: Performance of spectrum selection algorithm

In the following the results of the 4 experiments defined in Table 8 of section 5.1.5.2 are presented, comparing the behaviour of the fitness factor-based spectrum selection algorithm against the random spectrum selection. For that purpose, each experiment has been carried out two times, one per algorithm.

Figure 105 plots the results of experiment 1 in terms of efficiency observed by the ON link. Note that only the periods in which a session in the ON link has been established are plot. The results for the execution of the random algorithm are plot in Figure 105(a) and the results for the fitness factor-based algorithm are plot in Figure 105(b). Notice that, although the statistical pattern is the same for the two executions, the actual durations of each session are different due to the randomness in the session generation. In this experiment, the interferer in one of the spectrum blocks is active 50% of the time, with an average duration much longer than the session duration of the ON link. Correspondingly, in the random spectrum selection (see Figure 105(a)) spectrum handovers need to be carried out soon after the ON link session has been established if the allocation has been performed in this block, or during the ON maintenance phase in case the interference arises in the allocated block. This can be observed in the figure because the efficiency falls below the limit of 80%. The resulting spectrum handover rate observed during the whole execution for the different experiments with the random algorithm is indicated in Table 20. On the contrary, with the

fittingness factor based spectrum selection algorithm the efficiency is kept at a high level during the whole execution and correspondingly no spectrum handovers are required.

Figure 106 plots the results corresponding to experiment 2. In this case, the duration of the interferer activity is much lower (16% of the time with an average duration of 60s). As it can be noticed in Figure 106(a) and Table 20, the resulting SpHO rate for the random case is more reduced than with experiment 1. In any case, the fittingness factor achieves a better efficiency (see Figure 106(b)).

In experiment 3, the activity factor of the interference is 83%, so it is most of the time interfered. As a result, it can be observed in Figure 107(a) that the random selection algorithm is able to keep a good degree of efficiency by executing a high number of spectrum handovers, resulting in the largest SpHO rate among all the experiments, as seen in Table 20. Again, the fittingness factor spectrum selection provides the best performance.

Finally, experiment 4 considers that the interferer has the same activity pattern as in experiment 1 (50% of activity) but with much longer session durations in the ON link. In this case, the spectrum HO rate for the random selection case is more reduced than with experiment 1. The reason is that, once a SpHO is executed during the ON link session, if the new allocation is done over the spectrum block with less interference, it is possible to keep it until the end of the session. In any case, fittingness factor based spectrum selection is able to provide again a much better performance.

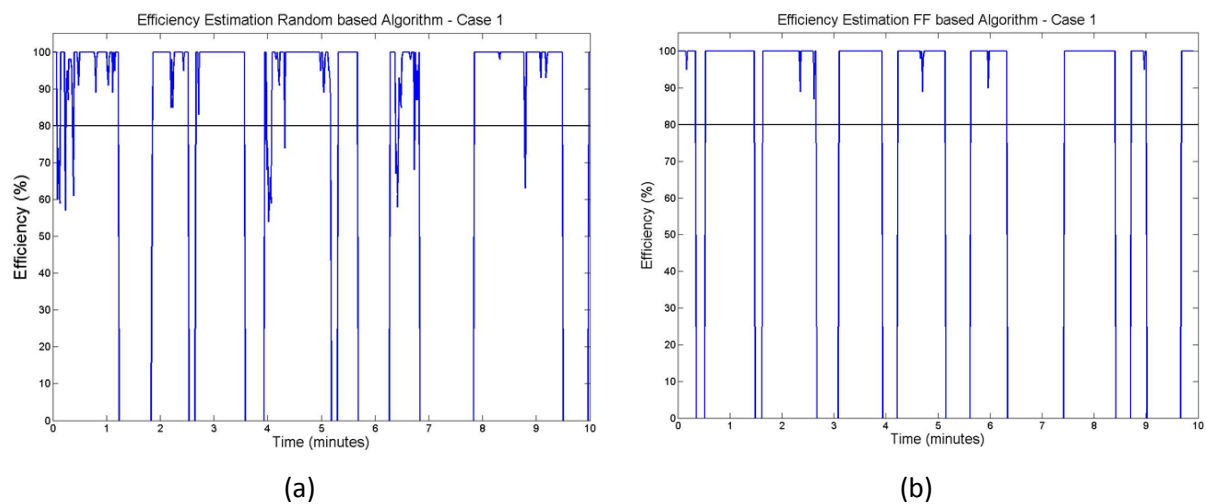


Figure 105: Results of experiment 1: (a) Random selection, (b) Fittingness factor-based selection

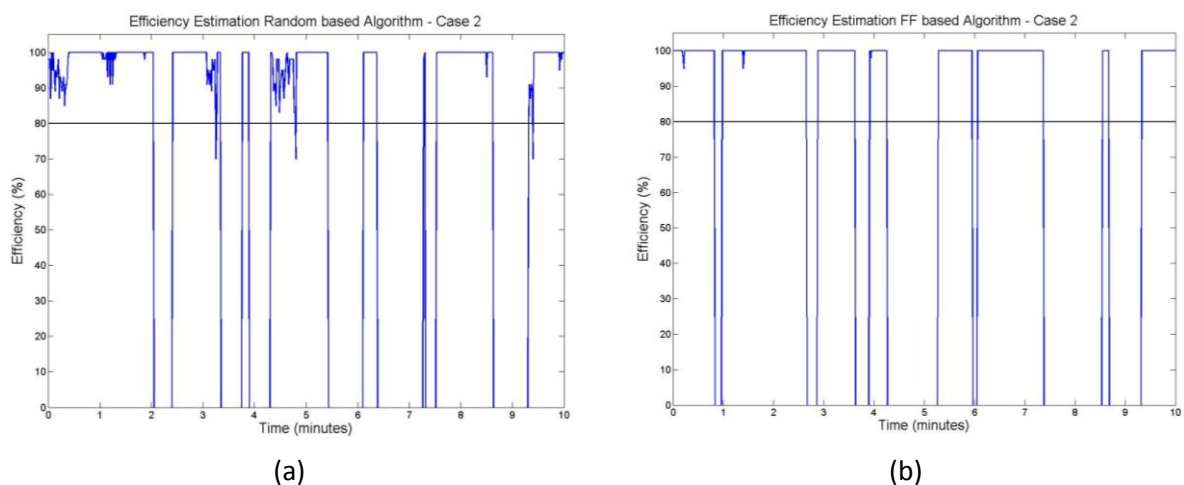


Figure 106: Results of experiment 2: (a) Random selection, (b) Fittingness factor-based selection

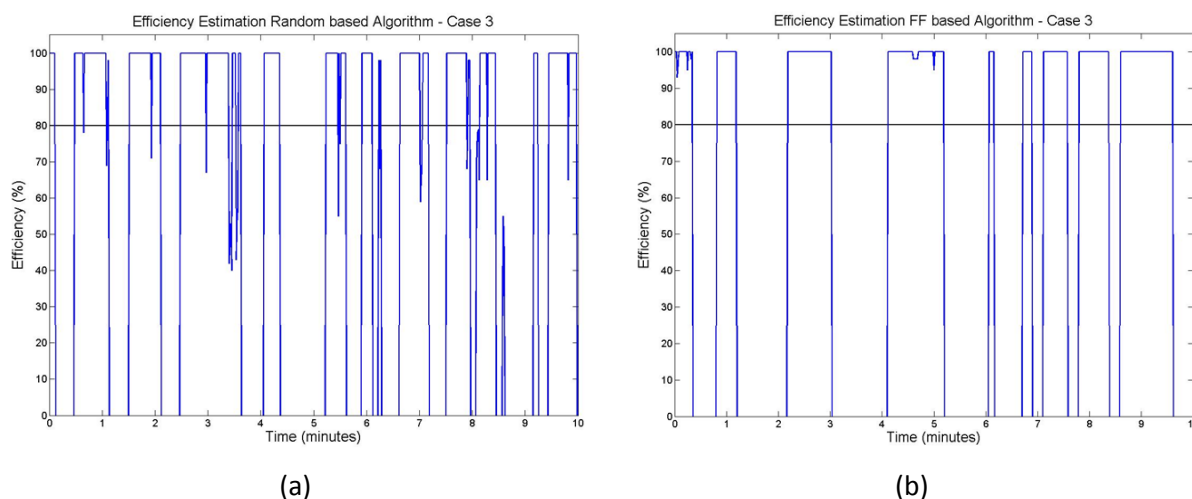


Figure 107: Results of experiment 3: (a) Random selection, (b) Fittingness factor-based selection

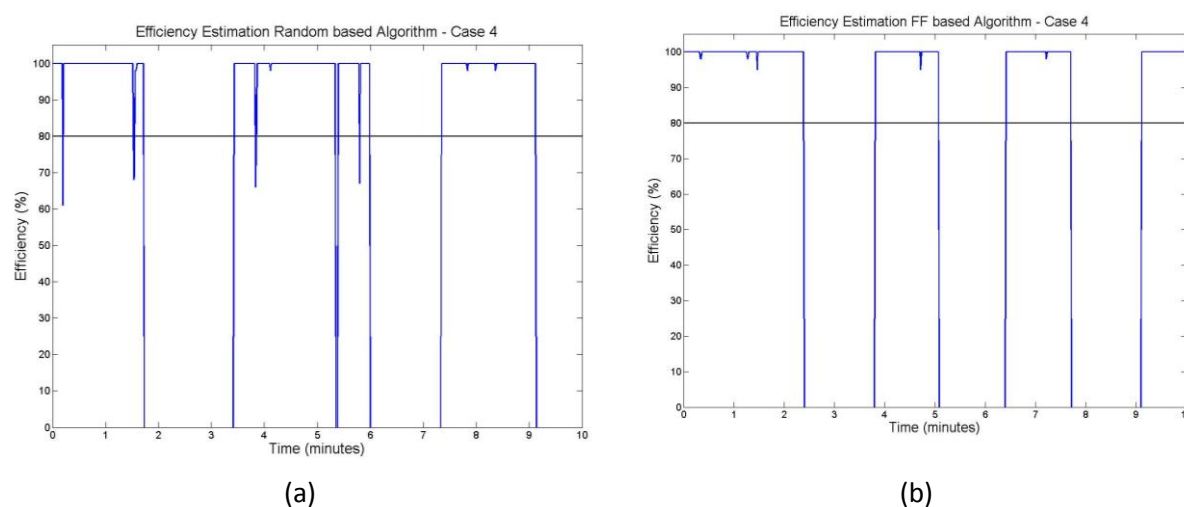


Figure 108: Results of experiment 4: (a) Random selection, (b) Fittingness factor-based selection

Table 20: Spectrum HO rate for the random selection

Experiment	SpHO rate (HO/min)
1	2.2
2	0.5
3	2.8
4	0.6

The different experiments shown in this section have revealed that the proposed fittingness factor-based spectrum selection, which takes into account some knowledge about the statistical behaviour of the different channels, is able to provide a better performance than a random selection algorithm. In the latter case, the spectrum HO ratio has to increase in order to keep the efficiency level in the communication at the desired value. This is particularly critical in case of spectrum blocks having large duration of the interference activity.

### 5.3 Results analysis and conclusions

Platforms related to Scenario 3 mimic the conditions where an ad-hoc Opportunistic Network is constituted among end users and APs, with few or none infrastructure nodes, but yet with the assistance of the Operator to allocate radio resources and provide context information. The ON is therefore created in order to serve to a specific, geographically-limited, temporary service established among users and nodes, such as a home network, a location service, a geographical social network or an offloading situation.

Results on the device-to-device testbeds show that infrastructureless communication can offer interesting advantages compared to one that includes infrastructure nodes:

- Nearly the same throughput values
- Less radio resources are needed
- Low PER values

This proves that establishing a D2D-based network, with no links to infrastructure nodes pose a very efficient mechanism to deal with offloading and location-based networking problems.

Concerning the spectrum opportunity identification and selection in this scenario, the validation has been performed using a testbed based on USRP modules that emulate the behaviour of the infrastructure node and the terminals in an ON. Different tests have been performed to validate the performance of the different functionalities. In particular, the tests on the spectrum opportunity identification have revealed that it is possible to detect the spectrum occupation in the considered scenario. From this occupation, the spectrum blocks that constitute the basis for the spectrum selection function are built. In turn, the tests on the spectrum selection functionality have shown first that the ON is able to trigger the necessary ON modification procedures and associated spectrum Handovers to react in front of changes in the interference that arises in the different spectrum blocks. Thanks to this feature, it is possible to keep the on-going communication in the ON link. Then, a performance comparison of the proposed spectrum selection algorithm has been carried out against a random selection, revealing that the knowledge about the statistical behaviour of the different spectrum blocks provided by the proposed approach is able to reduce the spectrum HO ratio while keeping the desired efficiency level of the communication.

Finally, an example service built upon the underlying Opportunistic Network has been designed and successfully tested, showing that it is possible to develop efficient ways of capitalizing the features of ONs providing novel services to the end users.

In general, the prototypes created for the scenario 3 have successfully focused on opportunistic ad hoc networking and prove that the proposed algorithms and techniques can provide the operator with the necessary tools to supervise and manage infrastructureless networks. Results show that the operator can efficiently allocate radio resources and monitor the stages of the lifetime of the ON. Moreover, it has been shown that a network operator can capitalize on the particular features of opportunistic networks to provide novel services which offer added value to the customers and can be monetized to obtain a new source of revenues.

## **6. Validation of Scenario 5 “Opp. resource aggregation in the backhaul”**

### **6.1 Set-up of test platforms**

#### **6.1.1 Platform 9 “Open platform wireless mesh network test-bed”**

Platform used for validation of the OneFIT scenario 5 specific use cases is described in section 2.2.9 of this document. This platform represents 802.11 based WMNs which, because of their wireless backhaul communication among WMN nodes, can benefit the most from opportunistic backhaul resource management. The comprehensive OneFIT algorithmic solution for the scenario 5 is presented in D4.3 [11]. Three of the OneFIT algorithms are utilized for validation of this scenario. The application cognitive multipath routing algorithm and algorithm for context aware node selection for content placement address scenario 5 specific node and route identification/selection. The algorithm for fittingness factor-based spectrum selection is used for selection of backhaul communication channels in the WMN (channel assignment to additional backhaul links which provide BW resource aggregation and sharing throughout the WMN). The roles of these three algorithms in the Scenario 5 are described in detail in section 4.5 of the [11].

##### **6.1.1.1 Configuration**

As mentioned above, the Open platform WMN test-bed is configured as 802.11 based WMN. Mesh topology provides many possibilities for backhaul resource management through aggregation and sharing. Context awareness plays a key role in efficient resource management in the backhaul of WMNs. This feature of the resource management system is ensured through constant system monitoring and knowledge based trigger recognition. The trigger recognition process behind the backhaul resource management system is described in D4.3 [11]. This recognition process is implemented together with the application cognitive multipath routing algorithm. The process is based on detection of values of key contextual parameters (enabled through utilization of the SNMP protocol) and recognition of the end user’s request for service/application (for details see [11]). Triggers for ON suitability determination phase are composed of the detected QoS capabilities of currently established backhaul paths in the WMN and recognized application/service request with accompanied QoS requirements. If QoS capabilities of the current backhaul path cannot provide QoS required by the requested application/service the ON suitability determination starts.

##### **a) Configuration of the test-bed for validation of the scenario 5 challenge related to opportunistic backhaul bandwidth aggregation**

The open platform WMN testbed (see subsection 2.2.9 and Figure 109) is used for validation of this scenario 5 related challenge. The bandwidth aggregation is achieved with “Application cognitive multipath routing in wireless mesh networks” algorithm [10] [11]. The nodes shown in Figure 109 are named after Serbian rivers. The web interface used for algorithm testing and demonstration can be accessed from the Internet while the shown test-bed is located in the LCI’s premises.

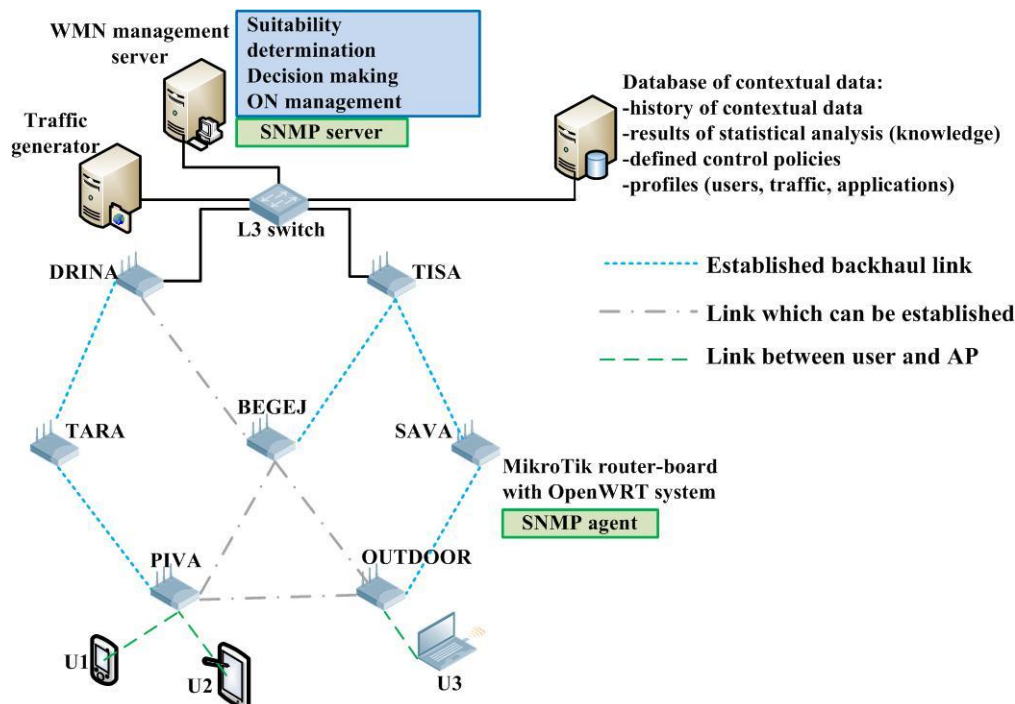


Figure 109: The test-bed used for realization of the scenario 5 use case

The test-bed shown in Figure 109 represents a well-constructed standard WMN. This is due to the facts that:

- WMN nodes have three radio interfaces (one for access and two for backhaul communication);
- Access is provided over the 802.11b/g standard;
- Backhaul communication is provided over the 802.11a standard;
- Topology allows every WMN node to “see” at least two other WMN nodes;
- Topology allows at least one path from every WMN node to all of available WMN GWs;
- Standard OLSR routing protocol used (developed for WMNs);
- Monitoring is done over SNMP protocol which is supported by all commercial devices.

Various static (links manually created) and dynamic (links created by the underlying MAC and routing protocols) topologies of the open platform WMN test-bed are investigated. Topology depicted in Figure 109 is selected as the one which provides the most possibilities for multiple paths selection, which allows the implemented algorithm to find solutions among sets of available solution thus demonstrating the decision making ability of the algorithm.

#### **b) Configuration of the testbed for validation of the scenario 5 related challenge to opportunistic backhaul storage aggregation and management**

This Scenario 5 related challenge will be demonstrated through validation of a variant of the OneFIT algorithm “Content conditioning and distributed storage virtualization/aggregation for context driven media delivery” [10] [11]. This algorithm variant will demonstrate algorithm’s ability to make a context informed selection of nodes in WMN topology with goal of providing (sub)optimal utilization of network’s capacity.

Research presented in [20] shows that content placement on WMN APs has the same impact on total streaming capacity of the WMN as turning these APs into WMN GWs (from perspective of the

stored content). Therefore, the node selection capability of the algorithm will be used for performing context informed decision making regarding selection of GW placement within the established WMN topology. The test-bed is configured so that in any moment the exact number of WMN GWs can exist in the WMN topology (the goal is to control utilization of cable backhaul links). The position of WMN nodes is fixed and power levels of their interfaces are configured in a way which ensures that the complete WMN topology is known (all possible wireless backhaul links are known). This WMN topology is presented as a network graph where edges represent backhaul links while vertices represent WMN nodes. User request distribution is established with real mobile devices (laptops, smart-phones and tablets) and with dummy traffic sinks at WMN nodes. The UDP traffic generator is located in the core part of the test-bed. The SNMP based monitoring system gathers information about where mobile end users are connected (on which WMN APs) every 20 seconds. The initial request distribution is established with test-bed configuration presented on Figure 110. This distribution of end users is used, together with the derived network graph representing the test-bed topology, as input for the MILP (Mixed Integer Linear Program) model (see [9] and [10]) for node selection. The mathematical model is executed with limitation that only two nodes need to be selected and QoS related constraints (minimization of the number of wireless hops, BW capacity of backhaul links and QoS requirements of detected application) need to be satisfied. Nodes WMN1 and 3 are selected and they are configured as WMN GWs by bringing up their Ethernet interfaces. It is important to note that all WMN nodes are connected via cable to the layer 2 switch, however only WMN GWs have active Ethernet port and WMN APs are connected to them over 802.11a based backhaul links.

As the next step, certain mobile users walk between WMN APs thus changing the request distribution among WMN nodes. As the number of end users connected to different WMN nodes changes, the MILP model is executed with different request distribution. The new set of WMN nodes are selected and these nodes are reconfigured into the new WMN GWs while the old WMN GWs are reconfigured into WMN APs and connected to corresponding GWs via wireless backhaul links.

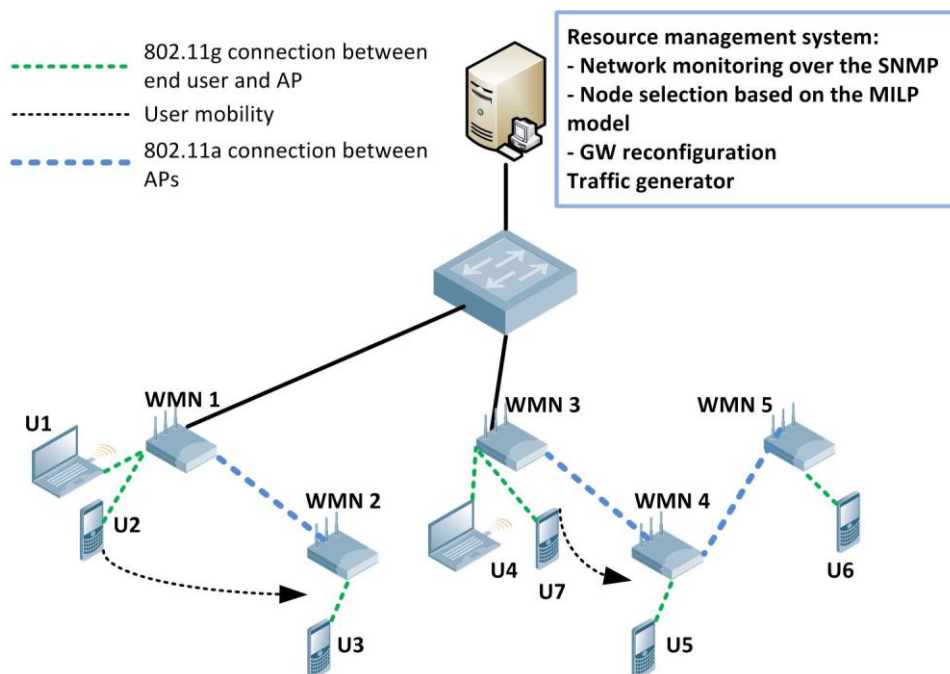


Figure 110 – Set up of the open platform WMN test-bed for validation of the GW selection algorithm

### 6.1.1.2 Test plan

Test-plan for validation of the scenario 5 challenge related to opportunistic backhaul bandwidth aggregation

This scenario 5 related challenge is validated through validation of the application cognitive multipath routing algorithm. The same test plan as the one presented in section 3.13 of [10] is used for practical validation of the opportunistic backhaul BW resource aggregation and sharing.

Metrics selected for validating the use case:

- Achieved aggregated bandwidth – total bandwidth which can be provided on access side of the struggling WMN AP (limited by access radio technology – 802.11g) by establishing multiple paths in WMN backhaul.
- Impact of multi path packet routing on QoS provided to end users.
- Signalling overhead – trade-off between the amount of gathered contextual data and performance of the algorithm will be examined (provided in D3.3).

The proof of concept experiments are conducted in order to assess ability of the proposed algorithm to find appropriate multiple path solution and enable the backhaul bandwidth aggregation for struggling APs. Experiments are validated on WMN test-bed shown in Figure 109. Traffic generator is sending UDP packet streams to nodes of the experimental network in order to simulate different backhaul traffic patterns.

All of the wireless links in the WMN can support maximum of 30Mbit/s of user data traffic (in accordance to 802.11a and g standards). The threshold for the number of hops for candidate paths is set to 3 (in order to speed up the decision making process and in line with practical limitations). We demonstrate ON creation in order to achieve backhaul bandwidth aggregation relative to AP4 and AP5 (see Figure 111). AP1, AP2, AP3, U1, U2 and U3 will be configured as sinks for the UDP streams. In the access side of the AP4 we consider the *type 4* (see section 2.12 of the D4.2 [10] for definition of traffic types) access traffic. Access traffic for AP5 can be considered as *type 2* or *type 3*. We will present 4 experiments for the WMN topology presented in Figure 111. Setups of the proof of concept experiments and their results are presented in Table 21.

Table 21: Setup and results of the proof of concept experiments for backhaul bandwidth aggregation validation

Exp#	AP1 sink	AP2 sink	AP3 sink	AP4 req	AP5 req	AP4 bottle	AP4 solution	AP5 bottle	AP5 solution
1	15	20	25	10	15	OK	OK	AP3-GW2 (5)	AP5-AP2-GW2 (10)
2	28	20	15	11	10	AP1-GW1 (2)	AP4+AP2-GW2 (9)	OK	OK
3	15	25	15	5	25	OK	OK	AP3-GW2 (15)	AP5-AP4-AP1-GW1 (10)
4	20	25	10	20	10	AP1-GW1 (10)	AP4-AP5-AP3-GW2 (10)	OK	OK

The main concern when using multipath routing for aggregation of backhaul BW resources in WMNs is its impact on QoS provided to end users. The multipath routing provides more bandwidth to the end users, but tends to increase interference in the backhaul paths, which results in more retransmitted packets, and result in packet reordering problems and increased jitter levels. The implemented multipath routing algorithm provides opportunistic creation of multiple paths for transmitting users' data, which means that multipath routing will be utilized if the underlying single path routing protocol struggles to provide required level of QoS while the RAT imposed limitations are not yet met (i.e. access interface of a WMN node has capacity of 30Mbit/s, but backhaul path to the GW has capacity of 20Mbit/s). In addition, the implemented multipath routing algorithm provides application/service awareness through earlier described autonomic trigger recognition.

The results of impact of multipath routing on QoS provided to the end users will be shown and discussed for a test-bed setup as shown in Figure 111.



There are two users. U1 is connected to WMN AP4, which is considered a candidate for multipath routing (together with AP5 – topology limitation). U2 is connected to AP1. There are two main test cases:

- U1 receives all the traffic over the path GW1-AP1-AP4
- U1 receives traffic over the new path GW2-AP2-AP4

Backhaul traffic patterns are established by sending traffic flows of selected bit rate to WMN nodes. These bit rates are gradually increased in order to simulate different levels of congestions among backhaul paths. Backhaul channels are carefully selected in order to minimize interference. Access interfaces of all WMN nodes, apart from AP1 and AP4 are turned off. However, interference in 2.4GHz band from environment are significant (23 different access networks are identified). Four types of applications are requested by U1 and U2:

- VoIP – bandwidth requirement 0.2Mbit/s;
- Video 1 – video stream of low quality with 1Mbit/s bandwidth requirement;
- Video 2 – video stream of medium quality with 1.5Mbit/s bandwidth requirement;
- Video 3 – video stream of high quality with 2.5Mbit/s bandwidth requirement.

Based on these requests a UDP traffic generator generates a constant bit rate stream of a certain rate to end users. IPERF QoS monitoring tool is installed on U1 and U2. Jitter levels, number of lost UDP packets and achieved throughput are monitored as QoS indicators. One test case consider one combination of requested applications (i.e. U1 requests Video 1 and U2 requests Video 3), one background backhaul traffic pattern and whether or not U1 receives its traffic over path GW1-AP1-AP4 or the new path GW2-AP2-AP4. There are 7 different backhaul traffic patterns and two combinations of requested applications (U1 requests Video 3 and U2 requests Video 1, U1 requests Video 2 and U2 requests VoIP). Every test case runs for an hour. After an hour average values for achieved throughput, percentage of lost packets and jitter level on every user is gathered. Total simulation time is 28 hours.

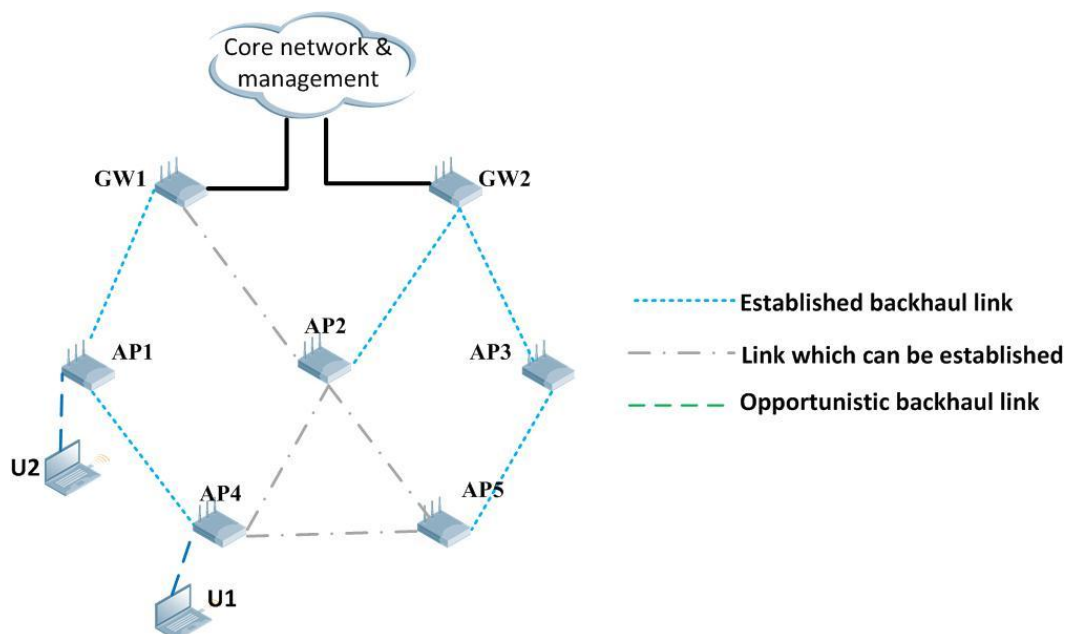


Figure 111: Test-bed setup for estimation of impact of multipath routing on QoS provided to end users

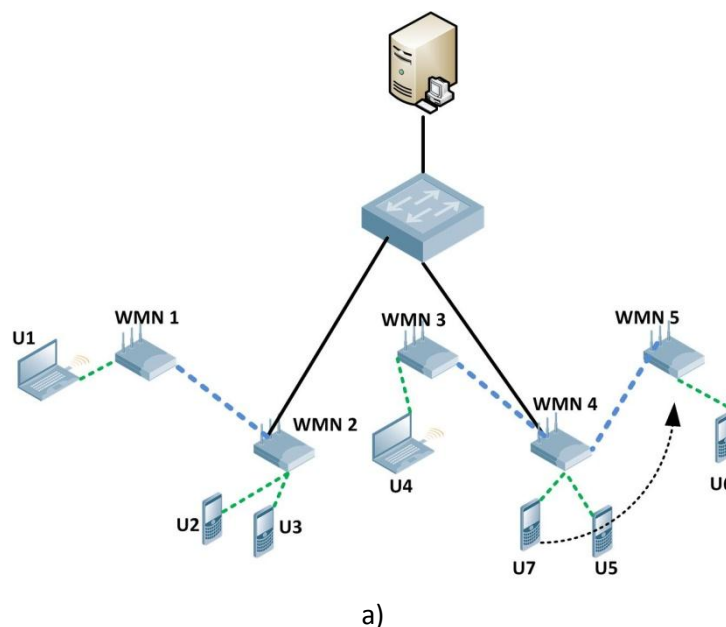
Test-plan for validation of the scenario 5 challenge related to opportunistic backhaul storage aggregation and management

The test-plan is based on a performance evaluation plan presented in section 2.14 of the [11]. The node selection capabilities of the implemented node selection algorithm are evaluated and confirmed in [9] and [10]. Therefore, the validation experiments are focused on the impact of GW reconfiguration on QoS indicators on end user devices. For simplicity we will focus on portion of the test-bed network composed of the WMN 3, 4 and 5 and user nodes U4-U7. All end users request the same service/application with the same QoS requirements. The mobile user U7 is walking from one WMN node to the other while other end users are static. All end users in the test-bed are requesting the same service. In the initial request distribution setup nodes WMN 1 and 3 are configured as WMN GWs. As the U7 walks from WMN 3 to the WMN 4, the request distribution changes. Handover of the U7 from the WMN 3 to the WMN 4 is detected by the SNMP protocol and the new request distribution triggers the new GW placement recalculation and GW reconfiguration. Mobility of the U7 triggers topology changes and GW reconfigurations as presented in Figure 110 and Figure 112.

The experiments are organized as follows:

- Three services are considered: VoIP (155Kbit/s), streaming of low quality video (Video 1 - 1Mbit/s) and streaming of high quality video (Video 3 - 3Mbit/s);
- Experiments are started when U7 starts walking towards the WMN 4;
- Three different service durations are tested while the U7 goes from the WMN 3 to the WMN 5: 1000, 2000 and 3000 seconds;
- Every experimental setup (service + service duration) is repeated 10 times.

The Iperf toll is used on nodes U4-U6 in order to check the impact of the GW reconfiguration on QoS indicators. The following QoS parameters are monitored on mentioned mobile users: achieved throughput, jitter level and packet loss percentage. The QoS on the U7 is not considered since this node experiences handover while moving between WMN nodes and its QoS would be affected whether or not the GWs are reconfigured.



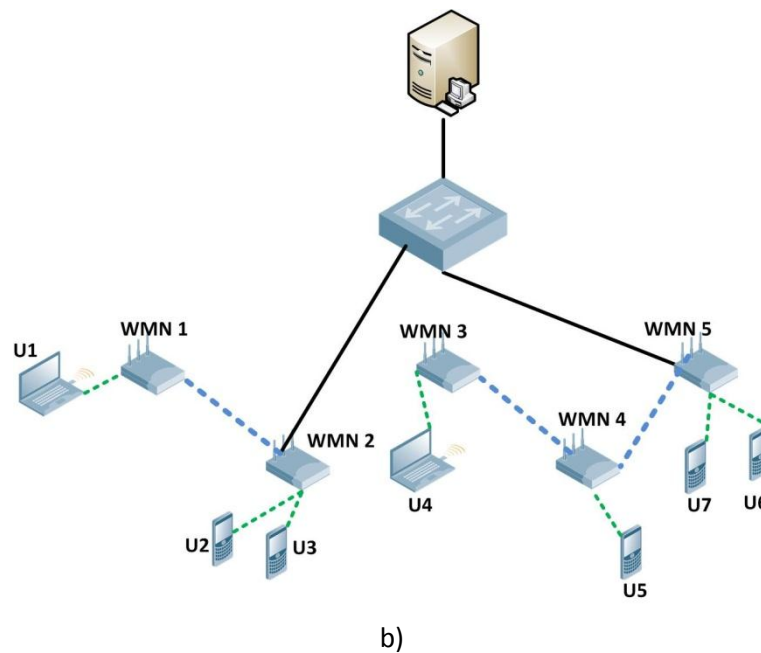


Figure 112 – User mobility results in change in request distribution and GW selection

## 6.2 Obtained results

### 6.2.1 Results from platform 9 “Open platform WMN test-bed”

#### Results from validation of the scenario 5 challenge related to opportunistic backhaul bandwidth aggregation

The results, regarding the ability of the implemented application aware multipath routing algorithm to properly select multiple backhaul paths for solving the recognized problem, are shown in the Table 21. For example, in the first experiment AP1, AP2 and AP3 (Figure 111) are set as sinks for UDP traffic streams. The bandwidth which is reserved by these sinks is presented in Table 21 in Mbit/s. Let's assume that users connected to AP4 require total of 10Mbit/s of UDP traffic and user at AP5 requires 15Mbit/s. Users connected to AP4 can be provided with the necessary bandwidth over the existing path AP4-AP1-GW1. However, user connected to AP5 cannot be provided with the required bandwidth, because no single path can be established with the sufficient capacity (in the light of the current bandwidth usage in the WMN). Therefore, the multiple path solution is derived. The implemented algorithm provides the solution (see Table 21) in the form of the path, which when joined with the current path AP5-AP3-GW2, with bottleneck link AP3-GW2 (marked red in the Table 21) which has 5Mbit/s available bandwidth capacity, provides aggregated backhaul bandwidth, which is enough to meet the current demand at the access side of the AP5. The additional path is AP5-AP2-GW2 (marked green in Table 21) and it provides 10Mbit/s (given in parentheses next to the path in Table 21). Solutions for all other experiments are given in Table 21 as well.

The implemented multipath routing algorithm runs on a well dimensioned centralized server which has access to contextual database with latest values of contextual parameters. This server performs management of the whole network and one of its management tasks is multipath routing control. Custom WMN monitoring system gathers a bulk of contextual parameters every one minute, therefore the algorithm will react to changes in contextual parameters in no later than one minute and a small time interval needed for decision making regarding multiple paths set selection. Regarding the power consumption of the multipath routing solution, it requires that dormant wireless interfaces of WMN nodes are turned on. This increases system power consumption. However, the implemented algorithm proposes opportunistic multipath routing when single path routing cannot deal with the increased congestion and poor load balancing in the backhaul segments

of WMN. Increased congestion results in more retransmissions as well as decreased bandwidth provided to end users. Less bandwidth provided to end users and more retransmission of packets means that they will spend more time communicating with infrastructure nodes which directly decreases the battery level of mobile users. Therefore, increased power consumption in the infrastructure side, as a result of utilization of additional network interfaces, is compensated by decreased number of packet retransmissions and increased bandwidth provided to end users, which allows them to finish their data transmission more quickly allowing them to turn off their wireless interfaces and thus save battery.

For the purpose of validating impact of the opportunistic backhaul BW aggregation/sharing on the QoS offered to the end users, the backhaul traffic patterns used in experiments are configured as shown in Table 22. UDP traffic generator is used for sending traffic of a selected bit rate towards nodes AP1, AP2 and AP4. For example, in case 6 8Mbit/s is sent to every of these nodes. This means that link GW1-AP1 transfers 16Mbit/s in total which makes it a bottleneck link and as a solution a path GW2-AP2-AP1 is created in order to offload a part of traffic from GW1 to GW2. UDP generator is used in order to avoid problems of packet retransmissions of TCP protocol.

The first case analyzed is when U1 requests Video 3 type of application and U2 requests Video 1 type of application. Average throughput provided to U1 and U2 for the case of backhaul bandwidth aggregation through multipath routing and in case when there is no backhaul bandwidth aggregation is shown in Figure 113. The results show that both U2 and U1 benefit from multipath routing (bandwidth aggregation) in a sense that average throughput increases for both users. Average throughput for U1 increases because he is rerouted to a less congested path GW2-AP2-AP4. Throughput of U2 increases because path GW1-AP1-AP4 is offloaded since U1 is rerouted over the new path towards GW2. The same logic stands for UDP packet loss percentage for U1 and U2 as shown in Figure 114. As the backhaul traffic pattern changes towards more congested situation, the packet loss percentage rises drastically. However packet loss percentage is less in case of multipath routing (bandwidth aggregation). Also, according to obtained results, relevant QoS parameters tend to show more stability in their values when multipath routing (backhaul BW aggregation) is established.

Table 22: Experimental setup

		Test case number (UDP traffic sent to WMN nodes)						
		1	2	3	4	5	6	7
WMN node	AP1	4Mbit/s	5Mbit/s	5.5Mbit/s	6.5Mbit/s	7Mbit/s	8Mbit/s	9Mbit/s
	AP2	4Mbit/s	5Mbit/s	5.5Mbit/s	6.5Mbit/s	7Mbit/s	8Mbit/s	9Mbit/s
	AP4	4Mbit/s	5Mbit/s	5.5Mbit/s	6.5Mbit/s	7Mbit/s	8Mbit/s	9Mbit/s

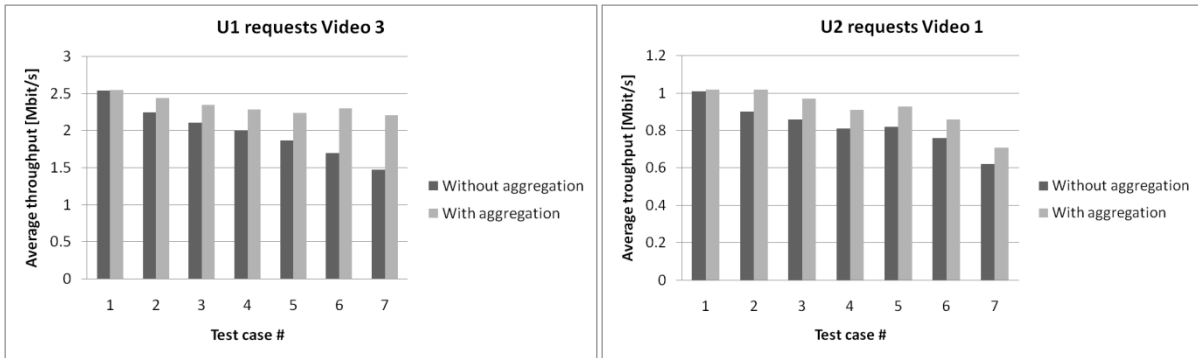


Figure 113: Average throughput achieved by U1 and U2

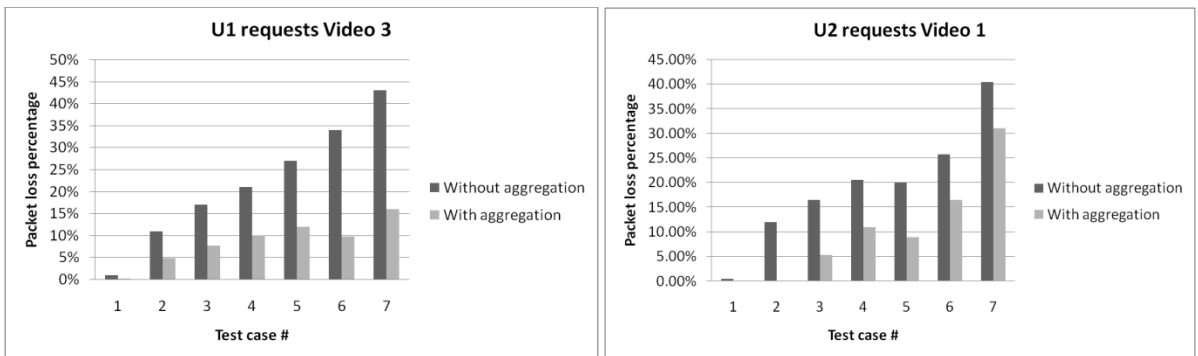


Figure 114: Packet loss percentage suffered by U1 and U2

Legacy multipath routing approaches in WMNs resulted in significant jitter related problems. The implemented application aware multipath routing algorithm avoided problems of packet reordering by providing application (access traffic) profile awareness. Results in Figure 115 show that multipath routing tends to achieve lower jitter level and more stable jitter value in contrast with the underlying single path routing protocol.

The second analyzed case is when U1 requests Video 2 and U2 requests VoIP type of application. Figure 116 shows how the average throughput received by both users is affected in case of multipath routing (backhaul bandwidth aggregation) and single path routing. These results are in line with results of the first test case. Also, packet loss percentage results shown in Figure 117 are in line with throughput related results. Results shown in Figure 118 confirm that the proposed application cognitive multipath routing achieves better jitter results when compared with underlying single path routing.

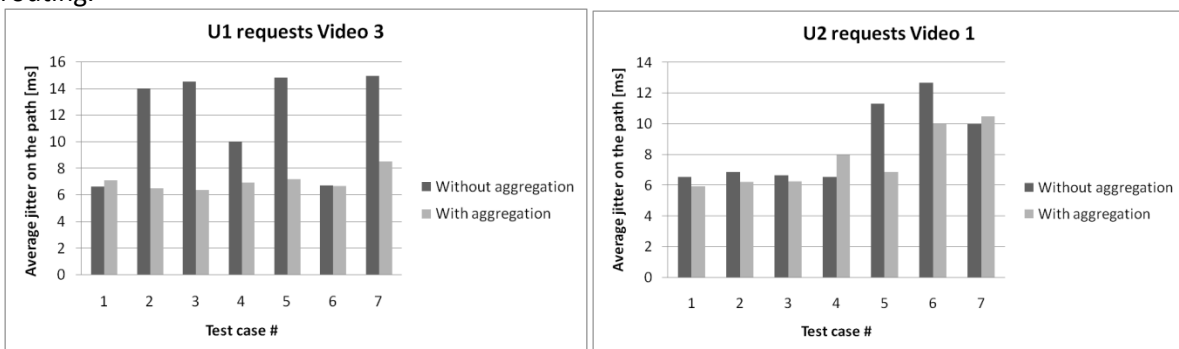


Figure 115: Average jitter on a path for U1 and U2

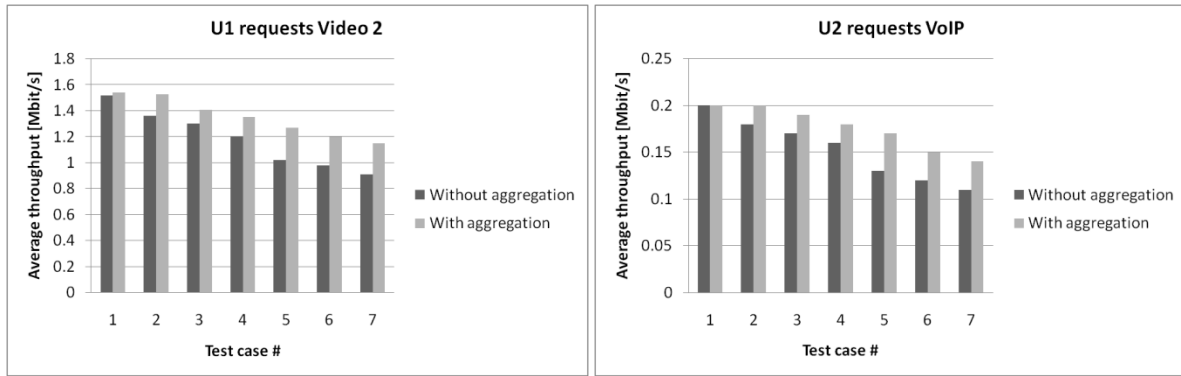


Figure 16: Average throughput achieved by U1 and U2

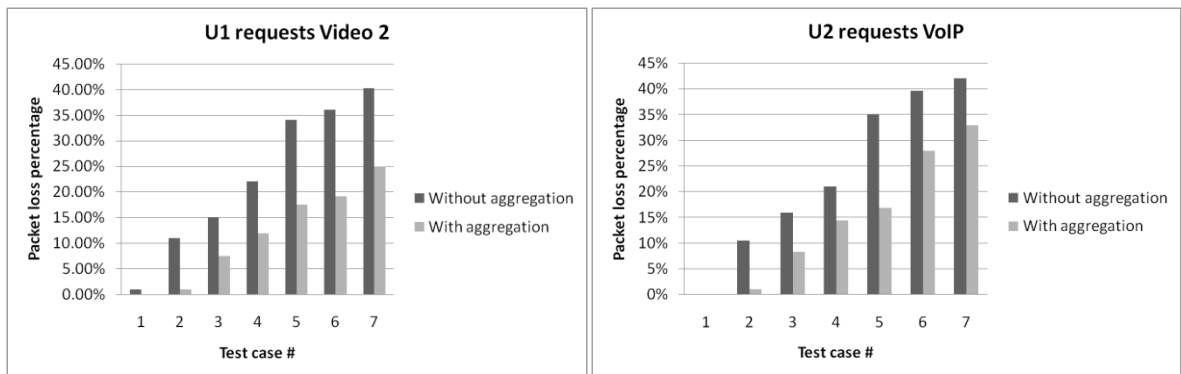


Figure 17: Packet loss percentage suffered by U1 and U2

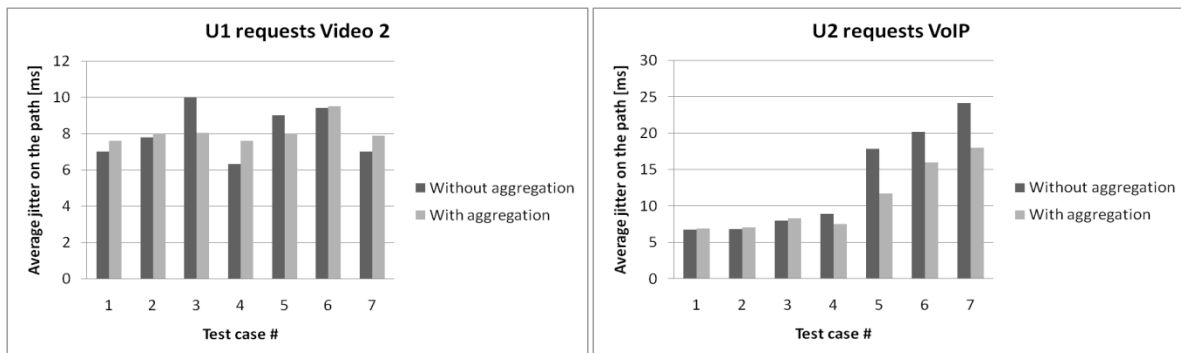


Figure 18: Average jitter on a path for U1 and U2

Results from validation of the scenario 5 challenge related to opportunistic backhaul storage aggregation and management

The following results show the impact of opportunistic GW reconfiguration on QoS offered to the end users. Experimental setup is described in section 7.1. Results which will be presented below are already presented and discussed in section 2.14 of the [11] in order to show performance evaluation of the node selection algorithm. In this document these results will be presented from perspective of validation of the scenario 5 challenge related to opportunistic aggregation of backhaul storage resources. Justification for the experimental approach (GW selection variant of the node selection algorithm) has already been given in D4.3 [11].

Figure 119 depicts the impact of GW reconfiguration on jitter levels at the side of the U4. GWs are reconfigured as result of U7's mobility. It is clear that jitter level increases as the WMN 3, to which the U4 is connected, becomes the first and the second AP on the backhaul path to the new GW. The longer backhaul paths (number of wireless hops) results in increased jitter and, consequently, decreased QoS. Figure 120 shows the impact of GW reconfiguration and service provision duration on packet loss percentage. During the GW reconfiguration phases the connections are lost for short

time interval (varying between 3 and 5 seconds) until the new GW is selected and addressing tables are updated. Since experiments are using the UDP traffic generator, packets sent during the GW reconfiguration phase are lost. Therefore, total packet loss rate at the U4 side increases in case where GW reconfiguration is executed. Service provision duration also impacts the total packet loss percentage in case when the same number of GW reconfigurations needs to be performed. The first 10 measures shown in Figure 120 correspond to the service session which lasts for 1000 seconds, the next 10 measures correspond to 2000 seconds long service session and finally the last 10 measures correspond to the service provision duration of 3000 seconds. The packet loss percentage in case when there is no GW reconfiguration is relatively constant in controlled environment. Longer session duration can be seen as impact of user's mobility speed on the packet loss rate when GWs are reconfigured in order to follow the mobile user. The first 10 measures in the Figure 120 can be seen as packet loss rate for very fast moving U7, while the last 10 results in this figure can be seen as packet loss rate in case where the U7 is moving slowly. The conclusion of this analysis is that the GW reconfiguration process should not address fast moving end users if there are static or slowly moving users in the same WMN. The GW reconfiguration should correspond to more general user mobility patterns and changes in request reconfigurations.

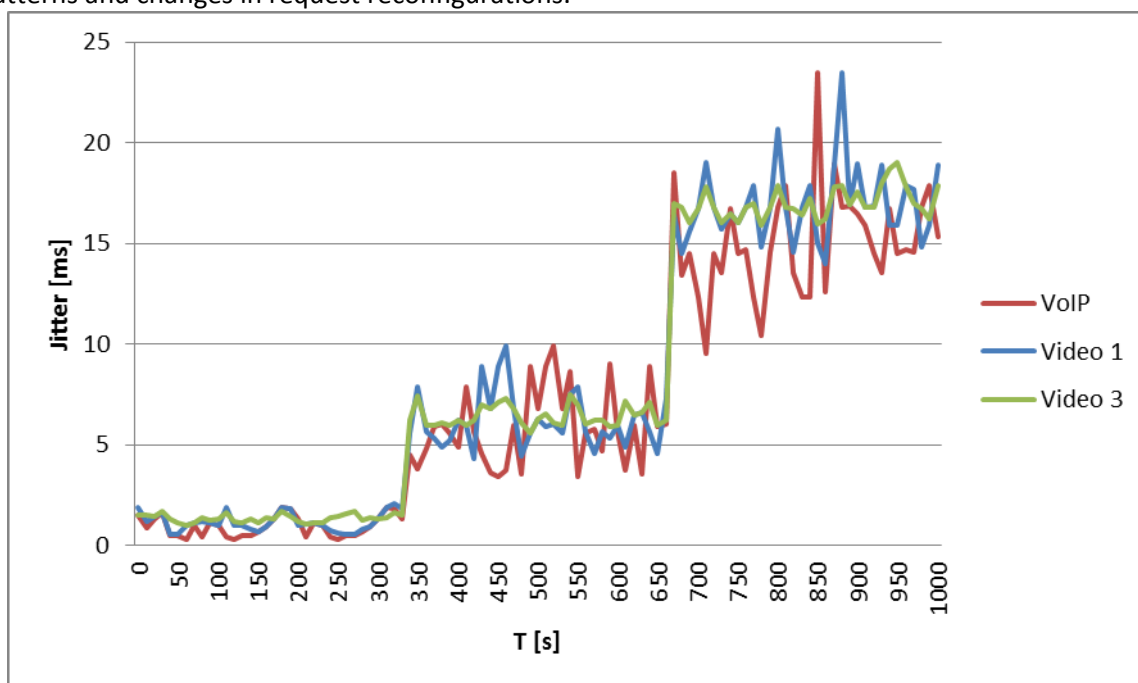


Figure 119 – Jitter levels measured at U4 side

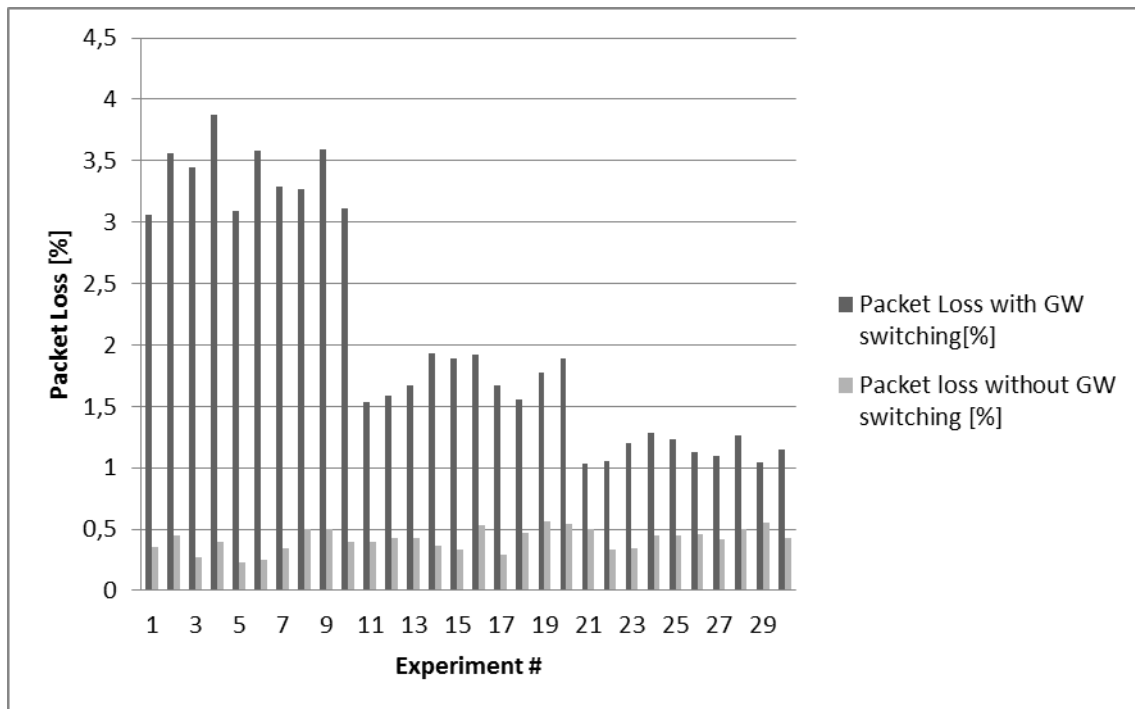


Figure 120 – Packet loss percentage measured at U4 side

The GW reconfiguration process has significant impact on QoS indicators at the side of end users which are not moving throughout the WMN. During the GW reconfiguration the connections is lost and, because the traffic generator sends UDP data streams, packets sent during this time are lost. However, GW reconfiguration can be significantly accelerated through proper reconfiguration and optimization of physical, MAC and routing protocols at WMN stations. There are practical solutions where WMN nodes are reconfigured “seamlessly” from perspective of end users (i.e. GW reconfigured in less than 10ms). In this case the GW reconfiguration process is able to address fast changing contextual parameters and to provide better resource utilization while not affecting the QoS delivered to the end users.

The ability of the node selection algorithm to make context informed GW selection, as request distribution changes, is successfully validated and obtained QoS related results are in line with expectations for WMNs where GW reconfiguration process is not optimized.

### 6.3 Results analysis and conclusions

Results are already analysed as they are presented in the section 7.2.

As stated before, algorithms presented in sections 2.12 and 2.14 of [10] and [11] are designed specifically for scenario 5 related challenges for opportunistic backhaul resource aggregation, sharing and management. Performance evaluation is conducted in custom built simulators and in the open platform WMN test-bed. The WMNs are selected for validation of scenario 5 related challenges because these networks can benefit the most from opportunistic resource management in the backhaul comprised of wireless links.

The challenge related to opportunistic backhaul BW aggregation is validated through validation of the implemented application aware multipath routing. The algorithm’s ability to properly select multipath set for solving problematic situations of service/application provision is confirmed. Also, the impact of the backhaul BW aggregation on the QoS delivered to the end users is assessed. The conclusion is that the proper opportunistic backhaul BW aggregation/sharing, supported with context aware multipath routing, can significantly improve QoS delivered to the end users when compared with BW management approaches without BW aggregation (without the multipath



routing in the backhaul). Also, the importance of the application/service awareness of the BW aggregation process is stressed. The implemented trigger recognition process is described and validated in the open platform WMN test-bed. This trigger recognition ensures that decision making for resource management is conducted in context informed manner. In practical implementation the multipath routing algorithm is supported with fittingness factor-based spectrum selection (described in section 2.4 of the D4.2 [10]) which ensures proper channel selection for additional backhaul links. This channel selection will ensure that the multipath routing solutions for backhaul BW resource aggregation don't impose additional interference in the WMN backhaul and that it is aware of the interference coming from the environment of the WMN. The role of the fittingness factor-based spectrum selection in the comprehensive OneFIT algorithmic solution for the scenario 5 is described in detail in section 4.5 of the D4.3 [11].

The backhaul storage resource aggregation challenge of the scenario 5 is covered by the "Content conditioning and distributed storage virtualization/aggregation for context driven media delivery" algorithm, which is described in section 2.14 of [10][11]. The algorithm performs selection of WMN nodes on which the multimedia content should be proactively placed in order to address detected/predicted request distribution and QoS capabilities of the underlying WMN. In line with conclusion of research presented in [20], the algorithm's node selection capabilities can be validated through implementation of context aware GW reconfiguration process. The results of practical validation show that the algorithm has the ability to make context informed selection of GWs. The GW reconfiguration processes impact on QoS is not considered as significant drawback since there are practical solutions for "seamless" node reconfigurations. When the equipment of the WMN test-bed is optimized for GW reconfiguration, the performance evaluation results of the autonomic, context informed GW selection should result in significant improvement of QoS offered to the end users (especially to users walking through the WMN).

The opportunistic BW and storage resource aggregation are important for delivery of multimedia over WMNs in context aware and knowledge based manner. LCI will continue working on the concept of wireless Content Delivery Networks (wCDNs) after the OneFIT is finished. The wCDN concept provides storage and BW resource management (aggregation and sharing) for multimedia delivery and distribution over WiFi networks. The algorithms for multipath routing and node selection will be the base for the wCDN decision making and resource management logic. How these two algorithms work together (with addition of the fittingness factor-based spectrum selection) can be seen in section 4.5 of the [11].

## 7. Global conclusions

This document has presented a comprehensive description of all the tests carried out in order to validate the OneFIT concept that has been developed during the last year and a half. From the beginning, five different business scenarios were specified, and since then they have driven the development of the architecture, entities, algorithms, mechanisms, protocols and procedures that comprise the whole OneFIT solution. Therefore, the validation activities have also been planned as scenario-oriented: for each scenario, a number of experiments have been carried out on one or more of the prototyping platforms designed in this Workpackage.

The first scenario proposes a situation where the infrastructure network needs to temporarily extend its coverage in order to provide service to a number of users that are out of reach. The results of the tests shown in section 3 prove that an Opportunistic Network approach efficiently copes with these problems, by creating an ad-hoc network among the target nodes and infrastructure-reachable nodes that uses the radio resources allocated by the operator after analysing the context information. Results also suggest the best way to accomplish this, showing what kind of nodes are more efficient, when to trigger D2D links and how to optimise energy consumption.

The second scenario addresses the situation where a specific area of the infrastructure network needs to temporarily serve more users than it is designed to, or to solve a congestion situation. The results from the experiments described in section 4 prove that the OneFIT approach efficiently tackles such situations, by creating an ON among neighbouring non-congested nodes that absorbs the excess of traffic from the infrastructure, under the requirements and policies stated by the operator after analysing the context and the availability of resources. Moreover, the results show the benefits on the packet delay and the delivery probability after the ON is created.

The third scenario depicts a situation where the operator needs to establish an ad-hoc network for a specific purpose (e.g. provide a proximity service, offload traffic, etc.) using the minimum amount of infrastructure resources. The results from the tests described in section 5 prove that creating Opportunistic Networks where the target users are diverted to, is an efficient solution to address such situations. Results also show good QoS values for the D2D links, the efficiency of the spectrum selection algorithms and the feasibility of developing end services specifically designed to run on top of ONs.

The fourth scenario proposes a situation where a number of closely located users request a set of applications to establish a communication with some entities beyond the service area region. The creation of an ON among these users allow a series of benefits, such as the aggregation of traffic, a reduction on the resource demand or cooperative caching of data. Due to the similarities of these use cases and those of Scenarios 3 and 5, no specific validation of Scenario 4 has been carried out, and most of the conclusions from those scenarios can be extrapolated for the fourth one.

According to the results presented in the section 6 of this document, the OneFIT approach can provide opportunistic resource management in the backhaul side of the infrastructure as well (other scenarios are focusing on the access portion of the infrastructure). The scenario 5 implementation focuses on wireless mesh networks (802.11 based) since specifics of this networking technology provide the most possibilities for cognitive backhaul resource management. Also, these networks can benefit the most from opportunistic backhaul resource management. Performed validation experiments (see section 6 of this document) show that the OneFIT system can provide opportunistic backhaul bandwidth aggregation and sharing in wireless mesh networks through utilization of application aware multipath routing. Also, the OneFIT system provides context aware selection of infrastructure nodes (wireless mesh network APs, BSs, Femto cells etc.) with the goal of providing opportunistic aggregation/virtualization and sharing of backhaul resources (bandwidth and storage).

Finally, we can conclude that this document has successfully addressed all the challenges posed by the scenarios described in D2.1 [4], and shown that the system developed during the lifetime of the OneFIT project is actually an efficient solution to tackle a wide variety of scenarios. All the algorithms and procedures have demonstrated their usefulness and the architecture and protocols developed have proved their design.

Therefore, the OneFIT concept has been validated as a necessary tool to address the challenges posed by the Future Internet.

## 8. References

- [1] ICT-2009-257385 OneFIT Project, <http://www.ict-onefit.eu/>
- [2] OneFIT Deliverable D5.1 "Validation platform specification", September 2011.
- [3] OneFIT Deliverable D5.2 "Validation platform implementation description", June 2012.
- [4] OneFIT Deliverable D2.1 "Business scenarios, technical challenges and system requirements", October 2010.
- [5] OneFIT Deliverable D2.2 "OneFIT functional and system architecture", February 2011.
- [6] OneFIT Deliverable D3.1 "Proposal of C4MS and inherent technical challenges", March 2011.
- [7] OneFIT Deliverable D3.2 "Information definition and signalling flows", September 2011.
- [8] OneFIT Deliverable D3.3 "Protocols, performance assessment and consolidation on interfaces for standardization", June 2012.
- [9] OneFIT Deliverable D4.1 "Formulation, implementation considerations, and first performance evaluation of algorithmic solutions", May 2011.
- [10] OneFIT Deliverable D4.2 "Performance assessment & synergic operation of algorithmic solutions enabling opportunistic networks", June 2012.
- [11] OneFIT Deliverable D4.3 "Performance evaluation of synergic operation of algorithms enabling opportunistic networks", December 2012.
- [12] Universal Software Radio Peripheral (USRP), <http://www.ettus.com/>
- [13] GNU Radio, <http://www.gnuradio.org>
- [14] Robin I.C. Chiang, Gerard B. Rowe, and Kevin W. Sowerby, "A Quantitative Analysis of Spectral Occupancy Measurements for Cognitive Radio", Vehicular Technology Conference (VTC) Spring, Dublin, April, 2007.
- [15] F. Bouali, O. Sallent, J. Pérez-Romero, and R. Agustí, "Exploiting Knowledge Management for Supporting Spectrum Selection in Cognitive Radio Networks," Cognitive Radio Oriented Wireless Networks and Communications (CROWNCOM) conference, Stockholm, June, 2012.
- [16] A. Keranen, J. Ott, K. Teemu, "The ONE Simulator for DTN Protocol Evaluation" in Proc. SIMUTools'09: 2nd International Conference on Simulation Tools and Techniques, 2009.
- [17] Java Agent DEvelopment Platform (JADE), Web site: <http://jade.tilab.com>
- [18] FIPA Abstract Architecture Specification. Foundation for Intelligent Physical Agents, 2000. <http://www.fipa.org/specs/fipa00001/>
- [19] D. Karvounas, A. Georgakopoulos, V. Stavroulaki, N. Koutsouris, K. Tsagkaris, P. Demestichas, "Resource Allocation to Femtocells for Coordinated Capacity Expansion of Wireless Access Infrastructures", EURASIP Journal on Wireless Communications and Networking: Special Issue on Femtocells in 4G Systems, 2012:310
- [20] M.Tosic, M.Cirilovic, O.Ikovic, D.Kesler, S.Dautovic, D.Bosovic, "Impact of different content placement and delivery techniques on streaming capacity of the wireless mesh networks", AdHoc Now 2012, Belgrade Serbia.
- [21] Rice University WARP Workshop, <http://warp.rice.edu/trac/wiki/Workshops/>, Aachen, Germany, May 2011

- [22] Ying-Chang Liang, "Sensing-Throughput Tradeoff for Cognitive Radio Networks", IEEE TRANSACTIONS ON WIRELESS COMMUNICATIONS, VOL. 7, NO. 4, APRIL 2008
- [23] P. Cheragi, "A novel low complexity differential energy detection for sensing OFDM sources in low SNR environment", Conference Publications, IEEE Globecom Workshops, pp. 378-382, Dec 2011
- [24] P. Cheragi, Yi Ma, Tafazolli R., "Cluster-Based Differential Energy Detection for Spectrum Sensing in Multi-Carrier Systems", IEEE Transactions on Signal Processing, Issue 99.
- [25] [www.wireshark.org](http://www.wireshark.org)
- [26] Real-time Transport Protocol RFC <http://www.ietf.org/rfc/rfc3550.txt>
- [27] Michel Bourdellès, Nicolas Ménégale "Routing optimization for network coding" IEEE/IFIP Wireless Days 2012, Dublin